BACE1 activity levels inversely influence peripheral axon regeneration: a potential therapy for nerve injuries and diseases

by

Carolyn Tallon

A dissertation submitted to Johns Hopkins University in conformity with the requirements for the degree of Doctor of Philosophy.

Baltimore, Maryland

December, 2017

Abstract

One of the many unsolved mysteries in neuroscience is why the peripheral nervous system can extensively regenerate its axons while the central nervous system is limited. Despite its capacity for regeneration, peripheral nerve regeneration is often unsatisfactory and slow, leading to limited functional recovery following traumatic nerve injuries or in response to motor neuron disease and peripheral neuropathies. In an attempt to identify mechanisms and targets for drugs, researchers have discovered many different regulators of peripheral nerve regeneration. Despite this intense interest in understanding how peripheral nerves regenerate, there are still no approved therapeutics for enhancing peripheral nerve regeneration. This thesis identifies BACE1 as a novel regulator of peripheral nerve regeneration and inhibitors of BACE1 as potential therapeutics. Previous research done in our lab demonstrated that BACE1 KO mice have enhanced peripheral nerve regeneration following a sciatic nerve crush injury. We then hypothesized that BACE1 activity levels have an inverse relationship with axonal regeneration. This thesis investigated this hypothesis using mice which overexpress BACE1 in their neurons and demonstrated impaired regeneration following a sciatic nerve crush injury. We then determined whether BACE1 inhibitors could be utilized as a potential therapy for enhancing peripheral nerve regeneration, both in terms of traumatic nerve injury as well as a peripheral neurodegenerative disease. BACE1 inhibitors were administered to WT mice after performing either a sciatic nerve crush or a partial nerve transection of the lateral thoracic nerve. Mice treated with the inhibitors had improved muscle reinnervation and electrophysiological function following the nerve crush, and enhanced terminal axonal sprouting following a partial nerve transection. BACE1 inhibitors were also able

to improve muscle innervation, electrophysiological function, and enhanced sprouting in the SOD1^{G93A} mouse model of ALS. Taken together, the data outlined in this thesis demonstrated that BACE1 activity not only negatively regulates peripheral nerve regeneration, but that providing mice with BACE1 inhibitors enhance axonal regeneration following both traumatic nerve injuries and motor neuron disease.

Mentor: Dr. Mohamed H. Farah

Thesis committee: Dr. Lee J. Martin, Dr. Charles G. Eberhart, and Dr. Barbara S. Slusher

Readers: Dr. Mohamed H. Farah and Dr. Lee J. Martin

Acknowledgements

At the risk of sounding cheesy, I think that the best way to begin my acknowledgements is with the proverb “it takes a village to raise a child.” Going all the way back to kindergarten, many people have been involved in encouraging and mentoring me to become the scientist I am today. I never would have been able to accomplish all of these things without all the support of my family, friends, and mentors.

I would first like to thank my family since none of this would have been possible without them. My mother and father have been my biggest supporters from day one and I don’t think I could ever thank them enough for all that they have sacrificed over the years in order for me to be here. Thank you for putting up with my hysterical phone calls after every exam panicking that I failed, only to later discover an A. Thank you for always encouraging me to strive to be the best that I could be but also supporting me when I fell short. Thank you for highlighting the importance of education and that the best way to feel successful was to make my own way in life with my own successes. I will be forever grateful for all the love and support given throughout my life. I would also like to thank my brother for also putting up with me and supporting me. I love you all so much.

I would next like to thank my thesis mentor, Mohamed, for all the support over the past 4 years. I don’t think I could have ever found a better mentor. He is always looking on the bright side of things, even when things were going horribly wrong. He taught me that there can always be a positive frame of reference to tackle a problem and that even unexpected setbacks can be great if you just take the time to think and learn from them. He always supported any ideas I had, even when those ideas were less than stellar, and allowed me to try things out in order to grow and learn as a scientist.

I also want to thank former members of the Farah lab; Katelyn Russell, Aniqa Tasnim, Lijuan Liu, Ping Xue, Nirmal Andrapalliyal, and Ashley Lea. I especially would like to thank Katelyn for teaching me all the electrophysiology methodologies, without her expertise this body of work would be nothing. To the current members of the lab, John Fissel and Katie Marshall, thanks for all the laughs along the way. Katie, you kept my sanity in the last few months by helping me out and I will be forever grateful. May the science gods be favorable towards your dissertations!

To my thesis committee members, Lee Martin, Charles Eberhart, and Barbara Slusher, thank you for all the guidance given to me over the past 4 years. My thesis would not be the coherent body of work presented here without the critiques and suggestions of all of you. I have truly grown as a scientist because of what I have learned from the wisdom of my committee. I would like to thank Lee for agreeing to read this thesis. I would also like to thank Barbara for continuing to support me through my post doc and providing me with support as I pursue my industry career goals.

A big thank you to Matthew Kennedy at Merck for generously agreeing to provide our lab with a clinically relevant BACE1 inhibitor and following the progress of my project over the past couple of years. I truly appreciate all the advice given to me about how to best achieve my goals of transitioning over to a position in industry.

I would also like to thank the Pathobiology program. I still remember sitting on the plane on my way to my interview and thinking that I should probably just head straight back home. As soon as I met with the Pathobiology people, however, my fears completely dissipated and I have never looked back since. To the past and present program administrators (Nancy Nath, Tracie McElroy, and Stacey Morgan), I never

would have gotten all the proper paper work in order and on time. To all the faculty members of the program, thank you for sharing your wisdom with me and helping to broaden my scientific mind. And lastly, to the group of students, thank you all for laughing and crying with me throughout these 4 years. I would take the time to give a shout out to each one of you individually, but that would probably add another 5 pages to this acknowledgement section. Just know that I cherish each and every one of you and all of the memories we've shared. You've made my time in the grad school truly memorable and if I could do it all over again I would choose the Pathobiology program every time.

I would also like to thank all of the teachers and professors who were instrumental to the lead up towards my entering graduate school. To my late grade 8 teacher Mrs. Chapman, you were the first teacher to truly believe in my potential and encourage me to push the envelope. To all my high school science teachers, thank you for instilling a love of science in me and sowing the seeds of scientific inquiry. I would like to thank Dr. Karine Auclair for giving me my first ever lab position. My time there was the catalyst needed to decide on pursuing a career in research over medical school. I would especially like to thank Kenward Vong and Aaron Larsen for taking the time to mentor me while I was in the lab and continuing to give me advice over the years. I would also like to thank Dr. Kathleen Cullen for taking me on to complete my honours thesis. Lastly, I would like to thank Dr. Claire Brown for teaching me all I know about microscopy. My thesis benefitted greatly from all the expertise I learned during my time in your lab.

This thesis is a testament to all of the support and encouragement of my own village and I thank every single person who has made me the person I am today.

Table of Contents

ABSTRACT II

ACKNOWLEDGEMENTS IV

LIST OF FIGURES XIII

LIST OF TABLES XV

CHAPTER 1: INTRODUCTION 1

INTRODUCTION 1

BETA SECRETASE AND ITS MANY SUBSTRATES 4

BETA-SITE APP CLEAVING ENZYME 1 (BACE1) 4

BACE1'S ROLE IN AMYLOID PRECURSOR PROTEIN PROCESSING 5

BACE1 IMPACTS PERIPHERAL MYELINATION VIA NEUREGULIN-1 TYPE III 5

BACE1 ACTIVITY INFLUENCES AXONAL GUIDANCE VIA MULTIPLE ADHESION MOLECULES 6

BACE2 8

HOW DO PERIPHERAL NERVES REGENERATE? 8

THE TYPE AND EXTENT OF PERIPHERAL NERVE INJURY AFFECTS REGENERATION EFFICACY 8

AXONAL SPROUTING FROM NEIGHBORING INTACT AXONS CONTRIBUTES TO REINNERVATION 11

REGENERATION ASSOCIATED GENES 13

MODELING PERIPHERAL NERVE INJURIES IN MICE 14

THE SCIATIC NERVE IS A SIMPLE MODEL TO STUDY NERVE CRUSH INJURIES 14

UTILIZING THE LATERAL THORACIC NERVE – CUTANEOUS MAXIMUS MUSCLE SYSTEM TO MODEL PARTIAL NERVE INJURIES 16

EXAMPLES OF DISEASES THAT LEAD TO PERIPHERAL NERVE DEGENERATION 18

CHARCOT-MARIE-TOOTH DISEASE 18

DIABETIC PERIPHERAL NEUROPATHIES 19

AMYOTROPHIC LATERAL SCLEROSIS 21

PROBLEMS IN PERIPHERAL NERVE REGENERATION 23

PERIPHERAL NERVES MUST OVERCOME MANY OBSTACLES FOR PROPER REGENERATION 23

PERIPHERAL NERVE REGENERATION IS FURTHER IMPAIRED BY AGE AND DISEASE 26

THERAPEUTIC OPTIONS FOR ENHANCING AXONAL REGENERATION ARE ABSENT 26

BETA SECRETASE AS A NOVEL REGULATOR OF PERIPHERAL NERVE REGENERATION 27

REDUCED BACE1 ACTIVITY LEVELS IMPROVE PERIPHERAL NERVE REGENERATION 27

BACE1 SUBSTRATES THEMSELVES INFLUENCE AXONAL REGENERATION 28

BETA SECRETASE INHIBITORS AS A POTENTIAL THERAPEUTIC STRATEGY FOR ENHANCING PERIPHERAL NERVE REGENERATION 31

BACE1 INHIBITOR DEVELOPMENT 31

BACE1 INHIBITORS DEVELOPED FOR AD HAVE GOOD SAFETY PROFILES 32

POTENTIAL ISSUES SURROUNDING THE USE OF BACE1 INHIBITORS FOLLOWING ACUTE PERIPHERAL NERVE INJURIES 33

BACE1 INHIBITOR TREATMENT MAY AVOID AXONAL GUIDANCE ISSUES IN ADULTS 36

BACE1 INHIBITORS MAY BE USEFUL IN EARLY STAGE PERIPHERAL NEURODEGENERATIVE DISEASES 37

CONCLUDING REMARKS OF THE INTRODUCTION 37

CHAPTER 2: OVEREXPRESSION OF BACE1 LEADS TO REDUCED PERIPHERAL NERVE REGENERATION AFTER ACUTE NERVE INJURY 39

INTRODUCTION TO CHAPTER 2 39

RESULTS 40

OVEREXPRESSION OF BACE1 DOES NOT ALTER UNINJURED AXON MORPHOLOGY OR PHYSIOLOGY 40

BACE1 OVEREXPRESSION DOES NOT ALTER AXONAL DEGENERATION AND DEBRIS CLEARANCE AFTER INJURY 43

BACE1 overexpression impairs axonal regeneration as early as 3 days after injury 46

Overexpressing BACE1 leads to impaired axonal regeneration 10 days after injury 49

BACE1 overexpression reduces reinnervation of the gastrocnemius muscle 15 days after injury 52

Overexpression of BACE1 causes a delay in the long-term recovery of the CMAP 55

Summary of chapter 2 **59**

CHAPTER 3: DECREASED BACE1 ACTIVITY ENHANCES PERIPHERAL NERVE REGENERATION FOLLOWING A NERVE CRUSH INJURY 60

Introduction to chapter 3 **60**

Results **61**

BACE1 inhibitors target BACE1 activity 61

BACE1 inhibition enhances neurite branching and outgrowth in vitro 64

BACE1 inhibitors do not alter normal, uninjured axon morphology 65

BACE1 inhibition enhances axon regeneration after a sciatic nerve crush injury 69

Summary of chapter 3 **73**

CHAPTER 4: AXONAL SPROUTING FOLLOWING A PARTIAL NERVE INJURY IS ENHANCED BY BACE1 INHIBITION 75

Introduction to chapter 4 **75**

Results **76**

Partial nerve transections can be performed in the lateral-thoracic nerve-cutaneous maximus muscle system 76

The CMM is a thin muscle exclusively comprised of type II muscle fibers 78

Whole-mounted LTN–CMM can be stained with antibodies 82

Reduced BACE1 activity increases axonal sprouting following a partial nerve injury 83

SUMMARY OF CHAPTER 4 **88**

CHAPTER 5: MONITORING PERIPHERAL NERVE DEGENERATION IN A CHRONIC NEURODEGENERATIVE DISEASE MODEL **89**

INTRODUCTION FOR CHAPTER 5 **89**

RESULTS **90**

NEITHER AXON NOR TERMINAL DEGENERATION WAS DETECTED AT 30 DAYS OF AGE 90

MARKED DEGENERATION APPEARS AT THE CAUDAL REGION BY 60 AND 90 DAYS 93

PHYSIOLOGICAL CHANGES AT THE DISTAL LTN OCCURS EARLIER THAN THE SCIATIC NERVE 98

LIMITED SPROUTING OF THE SURVIVING LTN AXONS 100

SUMMARY OF CHAPTER 5 **102**

CHAPTER 6: BACE1 INHIBITORS AS POTENTIAL THERAPEUTICS TO ENHANCE PERIPHERAL NERVE REGENERATION IN THE ALS MOUSE MODEL **103**

INTRODUCTION **103**

RESULTS **104**

BACE1 INHIBITORS IMPROVE MUSCLE INNERVATION AND ELECTROPHYSIOLOGICAL VALUES IN AN ALS MOUSE MODEL AFTER 1 MONTH OF TREATMENT 104

BACE1 INHIBITOR TREATMENT ONLY IMPROVES MORPHOLOGICAL REPAIR AFTER 2 MONTHS OF TREATMENT 109

AXONAL SPROUTING IS ENHANCED BY REDUCING BACE1 ACTIVITY 112

L1/CHL1 EXPRESSION LEVELS ARE INCREASED IN $SOD1^{G93A}$ MICE FOLLOWING BACE1 INHIBITION 114

SUMMARY OF CHAPTER 6 **115**

CHAPTER 7: CONCLUSIONS **117**

INCREASED BACE1 ACTIVITY LEVELS ARE DETRIMENTAL TO PERIPHERAL NERVE REPAIR **118**

POTENTIAL BACE1 MECHANISMS **119**

BACE1 ACTIVITY LEVELS MAY BE FURTHER COMPLICATING REPAIR IN DISEASE AND AGEING **120**

THE LTN-CMM SYSTEM IS USEFUL FOR STUDYING PERIPHERAL NERVE REPAIR FOLLOWING ACUTE NERVE TRAUMA AND IN NEURODEGENERATIVE DISEASES **121**

BACE1 INHIBITORS AS A THERAPY FOR TRAUMATIC PERIPHERAL NERVE INJURIES **125**

EARLY TREATMENT WITH BACE1 INHIBITORS IMPROVES CMM INNERVATION IN AN ALS MOUSE MODEL **128**

FINAL CONCLUSION **130**

CHAPTER 8: METHODS **131**

ANIMALS **131**

BACE1 OVEREXPRESSION EXPERIMENTS 131

BACE1 KO EXPERIMENTS 131

INJURY EXPERIMENTS IN WT MICE 132

SOD1 EXPERIMENTS 132

MOUSE PERFUSION 133

TISSUE PROCESSING FOR LIGHT AND ELECTRON MICROSCOPY **134**

NERVE INJURY PROTOCOLS **135**

SCIATIC NERVE CRUSH 135

SCIATIC NERVE TRANSECTION 135

PARTIAL LTN TRANSECTION 136

DRG PRIMARY CULTURE **136**

ELECTROPHYSIOLOGY PROTOCOLS **137**

SCIATIC NERVE ELECTROPHYSIOLOGY 137

LTN–CMM ELECTROPHYSIOLOGY 138

TISSUE STAINING **139**

CULTURED DRG NEURONS 139

SCIATIC NERVE STAINING 140

GASTROCNEMIUS MUSCLE STAINING 140

LTN–CMM STAINING 141

MUSCLE TYPE STAINING 141

REGENERATION ANALYSIS **142**

SCIATIC NERVE REGENERATION 142

EARLY REGENERATION ANALYSIS 142

MACROPHAGE QUANTIFICATION 143

NMJ REINNERVATION 143

AXONAL SPROUTING 144

WESTERN BLOT **144**

STATISTICAL ANALYSIS **145**

REFERENCES **146**

CV **163**

List of Figures

Fig. 1. BACE1 activity levels inversely regulate peripheral nerve repair. 3

Fig. 2. Peripheral nerves can regenerate by sending out sprouts from the proximal stump. 10

Fig. 3. Intact axons can send out axonal sprouts following partial nerve injuries. 12

Fig. 4. Problems in peripheral nerve regeneration. 25

Fig. 5. Potential mechanism for how BACE1 activity levels regulate peripheral axon growth. 30

Fig. 6. BACE1 overexpression does not affect nerve morphology and electrophysiology. ... 42

Fig. 7. BACE1 overexpression does not alter degeneration 5 days after complete sciatic nerve transection. 44

Fig. 8. BACE1 overexpressing mice have reduced early regeneration 3 days after a sciatic nerve crush. 47

Fig. 9. Fewer axons extend distally from the crush site in BACE1 transgenic mice 3 days following injury. 49

Fig. 10. BACE1 overexpression hinders axonal regeneration 10 days after sciatic nerve crush. 50

Fig. 11. Neurofilament staining with BACE1 overexpression is reduced 15 days following a sciatic nerve crush. 52

Fig. 12. BACE1 overexpression reduces NMJ reinnervation in the gastrocnemius muscle 15 days after sciatic nerve crush. 53

Fig. 13. BACE1 overexpression leads to delayed functional recovery after a sciatic nerve crush. 57

Fig. 14. Oral BACE1 inhibitors reduce full length APP. 62

Fig. 15. Cultured adult mouse neurons have enhanced neurite branching after BACE1 inhibitor treatment. 65

Fig. 16. BACE1 inhibitors do not alter normal axon morphology and physiology. 67

Fig. 17. BACE1 inhibitors enhance axonal regeneration following a sciatic nerve crush. 70

Fig. 18. BACE1 inhibition enhances functional repair following a sciatic nerve crush injury. 72

Fig. 19. Utilizing the LTN-CMM system to perform partial nerve transections. 77

Fig. 20. The CMM is exclusively comprised of type II muscle fibers. 80

Fig. 21. Reliable antibody staining of the neuromuscular synapse components in the whole, intact CMM. 83

Fig. 22. Genetically knocking out BACE1 enhances axonal sprouting following a partial nerve transection. 85

Fig. 23. BACE1 inhibitors enhance terminal axonal sprouting following a partial nerve injury. 87

Fig. 24. No evidence of axonal degeneration in 30-day-old SOD1 mice. 91

Fig. 25. Axonal degeneration is evident by 60 days in SOD1 mice at the caudal site but not the rostral site. 94

Fig. 26. Axonal degeneration is apparent at the rostral site at 90 days of age in SOD1 mice. 96

Fig. 27. The sciatic nerve shows a decrease in CMAP amplitude at 90 days. 99

Fig. 28. SOD1 mice show very limited axonal sprouting. 101

Fig. 29. 1 month MBI-9 BACE1 inhibitor treatment improves morphological and physiological repair in SOD1 mice. 106

Fig. 30. 1 Month of LY2886721 BACE1 inhibitor treatment enhances morphological and electrophysiological values in SOD1 mice. 108

Fig. 31. 2 month Merck BACE1 inhibitor treatment improves morphological repair but not functional repair. 110

Fig. 32. BACE1 inhibition enhances axonal sprouting in disease. 113

Fig. 33. BACE1 inhibition alters L1/CHL1 expression levels in SOD1 mice. 115

List of Tables

Table 1. Antibodies used for tissue staining. 139

Chapter 1: Introduction

Introduction

One of the many unsolved mysteries in neuroscience is the unknown reasons why the peripheral nervous system (PNS) is able to regenerate its axons following injury while the central nervous system (CNS) has limited growth capacity. The search for understanding this fundamental difference between the peripheral and central nervous systems has led to many discoveries of the cellular changes, differential gene expression, and pathways that regulate how the PNS is able to regenerate. There is now a good understanding of the steps required for the peripheral nerve to begin to regenerate and how these steps differ from the CNS. After axonal injury, the axolemma begins to degenerate and the myelin sheath breaks up. Following this degeneration, axonal and myelin debris is cleared in order to make space for regenerating axons to grow. In the PNS, macrophages, and to some extent Schwann cells, the myelinating cells in the PNS, begin to phagocytose axonal and myelin debris (*1-4*). In the CNS, resident microglia, and an influx of blood-borne macrophages, are responsible for debris clearance, however, there is some evidence that the CNS response to debris clearance is very slow and contributes to the limited axonal regeneration (*5-7*). Next, the supporting cells need to provide aid to the regenerating axons by guiding them towards the correct end target. The Schwann cells of the PNS carry this out by undergoing dedifferentiation and creating Schwann cell tubes, called Bünger bands, for which the regenerating axons can enter and grow through before reaching their target and getting remyelinated (*8-10*). In the CNS, astrocytes become activated and begin to proliferate and secrete inhibitory proteoglycans,

which make up a majority of the glial scar (*8*). This process is detrimental to axonal regeneration and provides a significant barrier for repair following CNS trauma. Another step that must occur for successful regeneration is when neurons and supporting cells alter their gene expression profiles to a pro-regenerative state. The cells of the PNS upregulate various growth factors, transcription factors, and adhesion molecules, collectively termed regeneration associated genes (RAGs), which all work together to enhance axonal outgrowth (*11-14*). On the other hand, CNS cells generally do not express high levels of RAGs. In fact, oligodendrocytes, responsible for myelination in the CNS, express various myelin-associated inhibitors, such as Nogo-A and myelin-associated glycoprotein, while neurons express axon regeneration inhibitor molecules, like repulsive guidance molecule and Semaphorin A (*11*).

Our lab has discovered a novel role of beta-site APP-cleaving enzyme 1 (BACE1), or beta secretase, in regulating peripheral axonal regeneration. BACE1 is a transmembrane protease that is involved in the cleavage and processing of a wide variety of membrane bound proteins (*15-23*). What is interesting with regard to peripheral nerve regeneration is that many of BACE1's substrates have been implicated in the regulation of axonal regeneration and neurite outgrowth. Some have even been identified as genes which are upregulated following nerve injury. We have demonstrated, using BACE1 KO mice, that lacking beta secretase enhances peripheral axonal regeneration following axonal injury. When beta secretase was genetically knocked out, we observed an increased number of regenerating axons following a sciatic nerve crush (*24-26*). This finding has led us to hypothesize that BACE1 activity levels may inversely influence peripheral nerve regeneration following injury, as diagrammed in Figure 1.

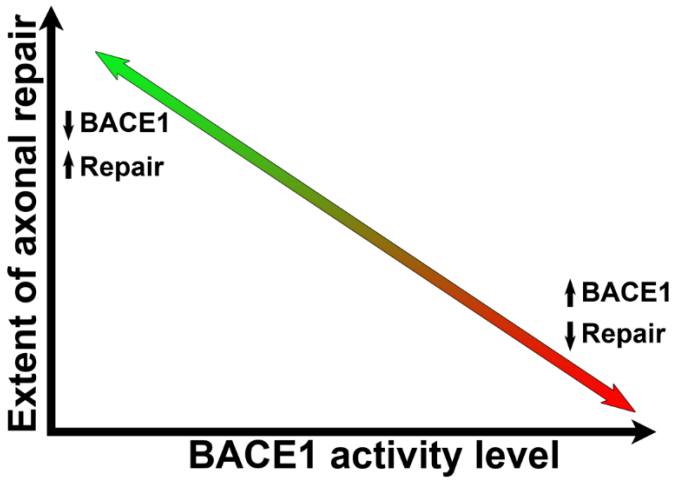

Fig. 1. BACE1 activity levels inversely regulate peripheral nerve repair.
Hypothetically, we propose that with low levels of BACE1 activity, peripheral nerve repair is accelerated. When BACE1 activity levels are high, axonal repair is reduced. We hypothesize that this relationship is on a sliding scale where changes in BACE1 expression have a small effect on repair process effectiveness.

Despite peripheral nerves' ability to regenerate, the outcome of this regeneration is often poor and insufficient (*9, 10, 27, 28*). Peripheral nerve regeneration must overcome many obstacles, including slow regeneration rates, inefficient axonal guidance, and the degeneration of supporting cells' end targets. Currently, the only available treatment option for patients is the surgical reconnection of the nerve (*29*). Various novel therapeutic options are being explored to improve outcomes such as enhanced nerve conduits, stem cell treatments, and small molecule drugs to enhance regeneration (*13, 29*). Our recent data, together with the greater body of research on BACE1's substrates' impact on axonal growth, points towards a possible novel application for BACE1 inhibitors currently being investigated in clinical trials of Alzheimer's Disease (AD).

Beta secretase and its many substrates

Beta-site APP cleaving enzyme 1 (BACE1)

BACE1 mRNA is widely expressed in many tissues throughout the body, however, the highest expression levels are found in the brain and pancreas (*15, 30*). In the normal CNS, BACE1 expression is highly localized to neuronal tissue and is not expressed in the surrounding glial cells (*30*). The expression mRNA pattern of BACE1 is closely correlated with BACE1 activity (*30*). Interestingly, BACE1 activity levels in the pancreas are rather low compared with the levels of mRNA expression. It was later determined that the BACE1 mRNA in the pancreas was actually a splice variant missing most of exon 3 which abolished its enzymatic ability (*31, 32*). Two inactive splice variants of BACE1 have been identified, with both being expressed in the pancreas and only 1 being expressed in the brain (*32*).

BACE1 is an approximately 70 kDa protein whose structure consists of a single transmembrane domain with a luminal Asp32-Asp228 catalytic domain (*33, 34*). Since the optimal pH range for BACE1 activity is fairly acidic (*15, 35*), it primarily localizes to the Golgi apparatus and endosomes (*16, 17, 36, 37*). BACE1 is first synthesized as a pro-enzyme in the endoplasmic reticulum (*38*). On its way to the Golgi apparatus, the pro-enzyme gets glycosylated and acetylated before carbohydrates are attached and the N-terminal prodomain is trimmed (*38*). BACE1 is then cycled between the cell surface and early endosomes which is regulated by Ser 498 phosphorylation and di-leucine motif (*38*).

BACE1's role in amyloid precursor protein processing

BACE1 has been well studied in the context of AD as it is one of the main enzymes responsible for generating amyloid beta plaques (Aβ), a pathological hallmark of the disease (*15-17, 39-41*). In order to generate Aβ, BACE1 cleaves amyloid precursor protein (APP) into a membrane bound C-terminal fragment (CTF) and a soluble APPβ fragment. The CTF is then further cleaved by gamma secretase to generate the Aβ fragment that then goes on to aggregate and form plaques. A reduction in beta secretase activity, either genetically or pharmacologically, leads to a decrease in the production of Aβ (*15, 39-42*). Conversely, when human BACE1 is overexpressed in mice, APP processing is increased leading to amyloid deposition and synaptic defects or neurodegeneration (*43, 44*). The fact that BACE1 is one of two important enzymes involved in generating Aβ plaques has led many drug companies to investigate BACE1 inhibitors as potential therapeutics for AD (*42, 45-48*). This large interest in inhibiting BACE1 has led many to ask the question, what other substrates, if any, does BACE1 cleave?

BACE1 impacts peripheral myelination via neuregulin-1 type III

As it turns out, BACE1 is a rather promiscuous enzyme and over 60 putative substrates have been identified (*18, 49-53*). Fortunately, despite the large number of substrates, BACE1 knock out mice are viable, with some moderate behavioral phenotypes (*39-41*). One of the more striking phenotypes observed was the reduction in the myelination of the peripheral nerves in these mice. The thickness of the myelin sheath is markedly decreased, but not completely absent, and the presence of an increase in

unmyelinated groups of axons, called Remak bundles, can be seen in nerve bundles in the periphery (*22, 23, 54, 55*). While reduced peripheral myelination is cause for concern when treating patients with BACE1 inhibitors, this phenotype appears to mostly be a developmental issue. When adult mice are given a BACE1 inhibitor, others (*46*) and our lab (unpublished observation) have observed that the myelination of uninjured peripheral axons is not changed. This observation of altered myelination gave a clue as to what other substrates BACE1 may be cleaving. As it turns out, BACE1 is involved in the cleavage of neuregulin-1 type III (NRG1) (*22, 54*). NRG1 type III is the molecule responsible for determining the levels of myelination in the peripheral nervous system (*56, 57*). Fortunately, its cleavage and activation is not solely dependent on BACE1 as it is also cleaved by ADAM17 (*58*). This parallel pathway allows for some myelination to occur and may be the reason for the presence of some myelination in total KO mice.

BACE1 activity influences axonal guidance via multiple adhesion molecules

Another phenotype that has caused some concern for BACE1 inhibitor use is the potential issues with axonal guidance. In BACE1 KO mice, there appears to be some defects in axonal connections in the central nervous system, most notably in the olfactory bulb and mossy fiber projections (*59*). This finding has led to the speculation that BACE1 inhibitors may negatively impact memory and learning by impairing synaptic plasticity. Since some of the potential BACE1 substrates are involved in cell-cell adhesion, such as neural cell adhesion molecule 1 (NCAM1) (*18*), it likely follows that this may be the reason behind the axonal guidance issues. Indeed, two of BACE1's identified substrates, L1 and close homolog of L1 (CHL1) (*60*), are thought to be involved in axonal guidance

(*49*). These molecules are members of the immunoglobulin superfamily and have been identified as being important in proper neurogenesis. A loss of L1 or CHL1 leads to behavioral abnormalities and decreased cognitive function in mice (*61, 62*). There are also known mutations in humans, which lead to mental retardation as well as schizophrenia (*63-66*).

Another protein that was identified as a BACE1 substrate is contactin-2, also known as Axonin-1 or transiently expressed axonal surface glycoprotein-1 (TAG-1) (*60*). This protein is also a member of the immunoglobulin superfamily and is expressed on the surface of axons as well as the Schwann cells of the PNS (*67, 68*). A loss of contactin-2 led to a reduced axonal growth speed and impaired guidance in zebrafish (*69*). Following a sciatic nerve crush, contactin-2 was found to be upregulated in Schwann cells near the lesion (*70*). BACE1 cleavage of contactin-2 also appears to have a negative impact on the level of contactin-2 found on the cell surface of primary mouse neurons (*71*).

One more BACE1 substrate that has been identified as being an important regulator for neurite outgrowth is Seizure-related gene 6 (Sez-6)(*60*). It has been implicated as having an important role in regulating neurite outgrowth and connectivity in the developing neocortex. Cultured cortical neurons from Sez-6 null mice showed more extensive neurite branching, however, they also had a reduction in neurite length (*72*). Another group also observed a decrease in neurite length when administering an shRNA against Sez-6 in PC12 cells treated with NGF (*50*).

As many of BACE1's substrates appear to be important in regulating axonal outgrowth and neurite branching, regulating BACE1 activity levels may have

implications going beyond AD. Our lab has been studying the effects of BACE1 activity levels on the efficacy of peripheral nerve regeneration following acute nerve injury.

BACE2

In addition to the identification of BACE1, there was also the discovery of a closely related homolog, named BACE2. Like BACE1, BACE2 is a membrane bound aspartyl protease with a very similar structure (*73*). BACE2 is also expressed in a wide variety of cell types, however, its expression levels in the brain are very low and only in very specific regions of the brain (*38*). BACE2 expression appears to be higher in the pancreas (*74*) and is involved in proper β cell function (*75*). BACE2 also differs in the way that it cleaves APP in a more α-secretase manner than a β-secretase manner (*76*). In addition to the Asp+1 cleavage site, BACE2 can also cleave at Phe+19 and Phe+20, indicating that it may have different processing preferences than BACE1(*77*). Another way that BACE2 differs is that it appears to regulate melanocyte function in zebrafish and hair pigmentation in mice (*73, 78, 79*). BACE2 knockout zebrafish also do not have any defects in the myelination of their nerves unlike BACE1 knockouts indicating that BACE2 most likely is not involved in myelination (*78*). All of this data points towards BACE2 having distinct functions from BACE1.

How do peripheral nerves regenerate?

The type and extent of peripheral nerve injury affects regeneration efficacy

The type and severity of a nerve injury can have a profound effect on how peripheral nerves regeneration and the efficacy of this regenerative process. In less severe

injuries, such as a nerve crush, the endoneural tube and basement membrane surrounding the axon remains intact, while the axon itself becomes disconnected. The regenerating axonal sprouts may be able to navigate their way back into the denervated Schwann cell tubes still connected to the proximal portion of the nerve. This is advantageous as the neural tube acts as a highway for the axon to be properly guided towards its appropriate target (Figure 2). In more severe injuries, such as a partial or complete nerve transection, the Schwann cell tube is no longer connected and the proximal axonal sprout can have a difficult time correctly navigating towards the open end of the tube. Depending on the location and extent of the nerve transection, the difficulty that proximal axonal sprouts have to re-enter the distal tube may leave the target organ insufficiently innervated for an extended period or, in the worst case, permanently denervated. Axonal sprouts that are unable to reach the vacated Schwann cell tubes and reinnervate the target muscle are generally pruned back to the main axon branch. In some cases, the unguided sprout can become tangled up and form a neuroma.

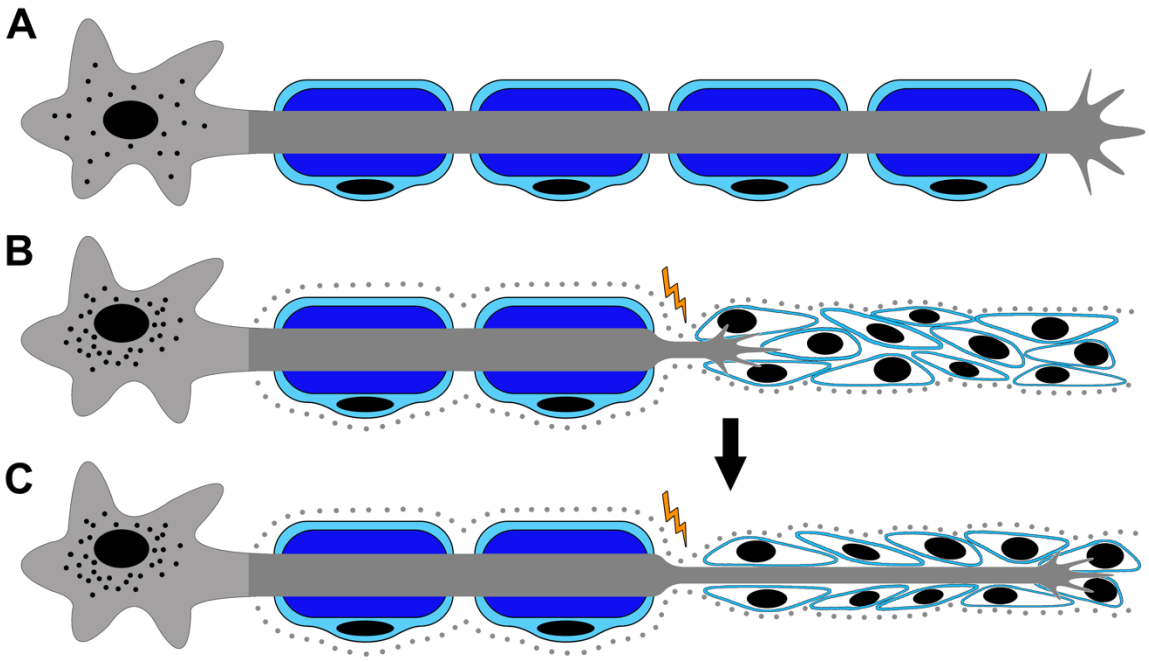

Fig. 2. Peripheral nerves can regenerate by sending out sprouts from the proximal stump. A) Uninjured peripheral axons (dark gray) are wrapped in a discontinuous myelin sheath (dark blue) generated by closely associate Schwann cells (light blue). Their nuclei are centrally located with disperse Nissl staining bodies (black dots) B) Following a nerve crush injury, the axonal portion distal to the crush site degenerates and the cell body carries out a chromatolytic response where the nucleus becomes peripherally located with chromatolytic bodies nearby (represented by the black dots around the nucleus). The proximal stump connected to the cell body will begin to send out a small axonal sprout through the crush site (yellow lightning bolt) directed to the now vacated Schwann cell tube made up of many proliferating Schwann cells (empty blue cells) encapsulated by the still intact basement membrane (gray dots). C) If the sprout is able to connect with the Schwann cell tube, it begins to elongate into the tube and grow towards the end target with the support of the surrounding Schwann cells.

Axonal sprouting from neighboring intact axons contributes to reinnervation

When the distal portion of the axon is unable to regenerate, or the area of denervation is too far away from the proximal site, neighboring intact axons can also send out axonal sprouts from their own axon to reinnervate nearby denervated neuromuscular junctions (NMJs) as an alternative process to enhance target organ reinnervation (*80*). The terminal Schwann cell sitting on the denervated NMJ will become activated and send out numerous processes (*81-84*). Eventually, a process will connect with a nearby intact axonal sprout and create a bridge between the intact axonal sprout and the denervated NMJ. This then allows the axonal sprout to be guided towards the denervated NMJ where it can then reinnervate the NMJ. These axonal sprouts can form from multiple regions along intact axons (Figure 3) (*85*). Axonal sprouts, termed nodal sprouts, can emerge along the main axon branch at the nodes of Ranvier, where the myelin sheath does not cover the axon. The sprouts can also emerge closer to the NMJs, called pre-terminal sprouts, where the myelin sheath ends just before the NMJ to allow for the terminal bouton to interact with the NMJ. Finally, there can also be terminal axonal sprouts which come directly from the terminal bouton innervating the NMJ. Terminal axonal sprouts are easiest to identify as the normal morphology of the terminal bouton at the NMJ only has one axonal connection (*85*). In cases of disease or injury, these terminal to terminal connections can be identified and scored as an axonal sprout.

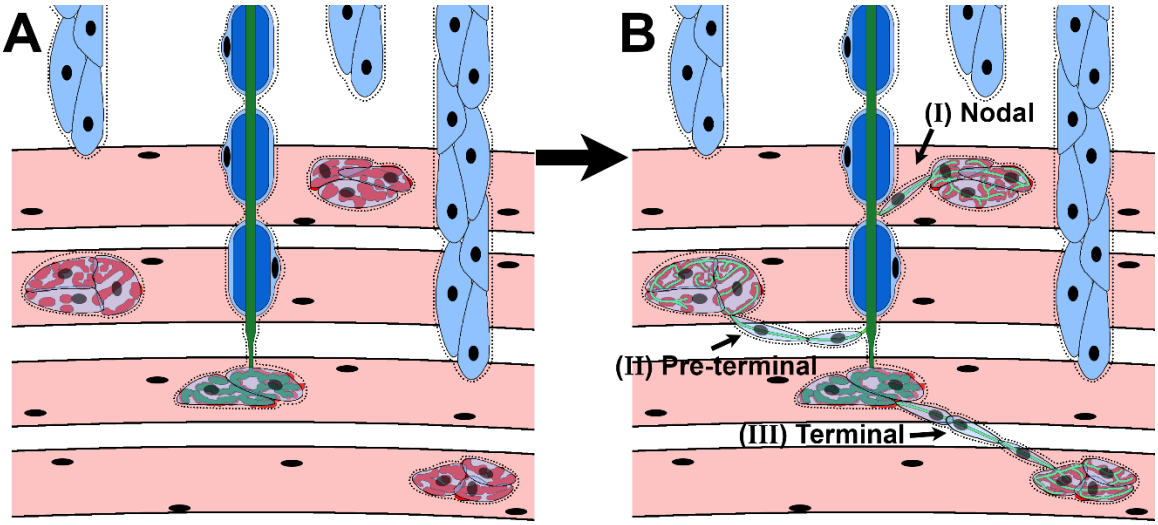

Fig. 3. Intact axons can send out axonal sprouts following partial nerve injuries.

A) When a nerve is partially injured, only some of the axons degenerate, as depicted by the empty Schwann cell tubes (light blue). A few intact axons (dark green) remain connected to their targets, in this case the NMJ (red), and can also be myelinated (dark blue). B) The intact axon has the option to send out axonal sprouts (lime green) to reinnervate the denervated NMJs nearby and can do so in three different ways. The first is a nodal sprout (I), where the sprout originates at the nodes of Ranvier. The second way is a pre-terminal sprout (II) that branches out from the unmyelinated portion of the axon just before synapsing on the NMJ. The final way for an axon to sprout is to send out a terminal sprout directly from the terminal bouton portion at the NMJ (III).

While axonal sprouting to neighboring targets is an important process to maintain connections under conditions of axonal and neuronal cell loss, it is a limited process. The size of any particular motor unit is bound by the surviving neuron's ability to metabolically sustain such a large number of connections (*86, 87*). Eventually, the motor unit becomes too large and the neuron cannot afford to continue to sprout axons. In addition to this limitation on the size of motor units, motor axons innervating different

muscle fiber types have varying sprouting capacities (*88*). Those motor axons innervating fast-fatigable, type IIb muscle fibers had a much lower terminal sprouting response to Botulinum A toxin induced terminal sprouting than the slow-twitch, type I muscle fibers (*88*). This finding may further complicate the efficacy of axonal sprouting depending on which nerves were injured, as some muscles are predominantly type IIb muscle fibers, such as the extensor digitorum longus (EDL) (*89*), and may not be as effectively reinnervated as a type I muscle, like the soleus muscle (*89*).

Regeneration associated genes

In order to initiate axonal sprouting, the gene expression profiles change to a pro-regenerative state. With the recent advances of microarrays, and now RNA Seq, the number of identified genes that are differentially expressed following acute peripheral nerve injury is ever growing (*12, 14, 90*). Many of these regeneration associated genes (RAGs) are anti-apoptotic, transcription factors, or are involved in cytoskeleton remodeling, cell growth, and cell-cell adhesion. In order to accommodate the rapid increase in transcription, many transcription factors become upregulated following injury and have been observed to enhance regeneration, with c-Jun, STAT3 and ATF3 being notable (*12, 91-93*). Many kinase cascades, such as the MAPK pathway, have been identified as RAGs, however, there is some debate over whether these pathways are involved in adult peripheral regeneration (*94*). Neurotrophic factors, such as IGF1, IGF2, NGF and BDNF, are also increased following injury and have been shown to positively impact axonal regeneration (*95-97*). There is also a large upregulation of the expression of cell adhesion molecules following nerve injuries, such as CHL1 (*98*). Proteins that aid

in the interaction between the cell surface and the cytoskeletal components of the cell, such as GAP43, are upregulated following injury in order to prepare for the large cytoskeleton remodeling involved in axonal outgrowth (*99-101*). The genes listed here are just a snapshot of the large number of genes whose expression levels are altered in order for neurons to undergo the extensive and complicated process of regeneration.

Modeling peripheral nerve injuries in mice

The sciatic nerve is a simple model to study nerve crush injuries

In order to study how BACE1 activity levels can influence peripheral nerve regeneration following an injury we need reliable models that reflect the various ways peripheral nerves can be injured. One of the ways a peripheral nerve can be injured is by crushing the nerve. This type of injury leads to the degeneration of the axon distal to the crush site and the breakdown of the myelin sheath. The Schwann cells and endoneural tube, however, are spared and provide a supportive track for the proximal portion of the axon to regenerate towards its normal end target (*102*). In order to easily perform a nerve crush, the most widely used model is the sciatic nerve crush in either a mouse or rat. This is easily performed by making a small incision along the thigh to expose the sciatic nerve and applying pressure on the nerve between a pair of tweezers or tying a suture tightly around the nerve. The recovery following a sciatic nerve crush injury can then be monitored both morphologically and functionally. Morphologically, one can look at the sciatic nerve itself and quantify the number of regenerating axons present in a cross section of the nerve (*25, 103, 104*). Additionally, the extent of reinnervation of the various muscles innervated by the sciatic nerve can also be sectioned and stained (*25,*

103-105). This system also provides the opportunity to monitor functional recovery by recoding the recovery of the compound muscle action potential (CMAP) from the various muscles innervated by the sciatic nerve (*102, 103*).

While the sciatic nerve provides an easy model to perform a reliable nerve crush injury, it does have some limitations. Since it is a mixed nerve of autonomic, sensory, and motor fibers, it can be difficult to determine whether there is a difference in regeneration between fiber types. To further compound this difficulty, there is some evidence that both motor and sensory fibers can be inappropriately recruited to target organs, however, this error can be corrected by pruning the aberrant innervation provided sufficient reinnervation has occurred (*106, 107*). Another issue is that the muscles which are innervated by the sciatic nerve are too large to completely stain and clearly image. Typically, the muscles need to be sectioned before staining in order to properly visualize the axons and NMJs. This is a confounding issue when trying to study axonal sprouting as it becomes rather tedious to reconstruct the muscle and trace the origin and end point of potential axonal sprouts. This can be partly improved by using the extensor digitorum longus (EDL) or tibialis anterior (TA) muscles as they are thinner than the gastrocnemius muscle and can be whole mounted (*104, 105*), however, the depth of staining penetration and imaging can be rather poor and may lead to difficulty tracing the extremely thin axonal sprouts. Finally, reliably performing partial nerve injuries in the sciatic nerve is fairly difficult. Traditionally, partial nerve injuries are performed by tightly tying a suture around 1/2 to 1/3 of the sciatic nerve or cutting half of the sciatic nerve (*108, 109*). However, it is rather difficult to injure a consistent number of axons as there is no way to objectively determine how much of the sciatic nerve is being ligated. Another way in

which a partial nerve transection can be performed using the sciatic nerve is to carry out a ventral root transection (*110*). While this procedure is able to produce a more reliable partial nerve injury, it is difficult to perform as the ventral roots are situated very close to the spinal cord and requires rather tricky surgical techniques to be performed.

Utilizing the Lateral Thoracic Nerve – Cutaneous Maximus Muscle system to model partial nerve injuries

While sciatic nerve crushes tend to be easy to perform in the mouse, these types of injuries tend to be less severe due to the endoneural tube and Schwann cell tube remaining connected to the portion of the nerve proximal to the crush site. A nerve axotomy, whether complete or partial, typically does not regenerate as well because the proximal portion of the nerve is no longer connected to the distal portion. In the case of a partial nerve transection, the intact axons respond to the denervation by sending out collateral axonal sprouts in an attempt to reinnervate portions of the denervated target organ. As discussed in the previous section, performing a partial nerve transection on the sciatic nerve has many technical issues. A more reliable model for performing partial nerve transections is needed before beginning to investigate whether pharmacological interventions can alter axonal sprouting in response to a partial nerve injury. Therefore, it would be beneficial to utilize a muscle-nerve system that can overcome many of the limitations of the sciatic nerve model.

The cutaneous maximus muscle (CMM) – lateral thoracic nerve (LTN) system may be the model that provides some of the answers to the problems of performing a partial nerve transection in the sciatic nerve. Our lab has previously characterized this

system (*111*). The LTN originates from the C7-T1 spinal nerves, exiting out from the brachial plexus towards the shoulder and eventually on to innervate the CMM. The CMM itself spans the entire back of the mouse and is located subdermally, in order to control the dorsal twitch reflex. The three main branches of the LTN are easily isolated by making a small incision along the ventral edge of the scapula and gently teasing apart the muscles (*111*). The relatively conserved organization of the LTN branches and the ease with which they can be accessed may offer a more consistent model for performing partial nerve transections. This would be beneficial as variable amounts of degeneration may have potential effects on the extent of axonal sprouting since axons only send out collateral sprouts in response to nearby degeneration.

Normally, the LTN extends caudally down the CMM, innervating various muscle fibers along the way. The left and right inputs from the spinal cord do not cross the midline and allows for one side to be used as an internal control when injuring one side of the LTN. Of particular note is that the LTN is a purely motor nerve, unlike the sciatic nerve, and the dorsal cutaneous sensory nerve is separated from the LTN. When removing the dorsal skin, the CMM is removed along with it as it lies directly below the dermis. The sensory nerves can then be removed by carefully removing the connective tissue on top of the CMM, with the skin side facing down. This separation of sensory and motor fibers allows for only the motor LTN nerves to be injured and may help to reduce confusion between sensory and motor sprouting when imaging the CMM.

In addition to being able to separate the sensory nerves, the CMM can also be whole mounted onto a slide and imaged because the CMM is an extremely thin muscle, only a few fibers thick (*111, 112*). The extreme thinness of the muscle has many

advantages over the muscles being innervated by the sciatic nerve. Firstly, it is quite easy to completely stain the CMM and image through the entire muscle. Secondly, the ability to image through the intact muscle allows for easy tracing of the beginning and end points of potential axonal sprouts. Lastly, because the LTN enters the CMM near the shoulder and spans the length of the mouse, it is possible to investigate the time course of regeneration in some of the shortest and longest axons in the mouse body. By contrast, in order to perform a similar experiment using the sciatic nerve, one would need to image multiple different muscles located in different regions of the body to get the longest and shortest axons from the sciatic nerve.

Examples of diseases that lead to peripheral nerve degeneration

In addition to acute trauma, peripheral nerves can also be injured as a result of neurodegenerative diseases and peripheral neuropathies. These diseases provide a more chronic model of peripheral nerve degeneration as many undergo a progressive loss of peripheral nerves as the disease advances. Here we outline a few key diseases which lead to progressive peripheral nerve degeneration and the mouse models used to study them.

Charcot-Marie-Tooth disease

Another disease which can lead to progressive peripheral axonal loss is Charcot-Marie-Tooth disease (CMT). This disease is characterized by extensive myelin loss and axonal degeneration. Patients typically present with distal sensory loss and muscle weakness, as well as reflex abnormalities. CMT can be broadly categorized into two main forms depending on whether the disease is primarily due to demyelination (CMT1) or

axonal defects (CMT2) (*113*). Despite this difference, both forms of the disease ultimately lead to axonal degeneration (*114*). Over the years, many mutations have been identified with respect to the pathophysiology observed in CMT (*113, 115*). Mouse models have been generated to study the disease progression using many of the more common mutations found to be associated with both CMT1 and CMT2 (*116*). One such mouse model is the Trembler J mouse, which expresses a mutant form of the peripheral myelin protein 22 (PMP22) and is a model for CMT1 (*117, 118*). These mice have myelin deficiencies and extensive peripheral axon degeneration, as well as abnormal NMJs (*111, 117, 119*). Other mouse models for CMT1 are those which express mutant connexin 32 (GJB1 gene) or myelin protein zero (MPZ gene) (*116*). For CMT2, 2 main mouse models have been generated. One encodes a mutant neurofilament light gene (NEFL) and the other a mutant heat shock protein B1 (HSPB1) (*116*). Unlike ALS, CMT involves both motor and sensory axons which provides the ability to study the degeneration of both sensory and motor axons. The extent of axonal regeneration of both sensory and motor fibers, both endogenous sprouting in the disease state as well as whether any therapeutic strategies can increase sprouting, can be studied in these models. Another interesting aspect to using CMT models is that there are also Schwann cell defects which may impact the ability of the axons to extend out axonal sprouts and highlight any importance in the role of Schwann cell involvement in axonal sprouting.

Diabetic peripheral neuropathies

Diabetic peripheral neuropathies (DPN) are characterized as a length dependent, sensorimotor polyneuropathy which generally shows symmetry. In addition to the axonal

degeneration, diabetic patients also have impaired axonal regeneration following a nerve injury, such as when the skin is cut (*120-122*). Since sensory nerves are the most susceptible to DPN, many patients experience extremely painful symptoms, such as burning, paraesthesia, or a stabbing pain. In addition to these painful symptoms, patients also have impaired abilities to detect small cuts on their extremities. This defect can eventually lead to infection and ultimately limb amputation if the patient is not attentive to checking extremities for cuts and accounts for a majority of limb amputations in the US. Currently, it is believed that both vascular changes as well as metabolic dysfunction in response to dysregulated glucose control play a role in the pathophysiology leading to the degeneration of peripheral nerves (*123*). The idea that hyperglycemia may be the main driver of DPN may not be completely correct. Type I diabetics are able to reduce their incidence of DPN more than Type II diabetics by controlling their glucose levels and many patients develop DPN despite having good control over their glucose levels (*124*).

While the majority of diabetes cases are not closely associated with specific mutations, a few mouse and rat models have been created. The most commonly used models are those that mimic type II diabetes as that is the most common form of diabetes. The most common genetic mouse models are the ob/ob mice, with mutations in leptin, and the db/db mice, with mutations in the leptin receptor, that both have impaired leptin signaling (*125*). In addition to mutant mouse models, it is also possible to generate a diabetic phenotype by placing the mice on a high-fat diet, which then go on to develop diet-induced obesity (*125*). All three mouse models recapitulate many of the symptoms seen in DPN patients. Nerve conduction velocities are reduced, abnormal axonal

morphology is evident, and they have reduced reactions to thermal stimuli (*125, 126*). Diabetic mouse models can provide data on how sensory axons are able to regenerate and sprout following a treatment intending to enhance axonal regeneration as sensory nerves are typically more severely impacted.

Amyotrophic Lateral Sclerosis

Amyotrophic lateral sclerosis (ALS) is characterized by a progressive loss of motor neurons, eventually leading to muscle wasting and finally death (*127*). While there are both sporadic and familial forms of ALS, there is very little known about the actual causes of the disease. Despite this, many mutations have been discovered to be associated with familial forms of ALS. One mutation, the glycine 93 to alanine point mutation in the superoxide dismutase 1 gene (SOD1) (*128*), has proven to be a useful manipulation for generating a popular mouse model of ALS by highly expressing the mutant $SOD1^{G93A}$ gene (*129, 130*). There have been many studies done on this mouse model to characterize the progression of the disease within the mouse. The earliest signs of disease begin to show up at around P45 and manifest as a significant decline in the number of innervated neuromuscular junctions (NMJs) (*88, 131-135*). This early denervation can also be detected as a decline in the amplitude of the compound muscle action potential (CMAP) using electrophysiological analysis (*131, 135*). It is only later, around 90 days, that clinical symptoms begin to appear and degeneration becomes evident in the ventral roots and motor neuron cell bodies (*88, 131-135*). This early peripheral nerve degeneration preceding abnormal motor neuron morphology was also identified in an ALS patient who died suddenly (*132*).

Studies have shown that type IIb, fast-fatigable motor fibers have a selective vulnerability for degeneration in the SOD1^{G93A} mouse compared with the type I or IIa subtypes (*88, 134, 136, 137*). It is also well known that the largest motor neurons die first, pointing toward an inability to keep up with a high metabolic demand (*135, 137*). Despite this, there have not been any extensive studies done on very long nerves of a single-nerve type within the SOD1 mouse. This is most likely due to the limitations set by using the sciatic nerve and its muscles to study the degeneration profile in these mice. As outlined in the previous section, utilizing the LTN-CMM system as a means of studying this length dependent degeneration may be an attractive alternative.

In order to accurately investigate the earliest signs of degeneration of the type II motor fibers, one must take into account the variations brought on by different genetic backgrounds. The B6SJL mixed background SOD1 mouse model, used in the studies mentioned earlier, present with overt clinical symptoms around P90 with a life span of around 130 days (*86, 131, 132, 135, 138*). In contrast, mice with the C57BL/6J background have a delayed disease onset of around 110 days and an extended life span of approximately 150 days (*129, 138-141*). The mice on the B6 background show an extended preclinical phase which provides a longer window to study the early stages of disease before the onset of clinical symptoms and to investigate potential therapeutics for enhancing muscle reinnervation. In addition to the B6 mice having a longer progression, there is also a mouse model which have a low copy number of mutant SOD1^{G93A} (B6.Cg-Tg(SOD1*G93A)dl1Gur/J) which have a disease onset around 200 days (*142*) and die around 266 days (*143, 144*).

Despite the ongoing degeneration in SOD1 mice, there is some extent of axonal sprouting from the surviving axons in an attempt to reinnervate the vacated NMJs. This is evident by an observed increase in the size of the motor units and some sparse reinnervation seen morphologically in the SOD1 mice (*87, 132, 133*). While this partial reinnervation may be useful in the early phase of the disease, as the motor units increase in size, so does the metabolic demand. This eventually catches up with the surviving axons and they can no longer support the increased motor unit size which, ultimately leads to the later phase of rapid decline (*131*). Another obstacle for regeneration, as mentioned above, is that the type II fast-fatigable fibers are fairly resistant to regeneration and do not sprout easily (*88*).

Problems in peripheral nerve regeneration

Peripheral nerves must overcome many obstacles for proper regeneration

The ability for regeneration in the PNS is especially important since peripheral nerves are less protected than those in the CNS and are injured much more frequently. While the peripheral nervous system contains the capacity for regeneration, it is often slow and incomplete, leading to less than favorable outcomes following severe nerve trauma (see Figure 4) (*9, 27, 28*). This is especially true in humans where the average rate of regeneration is around 2-5mm per day (*145*). Depending on the site of injury and how far away it is from the target muscle, the regeneration rate may be too slow for the axon to reach the muscle before other changes begin to happen that are detrimental to regeneration (*146, 147*). When a muscle is denervated for too long, the neuromuscular junctions begin to breakdown into fragments, which can greatly hinder the regenerating

axon's ability to reinnervate its target muscle (*148*). In addition to the breakdown of NMJs, supporting Schwann cells also become unable to aid regenerating axons due to gene downregulation and a reduced number of Schwann cells (*149*). All of these changes contribute to significantly limit the effectiveness of peripheral nerve regeneration and can lead to suboptimal clinical outcomes. Additionally, axonal regeneration is very inefficient and many of the axonal sprouts that are sent out never end up reaching their target. Another major setback is that even when the axon is able to reach its target, the myelination and ability of the nerve to fire correctly remains impaired, even long after the connection has stabilized (*10, 150*).

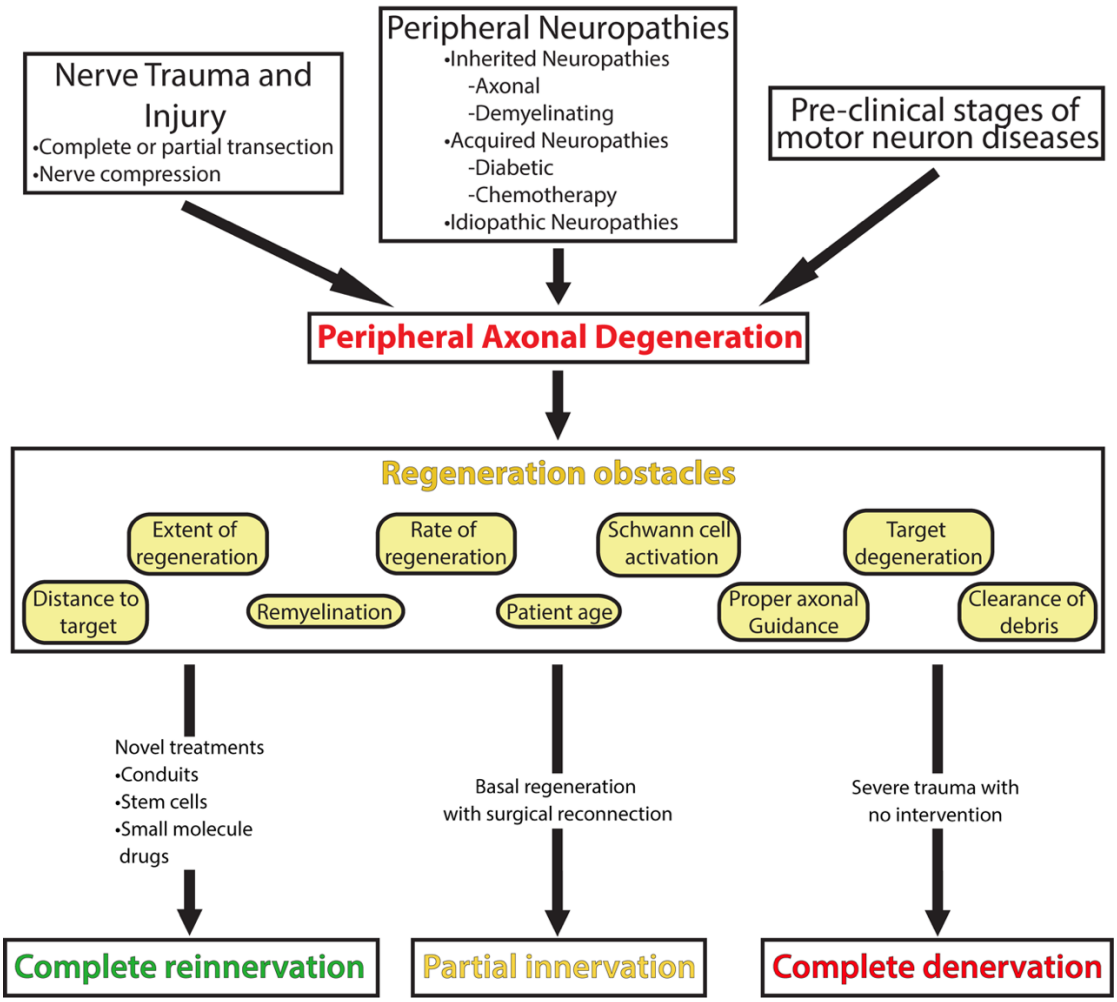

Fig. 4. Problems in peripheral nerve regeneration.

There are many ways axons of the PNS can get injured either by nerve trauma, various peripheral neuropathies, or the early stages of motor neuron diseases. The injuries that arise from these events leads to axonal damage and denervation. In order for regeneration to occur, many obstacles, which are detailed in the regeneration obstacles box, need to be overcome. With the current intervention of surgical repair and the basal state of regeneration, the extent of reinnervation is typically only partially complete. With the development of novel treatments, we hope that complete reinnervation can be achieved. In cases of severe trauma with no surgical intervention, there is a risk of no reinnervation occurring, leaving the target organ completely denervated.

Peripheral nerve regeneration is further impaired by age and disease

These issues are even greater when the repair process itself becomes reduced, either due to aging, neurodegenerative disorders, or peripheral neuropathies (*87, 88, 122, 151*). In terms of aging, the rate and number of regenerating axons in elderly patients and animals are significantly reduced following a peripheral nerve injury (*151*). All of the key steps in peripheral nerve regeneration are reduced in aged rats. The peripheral nerves do not sprout as extensively, myelin debris clearance is delayed and impaired, and Schwann cell activation is inhibited (*14, 87, 151*). In cases of peripheral neuropathies or motor neuron diseases with distal axonal degeneration, such as the three diseases discussed previously, the rate of axonal regeneration may be overwhelmed by the rate of axonal degeneration occurring via the disease process (*86-88, 122, 135*). This is further complicated by subsequent neuronal cell loss in ALS which reduces the number of available axons for regenerating. This then increases the burden on the surviving axons to generate axonal sprouts and increases their motor unit size.

Therapeutic options for enhancing axonal regeneration are absent

Despite insufficient repair following axonal insult to the peripheral nervous system, either due to trauma or disease, there are currently no therapeutics available to enhance regeneration. As it stands right now, the best available treatment is the surgical reattachment of the distal portion of the nerve to the proximal stump in hopes that the proximal stump can sprout into the vacated Schwann cell tubes to accelerate repair (*29*). Even with the best surgical techniques however, this still leaves many without full recovery. Current research to enhance regeneration focuses on developing nerve conduits

which improve the connection between the proximal and distal stumps (*152*). Unfortunately, this approach doesn't aid those who suffer from severely pinched nerves or those suffering from neurodegenerative diseases, nor does it address the slow rate of axonal growth. Other potential therapeutics have looked into electrically stimulating the nerves to enhance regeneration. Some research has shown that when the proximal portion of an injured nerve is stimulated, axonal growth is enhanced (*13, 153*). However, this strategy has the potential to be an invasive and painful experience for the patient. What is truly needed is a minimally invasive therapy, such as a small molecule drug, that can be administered following successful reattachment which can accelerate the growth rate.

Beta secretase as a novel regulator of peripheral nerve regeneration

Reduced BACE1 activity levels improve peripheral nerve regeneration

Our lab has identified a novel role for BACE1 in modulating peripheral nerve regeneration following injury. Based on our data, we have determined that BACE1 activity levels have a negative effect on the efficacy of peripheral nerve regeneration. We observed a significant improvement in peripheral nerve regeneration following a sciatic nerve crush in BACE1 KO mice when compared with their WT littermates (*25*). The nerves in the KO mice were able to grow further, on top of having a greater number of regenerated axons compared with WT mice. There was also an improvement in muscle reinnervation in the BACE1 KO mice. These experiments provided interesting data highlighting a novel role for BACE1 in regulating peripheral nerve regeneration. However, these experiments did not narrow down where BACE1 was exerting its effects. The enhanced regeneration could be due to increasing the outgrowth of the axons

themselves, enhanced macrophage recruitment and activity, or even enhanced Schwann cell activation and axonal support.

While BACE1 activity's influence over the neuronal component of peripheral nerve regeneration is an interesting piece of the puzzle, we also need to investigate the role that macrophage and Schwann cell BACE1 activity levels play in enhancing regeneration. Our study using global BACE1 KO mice indicated that macrophages are not only recruited in greater numbers, but also engulf more myelin debris following a peripheral nerve injury (*25*). We also observed an increased expression of tumor necrosis factor receptor 1 (TNFR1), a macrophage signaling receptor, in the distal stump of the injured nerve in both BACE1 KO mice and WT mice treated with a BACE1 inhibitor (*24*). While this data indicates that macrophages are influenced with reduced BACE1 activity, it does not determine whether this is due to BACE1 activity within the macrophages themselves or in the cells that the macrophages interact with. Data investigating how BACE1 activity levels influence the initial activation of Schwann cells following peripheral nerve injuries has not yet been studied. However, there is evidence which indicates that BACE1 activity is involved in peripheral nerve remyelination following axonal outgrowth and is important for proper remyelination to occur (*54, 154*). More studies need to be conducted investigating the role of BACE1 activity solely in the neurons, Schwann cells, and macrophages.

BACE1 substrates themselves influence axonal regeneration

In addition to our own data, there has been some evidence that some of the substrates of BACE1 are also involved in regulating peripheral nerve regeneration. A few

studies have found that the processing of APP itself has an effect on neurite outgrowth. Knocking out APP in cultured neurons has led to enhanced neurite outgrowth (*155, 156*), while soluble APPβ has been shown to have an inhibiting effect on neurite outgrowth (*157*). While interesting, the effects APP processing has on peripheral nerve regeneration has been inconclusive thus far. The processing of another BACE1 substrate, NCAM, has also been shown to have an impact on neurite outgrowth and branching. The cleavage of NCAM leads to the shedding of an ectodomain and reduces neurite outgrowth, which can be rescued by preventing the release of the ectodomain (*158*). Additionally, the cleavage of CHL1 by BACE1 also impacts neurite outgrowth. When the release of CHL1's cleavage product is prevented, the growth cone no longer collapses and promotes neurite extension (*159*). Taken together with our own data, we hypothesize that BACE1 activity on its various substrates plays an important role in regulating peripheral nerve regeneration by potentially modulating the expression of various cell adhesion molecules (Figure 5).

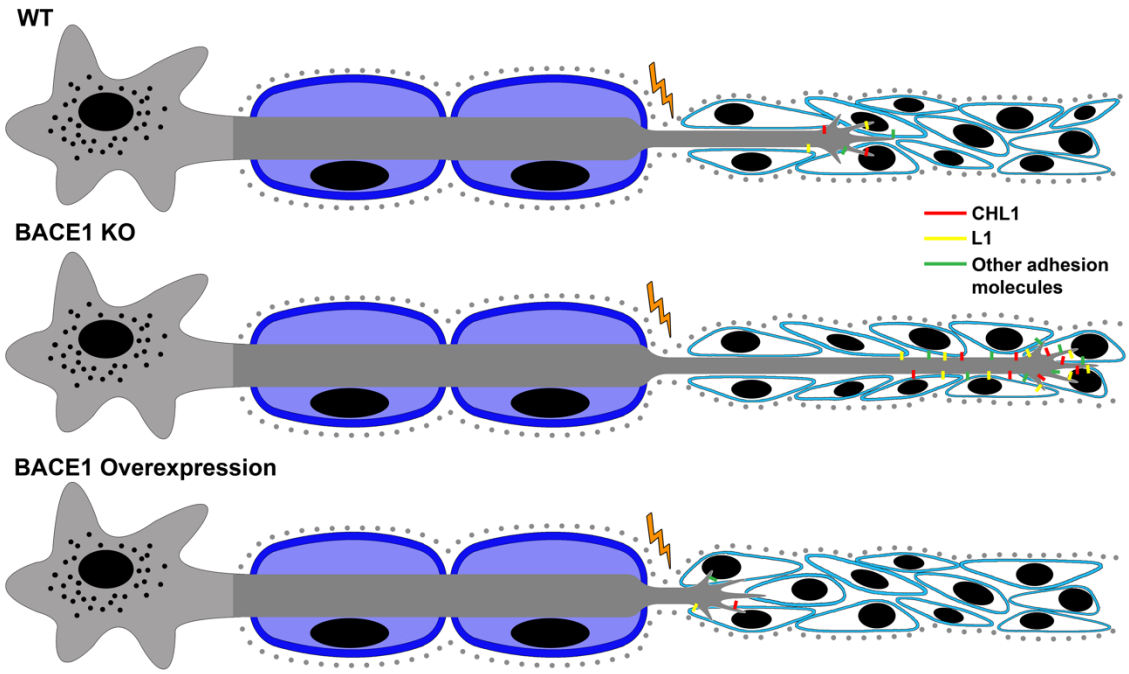

Fig. 5. Potential mechanism for how BACE1 activity levels regulate peripheral axon growth. Since adhesion molecules are essential for proper axonal outgrowth and interaction with Schwann cells (depicted in blue), I hypothesize that BACE1 regulates peripheral axonal outgrowth by modulating the cell surface expression levels of various adhesion molecules, such as CHL1 and L1. In WT mice, adhesion molecules are moderately expressed on the cell surface leading to basal regeneration rates. With reduced BACE1 expression, as in KO mice, adhesion molecules aren't cleaved and therefore remain at the cell surface in greater numbers, enhancing interactions with Schwann cells and leading to increased growth. When BACE1 is overexpressed, there is more cleavage causing fewer adhesion molecules to be expressed on the cell surface, impairing Schwann cell interactions and reducing axonal growth.

Beta secretase inhibitors as a potential therapeutic strategy for enhancing peripheral nerve regeneration

BACE1 inhibitor development

BACE1's important role as one of the two enzymes needed to generate Aβ plaques in AD has led to a robust interest in the development of BACE1 inhibitors in the hopes that reducing the Aβ burden may improve AD symptoms. Early efforts to develop a BACE1 inhibitor took advantage of a peptide molecule that was unable to be cleaved by BACE1, however, this molecule lacked the ability to cross the blood-brain-barrier and was not orally bioavailable (*160*). Due to this difficulty, researchers began to focus on developing small molecule inhibitors in the hopes that they would improve the desired pharmacological characteristics. Early generations of small molecule BACE1 inhibitors indeed had better cell membrane permeability and good target engagement, but unfortunately there were still issues with generating a high enough concentration in the brain, as well as some toxicity issues with retinal degeneration and abnormal liver biochemistry, which were thought to be related to off-target effects and not BACE1 inhibition itself (*160-163*). The most recent generation of BACE1 inhibitors are now able to enter the brain at high enough concentrations to achieve robust reductions in Aβ levels in animal models, are also orally bioavailable, and early phase I trials show no severe toxicity issues (*42, 45, 48, 160, 164*). Due to this vast improvement, many companies have begun clinical trials of their BACE1 inhibitors and we now have a large pool of data on safety profiles of various small molecule BACE1 inhibitors in humans.

BACE1 inhibitors developed for AD have good safety profiles

As mentioned earlier in this introduction, because BACE1 has a large role in generating Aβ plaques in AD, many pharmaceutical companies have made great efforts to develop small molecule BACE1 inhibitors. Early efforts were held back due a lack of small molecules that could penetrate the blood-brain-barrier as well as toxicity issues, such as the liver toxicity seen with the Eli Lilly BACE1 inhibitor LY2886721 during their phase 2 trials (*160*). This led many to speculate whether BACE1 inhibitors were a feasible target for AD. However, recent advances in the development of these drugs has shown more promise. Recently, Merck announced that their latest BACE1 inhibitor, verubecestat (MK-8931), was well tolerated at various doses in patients enrolled in their phase I clinical trial (*42*). Verubecestat also showed a robust decrease in CSF Aβ production, indicative of proper target engagement. In addition to verubecestat, AstraZeneca/Lilly also have a promising small molecule BACE1 inhibitor, AZD3293, currently in phase II/III clinical trials. This drug was also well tolerated in phase I trials and showed a marked decrease in CSF Aβ production (*48*).

Unfortunately, Merck recently stopped their mild/moderate Phase III trial for verubecestat due to a lack of significant clinical changes observed. Despite being a disappointing setback, this result was unsurprising to those in the field as Aβ levels tend to plateau and neuronal death is widespread by the time clinical symptoms begin to appear. While this is bad news for AD, all may not be lost for those who have sunk billions into developing BACE1 inhibitors. Since high BACE1 activity appears to have a negative impact on peripheral nerve regeneration, we hypothesize that BACE1 inhibitors may be a potential drug to fill the therapeutic void for enhancing peripheral nerve

regeneration. Indeed, when we administered an older BACE1 inhibitor, BACE1 inhibitor IV, for 7 days following a sciatic nerve crush, we observed an apparent increase in regenerated axons as well as enhanced axonal debris clearance (*25*). This is a promising start for determining whether BACE1 inhibitors may find a new life as peripheral nerve regeneration enhancers.

In addition to the generation of safe, well-tolerated BACE1 inhibitors, treating peripheral nerve injuries with small molecule inhibitors may not be impacted by the blood-brain barrier issues that hinders CNS drug development. Unlike the blood-brain barrier, the nerve-blood barrier is rather leaky and would most likely allow larger molecules through at lower concentrations (*165*). This may be beneficial and could potentially allow for the development of more potent BACE1 inhibitors that is unable to cross the blood-brain barrier, may be able to cross the nerve-blood barrier. Additionally, being able to get a high efficiency in nerves with a lower dose would also lower the risk of toxicity issues that has been seen with some BACE1 inhibitors at higher doses and would give a therapeutic advantage to treating peripheral nerve injuries with BACE1 inhibitors.

Potential issues surrounding the use of BACE1 inhibitors following acute peripheral nerve injuries

While utilizing BACE1 inhibitors as a means to enhance regeneration following a peripheral nerve injury has promise, due to BACE1's promiscuous nature, potential issues of inhibition need to be closely monitored. This especially concerning as the sustained plasma levels with the newer generation of BACE1 inhibitors are quite robust

(*42, 48*) and may lead to unintended side effects where chronic BACE1 inhibition in other tissues may alter the processing of any of its other substrates. Firstly, because BACE1's cleavage of NRG1 type III is involved in the myelination of peripheral nerves, it is important to think about how this may negatively impact peripheral nerve remyelination as well as the existing myelin on uninjured axons. In the case of uninjured nerves, their myelination does not appear to be altered with BACE1 inhibition as we have seen in our own lab (unpublished data) as well as by other groups (*46*). For regenerating axons, remyelination would most likely be reduced for as long as BACE1 activity is being inhibited. This hypomyelination would impact the ability of the axons to fire in a coherent manner and may have a negative impact on the effectiveness of the regenerated axons to engage with their targets correctly. How large this deficit would be is a factor that needs to be studied with regards to administering BACE1 inhibitors following a peripheral nerve injury. While this deficit could be similar to the hypo-remyelination observed in BACE1 KO mice (*54, 154*), it may be ameliorated by only administering the BACE1 inhibitors for a short time period, a couple of weeks at most, immediately following the injury. This dosage schedule would induce increased axonal outgrowth during the early stages of repair and once the inhibition of BACE1 is abolished, remyelination would be allowed to occur in a normal capacity and would hopefully allow for proper axonal firing to occur. Additionally, there is some evidence that BACE1 cleavage of NRG1 type III is not essential for the induction of myelination (*55*).

Another issue that could potentially arise when using BACE1 inhibitors is that there may be possible defects with the muscle spindles. In the absence of BACE1, mice have defects in muscle spindle formation and maturation (*166*). Additionally, when

BACE1 was inhibited in adult mice, Cheret et al. (*166*) found that muscle spindle maintenance was impaired, as was motor coordination. While this finding may be troubling for the use of BACE1 inhibitors, phase I clinical trial reports about adverse responses to BACE1 administration in human patients did not report any issues with motor coordination, even at the highest doses administered (*42*). This difference in adverse effects may be a result of species specific effects of BACE1 inhibition as a difference in behavioral studies and post-natal mortality were reported between knockout mice and rats (*167*). The lack of issues seen in human patients following BACE1 inhibitor treatment lead us to believe that many of the issues surrounding possible pitfalls associated with BACE1 inhibition may not be as severe as originally thought.

In addition to issues with inhibiting BACE1 itself, it is also possible that these compounds may inhibit other aspartyl proteases leading to off-target effects. Since BACE2's structure is extremely similar to BACE1, the BACE1 inhibitors currently in clinical trials usually have as strong of an affinity for BACE2 as they do BACE1 (*164, 168*). Fortunately, when these drugs were reported on following phase I clinical trials no significant adverse effects were reported in human patients (*42, 48*). Another concern is that these drugs may inhibit Cathepsin D, another aspartyl protease responsible for degradation and activation of various proteins in the lysozyme. Despite the similarities between BACE1 and Cathepsin D, the current generation of BACE1 inhibitors are not selective for Cathepsin D (*164, 168*).

BACE1 inhibitor treatment may avoid axonal guidance issues in adults

BACE1 inhibitors being used to enhance peripheral nerve regeneration may also be able to overcome many of the axonal guidance issues that have been identified. Many of these studies were performed in null mice, either of BACE1 or its substrates, and using an inhibitor that would not completely abolish BACE1 activity levels may lead to a less severe phenotype with regards to axonal guidance. Additionally, these studies were also focusing on how a loss of BACE1, or its substrates affects axonal guidance in the developing CNS. Due to the wide variety of BACE1 substrates, it may be possible that the substrates involved in impaired axonal guidance in the CNS may not be as important for similar functions in the peripheral nervous system. An alternative hypothesis is that these substrates may interact with different molecules and cells in the periphery which lead to a different phenotype. This makes sense, as axons in the CNS interact with oligodendrocytes and astrocytes while the PNS axons interact with Schwann cells. Indeed, our lab has not noticed any morphological differences in how NMJs are innervated in uninjured BACE1 KO mice. Another major issue to note with these studies is that many of the null studies may be related to developmental defects, as the mice are lacking BACE1 and its substrates from the beginning. In the developing mouse, many neuronal connections are being made, both in the CNS and PNS. Due to this high activity, a lack of BACE1 early on may be more detrimental than later in development. Using BACE1 inhibitors for the treatment of peripheral nerve injuries would occur after the bulk of the synaptic connections had been formed and would not effect a majority of the synapses formed in the adult. In addition to the adult nervous system being less plastic than a developing nervous system, depending on the type of neurodegeneration,

there would not need to be a very prolonged treatment and would allow proper guidance to occur in normal pruning. Both of these factors could potentially avoid any of the guidance issues observed in the BACE1 KO mice and would support the use of BACE1 inhibitors in adults.

BACE1 inhibitors may be useful in early stage peripheral neurodegenerative diseases

We also hypothesize that in addition to peripheral nerve injuries, these inhibitors may be helpful in the early stages of peripheral neurodegenerative disorders. In the earliest stages of motor neuron disease, axonal degeneration typically precedes neuronal cell body death (*88, 131-135*). The axons of these neurons also die back at different rates depending on their susceptibility to degeneration based on multiple factors such as fiber type, size, and length (*88, 134-137, 169*). We theorize that motor function, and therefore quality of life, may be prolonged in the early stages of these diseases if the surviving motor neurons could be encouraged to sprout and regrow in an attempt to reinnervate denervated muscle. It is true that even with a disease background, peripheral nerves do have the capacity to sprout, however limited it may be (*85, 87, 170, 171*). If the rate of axonal sprouting and outgrowth can be enhanced using a BACE1 inhibitor, it may be able to keep up with the rate of degeneration for a time, especially in slowly progressing disorders.

Concluding remarks of the introduction

Our current understanding of how BACE1 is involved in regulating axonal regeneration is still in its infancy. However, our lab has been able to identify an

interesting relationship between BACE1 activity levels and how effective axons are at regenerating following an acute nerve injury. Our own data has determined that reducing BACE1 activity levels improves axonal regeneration, but whether the inverse is true still remains to be understood. Additionally, we are still unclear as to which cells involved in peripheral nerve regeneration BACE1 activity levels are working on. Despite these gaps in knowledge, our original finding has interesting clinical implications. If the administration of BACE1 inhibitors following an acute nerve injury can help to increase the rate and efficacy of peripheral nerve regeneration, it would fill a much-needed therapeutic gap for acute nerve injuries. Additionally, BACE1 inhibitors may also be useful in the early stages of peripheral neuropathies as a means for enhancing the rate of axonal regeneration, which may be able to compensate for the progressive loss of axons and lead to prolonged function.

This dissertation sets out to answer 3 major questions related to how BACE1 activity levels influence peripheral nerve regeneration and how we can utilize this knowledge to develop potential therapeutics:

1) Does BACE1 overexpression, in neurons, lead to impaired axonal regeneration?

2) Can BACE1 inhibitors enhance peripheral nerve regeneration and axonal sprouting following acute nerve injuries?

3) Are BACE1 inhibitors able to improve early regeneration in the $SOD1^{G93A}$ mouse model of ALS?

Chapter 2: Overexpression of BACE1 leads to reduced peripheral nerve regeneration after acute nerve injury

Introduction to chapter 2

Before exploring how BACE1 activity levels can be manipulated pharmacologically as a potential therapeutic, we first wanted to further characterize how BACE1 activity is able to regulate peripheral nerve regeneration in response to a nerve injury. Our original data determined that a complete loss of BACE1 in all the components of the peripheral nerve regeneration machinery, namely the neurons, Schwann cells, and macrophages, led to an increase in peripheral nerve regeneration and enhanced axonal debris clearance and phagocytosis by macrophages (*25, 172*). While a promising first step, these studies do not address the question of whether the reverse is true. It also does not provide any information on the individual roles of BACE1 activity in the neurons, Schwann cells, and macrophages. In order to tackle some of these missing links, we carried out sciatic nerve crush experiments in mice that were engineered to overexpress human BACE1 under the neuronal specific Thy1.2 promoter generated from a modified Thy1 expression cassette which is expressed only in neurons and not in non-neuronal cells, such as the Schwann cells (*44, 173*). These mice were originally designed to study high BACE1 activity levels in AD and therefore there is very little information about potential phenotypes beyond enhanced APP processing and how it leads to altered Aβ deposition and neurodegeneration in the brain (*43, 44*).

In this chapter, we set out to characterize the normal peripheral axonal morphology in these mice in order to use them to study neuronal specific overexpression

of BACE1 and how it affects peripheral nerve regeneration following axonal injury. We then determined how these nerves degenerated and regenerated following a sciatic nerve crush injury and whether our initial hypothesis that BACE1 activity levels inversely influence peripheral nerve regeneration holds true with increased BACE1 activity levels.

Results

The following data was published in C. Tallon, E. Rockenstein, E. Masliah, M. H. Farah, Increased BACE1 activity inhibits peripheral nerve regeneration after injury. Neurobiol Dis 106, 147-157 (2017).

Overexpression of BACE1 does not alter uninjured axon morphology or physiology

Previous studies suggest that BACE1 activity levels influence the extent of peripheral nerve regeneration (*25, 26, 172*). A testable prediction of this postulate is that an increased expression of BACE1 would be expected to impede nerve regeneration. In order to investigate whether increased BACE1 expression reduces nerve regeneration, We used transgenic (Tg) mice where human BACE1 was driven by the Thy-1 promoter and has been shown to express BACE1 in neurons (*44*). These BACE1 Tg mice have been investigated in the field of Alzheimer's disease, but not in peripheral nerve studies (*44, 174*). Therefore, we first evaluated the sciatic nerves of the BACE1 Tg mice before injury and observed a marked increase in BACE1 expression in both the sciatic nerve and brain of the BACE1 Tg mice (Fig. 6A; WT $n = 5$; Tg $n = 5$). Morphologically, the sciatic nerves of both WT (Fig. 6B) and BACE1 Tg (Fig. 6C) mice were indistinguishable from one another, indicating that BACE1 overexpression did not alter the normal morphology

of axons in the sciatic nerve. We did not observe any difference in the amplitude of the CMAP recorded in the muscles of the footpad between WT (n = 15) or Tg (n = 19) mice with either ankle stimulation (WT = 19.22 ± 2.18 ms, Tg = 19.38 ± 1.55 ms; p = 0.951) or hip stimulation (WT = 13.42 ± 1.91 ms, Tg = 13.73 ± 1.04 ms; p = 0.883) (Fig. 6D). There was also no latency difference between WT or Tg mice with ankle stimulation (WT = 0.717 ± 0.103 ms, Tg = 0.886 ± 0.111 ms; p = 0.414) or hip stimulation (WT = 1.454 ± 0.128 ms, Tg = 1.554 ± 0.0982 ms; p = 0.534) (Fig. 6E). Both of these electrophysiological parameters support there being no difference in axon number and extent of myelination. Taken together, these data indicate that BACE1 overexpression does not affect the normal morphology or physiology of the uninjured sciatic nerve, allowing us to investigate the effect of BACE1 overexpression on nerve regeneration in response to injury.

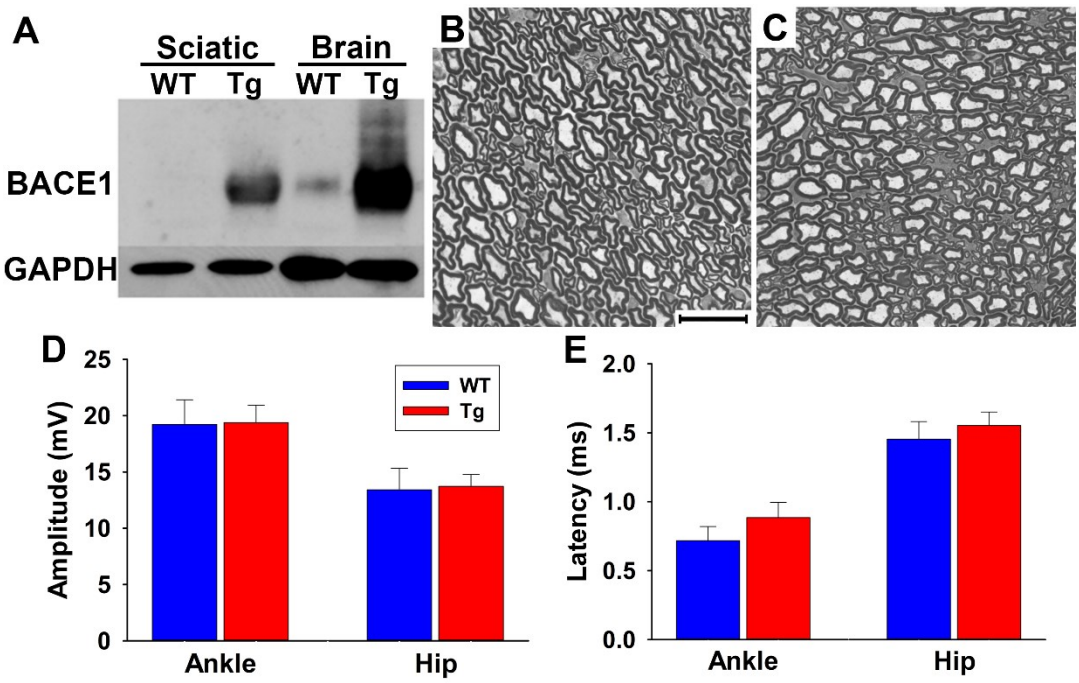

Fig. 6. BACE1 overexpression does not affect nerve morphology and electrophysiology. A) Western blot showing BACE1 overexpression in both the sciatic nerve and the brain of transgenic mice (Tg). B–C) Cross section of a WT (B) and Tg (C) sciatic nerve stained with toluidine blue. Both mice have normal axonal myelination. Scale bar represents 20 μm. D) The amplitude of the CMAP recorded at the foot was not altered between the WT (blue, n = 15) and Tg (red, n = 19) mice when the uncrushed sciatic nerve was stimulated at either the hip or the ankle. E) The latency of the CMAP was not altered in the Tg mice with either stimulation at the hip or ankle (WT n = 15, Tg n = 19). Bars represent mean ± standard error. *C. Tallon, E. Rockenstein, E. Masliah, M. H. Farah, Increased BACE1 activity inhibits peripheral nerve regeneration after injury. Neurobiol Dis 106, 147-157 (2017).*

BACE1 overexpression does not alter axonal degeneration and debris clearance after injury

While uninjured WT and BACE1 Tg nerves are electrophysiologically and morphologically similar, it is possible that increased neuronal expression of BACE1 might affect axonal degeneration and debris clearance following nerve injury since BACE1 KO mice have enhanced debris clearance and macrophage recruitment. We therefore examined myelin debris and macrophage recruitment in BACE1 Tg and WT mice after injury. We performed a complete sciatic nerve transection in WT ($n = 4$) and Tg ($n = 3$) littermates, collected the distal nerve segments and stained for myelin basic protein (MBP) and CD68, a macrophage marker. There was no observable difference between the amount of myelin debris nor the distribution of the debris (Fig. 7 C and D). There was also no observable difference between the number of macrophages present in WT or Tg mice, either before or after injury (Fig. 7 E–H). Quantifying the number of macrophages present after injury confirmed that there was no significant difference in the density of macrophages between the WT and Tg mice (Fig. 7 I, WT = 107,612 ± 16,371 macrophages/mm3 and Tg = 96,218 ± 2287 macrophages/mm3, $p = 0.529$). These results indicate that exclusively overexpressing BACE1 in neurons does not alter axonal degeneration nor does it affect the recruitment of macrophages.

Fig. 7. BACE1 overexpression does not alter degeneration 5 days after complete sciatic nerve transection.

A–D) Longitudinal sections of sciatic nerves stained for myelin basic protein. Scale bar represents 50 μm. A–B) Uninjured nerves from WT (A) and Tg (B) mice showing similar levels of myelination. C-D) Injured nerves from WT (C) and Tg (D) mice where the extent of degeneration was indistinguishable between genotypes. E-H) Longitudinal sections of sciatic nerves stained for macrophages with CD68. Scale bar represents 20 μm. E–F) Uninjured nerves from WT (E) and Tg (F) mice with very few macrophages present. G–H) Representative images of comparable macrophage influx between WT (G) and Tg (H) mice. I) Quantification of the volumetric density of macrophages in WT (n = 4) and Tg (n = 3) distal sciatic nerve stumps with no difference between WT and overexpressing mice. Bars represent mean ± standard error. *C. Tallon, E. Rockenstein, E. Masliah, M. H. Farah, Increased BACE1 activity inhibits peripheral nerve regeneration after injury. Neurobiol Dis 106, 147-157 (2017).*

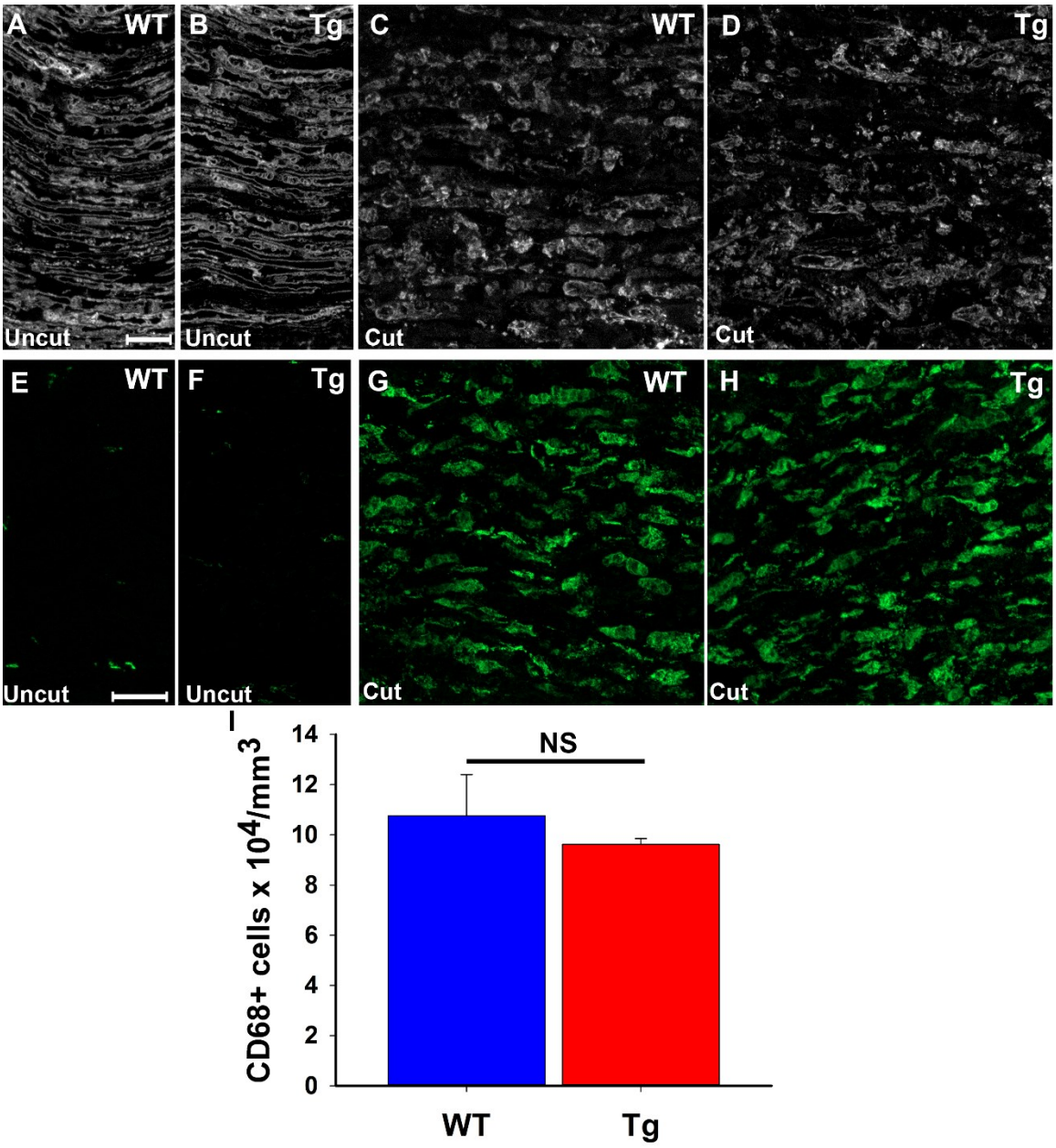

The data presented in Figs. 6 and 7 collectively indicated that BACE1 overexpression does not affect the normal morphology or physiology of the uninjured sciatic nerve nor does the nerve degeneration profile differ between BACE1 Tg and WT injured nerves. Thus, we proceeded to investigate the effect of neuronal BACE1 overexpression on nerve regeneration.

BACE1 overexpression impairs axonal regeneration as early as 3 days after injury

We first determined whether the initial outgrowth of regenerating axons was altered in the injured nerves of BACE1 Tg mice. We stained the nerves of 3 WT and 3 BACE1 Tg mice for GAP43 expression, a regeneration associated gene, and measured the extent of axonal outgrowth 3 days after a sciatic nerve crush. In uninjured nerves, no detectable GAP43 staining was present under our staining protocol (Figs. 8A and B). However, in the injured nerves, high levels of GAP43 staining was present near the crush site and extended distally, indicating the beginning of axonal regeneration (Fig. 8C and D). We measured the level of axonal outgrowth by measuring the length of the longest GAP43 positive axon from the crush site and found that there was a significant reduction in the length of the longest axon in the BACE1 Tg mice (Fig. 8 C–E). On average, WT axons regenerated 5.17 ± 0.368 mm while the transgenic mice only grew 2.86 ± 0.262 mm ($p = 0.00695$) 3 days after being crushed. We also observed a marked reduction in another early axonal regeneration marker, SCG10. Transgenic mice had a drastic reduction in staining while the WT mice had extensive staining distal to the crush site (Fig. 9A and B). We therefore conclude that overexpressing BACE1 reduces the initial early outgrowth of regenerating axons.

Fig. 8. BACE1 overexpressing mice have reduced early regeneration 3 days after a sciatic nerve crush.

A–B) Longitudinal sections from uninjured sciatic nerves of WT (A) and Tg (B) mice with very little GAP43 staining. C–D) Representative longitudinal sections from WT (C) and Tg (D) injured sciatic nerves. The crush site was located at the left of the image (white arrow) and the red arrows indicate the longest GAP43 positive axons. WT mice have more extensive GAP43 staining and longer axons when compared to Tg littermates. E) Quantification of the length of the longest GAP43 positive axons in WT (n = 3) and Tg (n = 3) mice. Tg mice have a 40% reduction in the length of the longest axon compared with WT littermates. * indicates $p < 0.05$. Bars represent mean ± standard error. Scale bar represents 500 μm. *C. Tallon, E. Rockenstein, E. Masliah, M. H. Farah, Increased BACE1 activity inhibits peripheral nerve regeneration after injury. Neurobiol Dis 106, 147-157 (2017).*

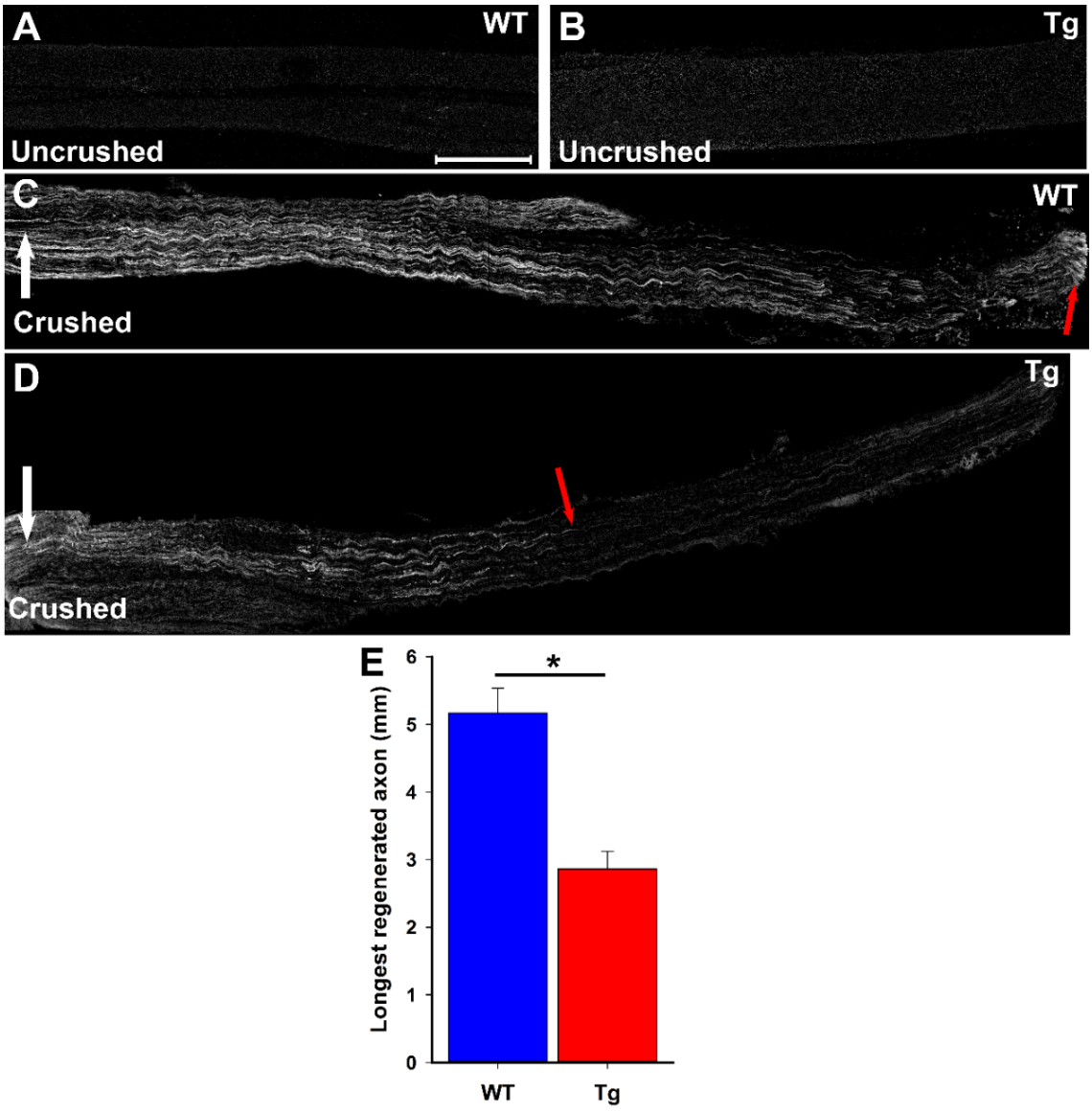
A
WT
Uncrushed
B
Tg
Uncrushed
C
WT
Crushed
D
Tg
Crushed
E
Longest regenerated axon (mm)
0
1
2
3
4
5
6
*
WT
Tg

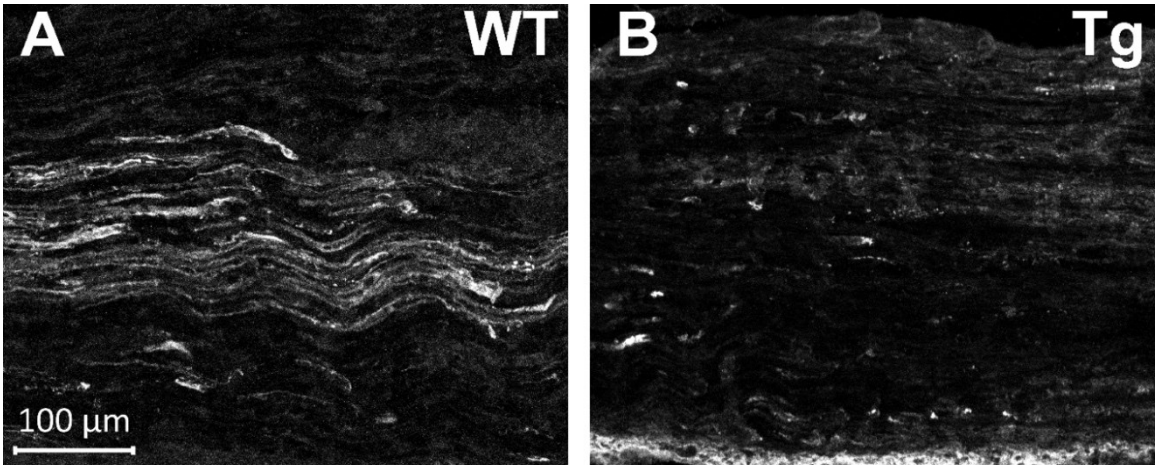

Fig. 9. Fewer axons extend distally from the crush site in BACE1 transgenic mice 3 days following injury.

A) Representative longitudinal section of a WT sciatic nerve stained with SCG10 antibody with extensive neurite outgrowth. B) Representative longitudinal section of a BACE1 transgenic sciatic nerve stained with SCG10 antibody where there are only a few axons growing out from the crush site. In both images the crush site is to the left. *C. Tallon, E. Rockenstein, E. Masliah, M. H. Farah, Increased BACE1 activity inhibits peripheral nerve regeneration after injury. Neurobiol Dis 106, 147-157 (2017).*

Overexpressing BACE1 leads to impaired axonal regeneration 10 days after injury

We next asked whether regeneration is impaired in BACE1 Tg mice at later time points. We analyzed distal segments of the sciatic nerves for axonal regeneration from 6 WT and 6 Tg mice 10 days after being crushed. BACE1 Tg crushed nerves had visually fewer regenerated myelinated axons compared to controls (Fig. 10A–D). The number of regenerated axons in BACE1 Tg mice was significantly decreased 10 days after performing a sciatic nerve crush when compared with WT mice (Fig. 10E; $p = 0.0035$). WT mice had on average 1139.67 ± 95.15 regenerated axons while the BACE1 Tg

littermates had only 653.00 ± 86.15 regenerated axons. We also observed a drastic difference in neurofilament (NF) staining of sciatic nerves cross-sectioned 15 days after performing a sciatic nerve crush, when most of the debris had been cleared. WT sciatic nerves had a lot of characteristic punctate axonal staining (Fig. 11A), while Tg mice had almost no punctate NF staining (Fig. 11B). Based on these findings, we conclude that overexpressing BACE1 leads to a reduction in the ability of axons to regenerate.

Fig. 10. BACE1 overexpression hinders axonal regeneration 10 days after sciatic nerve crush.

A-B) Representative cross-section images of sciatic nerves from WT (A) and Tg (B) mice 10 days post sciatic nerve crush illustrating a greater number of myelinated axons in the WT mice. The red arrows indicate regenerated axons. The yellow arrowheads indicate degenerated axons. Scale bar represents 20 μm. C–D) Representative cross-section EM images from WT (C) and Tg (D) mice again showing greater regenerated axons in the WT mouse. Scale bar represents 2 μm. E) Quantification of the number of regenerated axons in WT (n = 6) and Tg (n = 6) mice. The Tg mice show a drastically reduced number of regenerated axons 10 days after sciatic nerve crush. Bars represent the mean ± standard error. * indicates $p < 0.05$. *C. Tallon, E. Rockenstein, E. Masliah, M. H. Farah, Increased BACE1 activity inhibits peripheral nerve regeneration after injury. Neurobiol Dis 106, 147-157 (2017).*

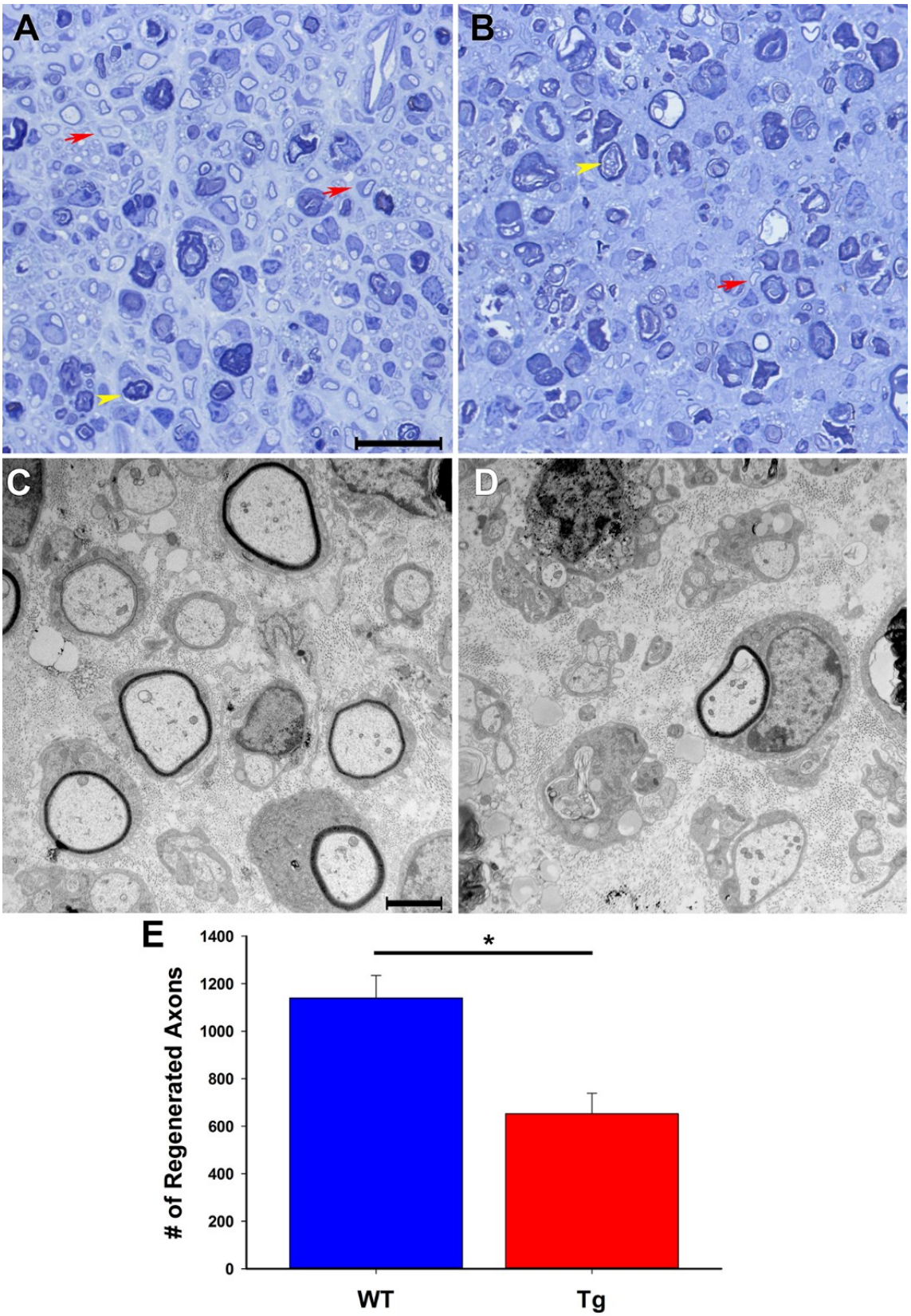
A
B
C
D
E
1400
1200
1000
800
600
400
200
0
# of Regenerated Axons
*
WT
Tg

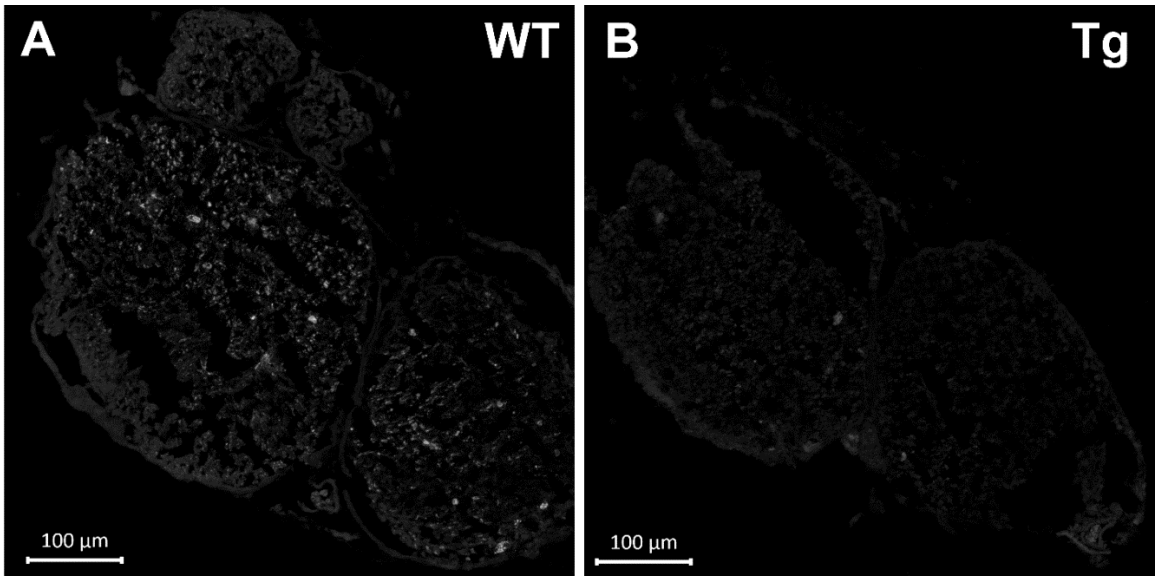

Fig. 11. Neurofilament staining with BACE1 overexpression is reduced 15 days following a sciatic nerve crush.

A) Cross-section of a WT sciatic nerve with small, punctate NF staining indicating regenerated axons have begun to repopulate the sciatic nerve. B) Cross-section of a BACE1 transgenic sciatic nerve with almost no punctate NF staining indicating very little regeneration has occurred. *C. Tallon, E. Rockenstein, E. Masliah, M. H. Farah, Increased BACE1 activity inhibits peripheral nerve regeneration after injury. Neurobiol Dis 106, 147-157 (2017).*

BACE1 overexpression reduces reinnervation of the gastrocnemius muscle 15 days after injury

We next determined whether the impaired regeneration seen in the BACE1 Tg crushed sciatic nerves was reflected by the extent of innervation of the gastrocnemius muscle. We collected the gastrocnemius muscles from 3 WT and 4 Tg mice 15 days after performing a sciatic nerve crush. Both a partial and complete overlap of the NF/SV2 staining with the post-synaptic α-bungarotoxin (α-BTX) were scored as innervated while

no overlap was scored as denervated. While the uninjured side showed no difference in innervation between WT (Fig. 12A) or Tg (Fig. 12B) mice, the injured Tg gastrocnemius muscles (Fig. 12D) had a reduced number of innervated NMJs when compared with their WT littermates (Fig. 12C). The quantification of the percentage of innervated NMJs is shown in Fig. 12E where BACE1 Tg mice showed 45.3 ± 7.6% innervation (n = 300 NMJs), while the WT littermates had 67.8 ± 2.8% of their NMJs innervated (n = 239 NMJs) (p = 0.0491). Thus, impaired axonal regeneration in the BACE1 Tg mice led to reduced reinnervation of the gastrocnemius muscle 15 days after injury.

Fig. 12. BACE1 overexpression reduces NMJ reinnervation in the gastrocnemius muscle 15 days after sciatic nerve crush.

A–D) Sectioned gastrocnemius muscles stained with neurofilament and SV2 (both green) as well as α-BTX (red) to identify innervated and denervated NMJs. Scale bar represents 100 μm. A–B) Representative images of gastrocnemius muscles from uninjured sciatic nerves of both WT (A) and Tg (B) mice with complete NMJ innervation. C–D) Representative images from injured sciatic nerve gastrocnemius muscles of WT (C) and Tg (D) mice. Tg mice have fewer innervated NMJs than WT littermates as illustrated by the lack of red and green staining overlap. E) Quantification of the percent of innervated NMJs in the gastrocnemius muscle of both the WT (n = 3) and Tg (n = 4) mice. 15 days after crushing the sciatic nerve, the WT mice had a significantly higher number of innervated NMJs. Numbers in parenthesis indicate the total number of NMJs counted. Bars represent the mean ± standard error. * indicates $p < 0.05$. *C. Tallon, E. Rockenstein, E. Masliah, M. H. Farah, Increased BACE1 activity inhibits peripheral nerve regeneration after injury. Neurobiol Dis 106, 147-157 (2017).*

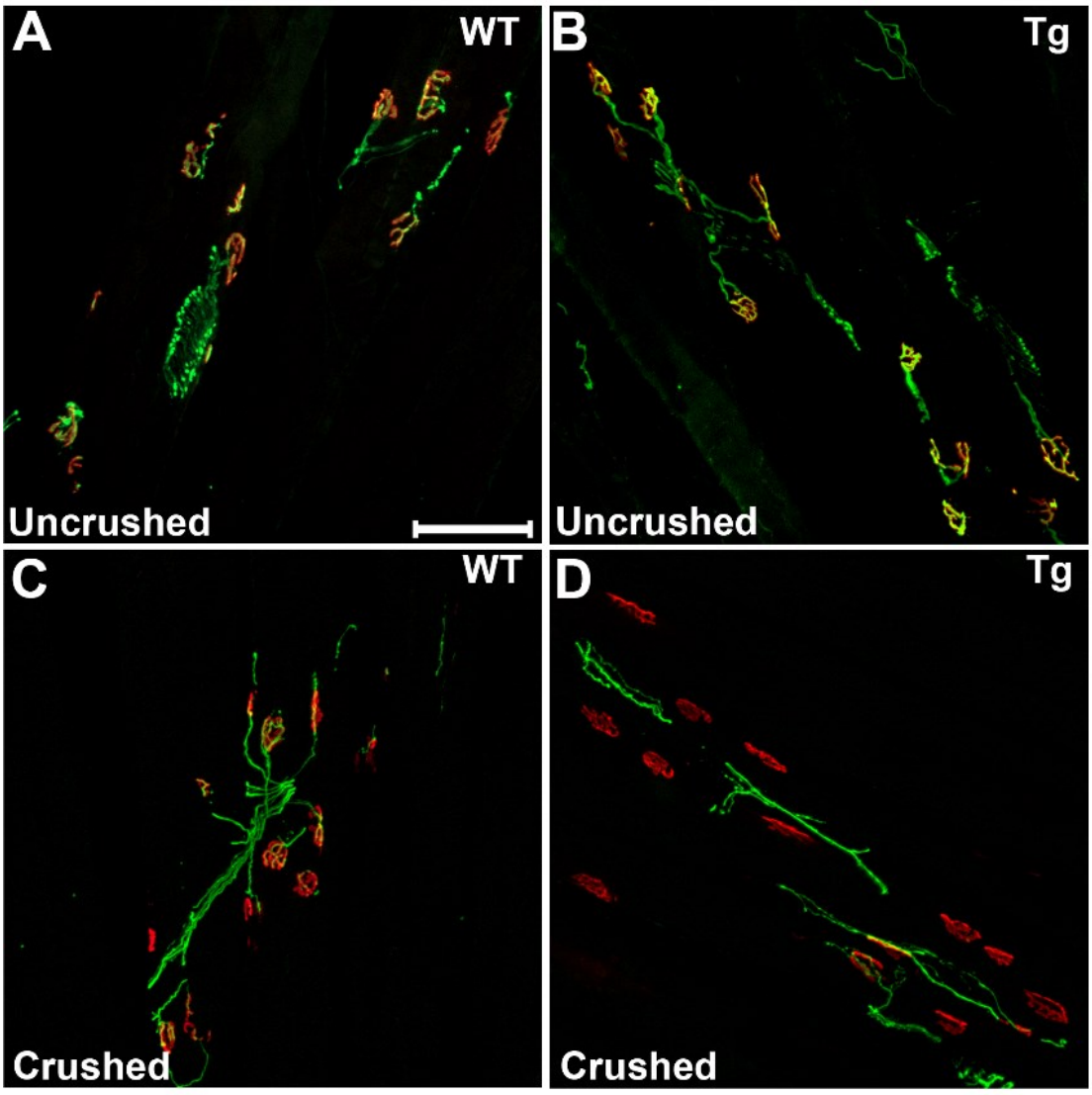
A
WT
Uncrushed
B
Tg
Uncrushed
C
WT
Crushed
D
Tg
Crushed

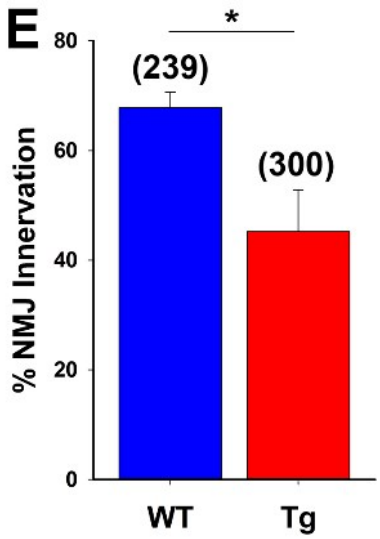
E
*
(239)
(300)
% NMJ Innervation
80
60
40
20
0
WT
Tg

Overexpression of BACE1 causes a delay in the long-term recovery of the CMAP

After establishing that BACE1 overexpression led to a deficit in axonal regeneration, as well as NMJ reinnervation, we determined whether there was a functional difference in the repair process between WT and Tg littermates. In order to do this, we recorded the CMAP in the muscles of the footpad at 2, 4, 6, and 8 weeks after injury as outlined in Fig. 13A. The sciatic nerve was stimulated by a short electrical pulse, at either the hip or ankle, on the same side as the injury. The recording electrode was placed in the muscles of the footpad. At the ankle stimulation site, we recorded from 6 WT and 11 Tg mice at the 2, 4, and 6-week time points. At 8 weeks, 15 WT and 19 Tg mice were used. Representative traces of the CMAPs recorded at the ankle for each time point over the 8 weeks are shown in Fig. 13B (WT) and 13C (Tg). Figs. 13D–E show the quantifications of the CMAP amplitudes at the ankle (Fig. 13D) and hip (Fig. 13E) stimulation sites over an 8-week period of recovery after a sciatic nerve crush. At our earliest time point of 2 weeks post-crush, the amplitudes of the CMAPs for both the WT and Tg mice were negligible when stimulated at the ankle (WT mean = 0.0043 ± 0.0043; Tg mean = 0.0059 ± 0.0040; $p = 1$). The same negligible amplitudes were seen in both the WT and Tg mice when stimulated at the hip (WT mean = 0.0093 ± 0.0032; Tg mean = 0.015 ± 0.0045; $p = 0.319$). By 4 weeks, WT mice had a significant improvement in the CMAP amplitudes when compared with their Tg littermates at both the ankle stimulation site (WT = 8.14 ± 0.67; Tg = 0.507 ± 0.075; $p = 0.001$) and hip stimulation site (WT = 2.74 ± 0.55; Tg = 0.50 ± 0.051; $p < 0.001$). Again, at 6 weeks, the Tg mice had amplitudes that were significantly lower than their WT littermates at both the ankle (WT = 13.5 ± 1.105; Tg = 3.84 ± 0.63; p = 5.99E-7) and hip (WT = 5.817 ± 1.06;

Tg = 1.598 ± 0.207; $p < 0.001$) stimulation sites. It is only at 8 weeks that the Tg littermates began to catch up with the WT mice. At the ankle stimulation site, while the WT mice were still higher, the difference was no longer statistically significant (WT = 11.977 ± 1.132; Tg = 9.443 ± 1.073; $p = 0.063$). At the hip stimulation site, the Tg amplitudes were closer to the WT values, but they were still significantly lower (WT = 8.005 ± 1.011; Tg = 5.412 ± 0.720; $p = 0.024$). This data strongly indicates that BACE1 overexpression is able to greatly delay the repair process of sciatic nerves after a nerve crush injury. While both WT and BACE1 Tg mice showed little improvement at 2 weeks, the CMAP amplitudes in WT mice were consistently higher than their Tg littermates at both the ankle and hip stimulation sites. Even at 8 weeks, the BACE1 Tg mice were worse off than the WT mice, indicating that this impaired regeneration is in effect throughout the repair process.

Fig. 13. BACE1 overexpression leads to delayed functional recovery after a sciatic nerve crush.

A) Schematic diagram indicating the crush site (red x), stimulating sites (yellow lightning bolts) and recording site (green needle). The hip stimulation site was performed just proximal to the crush site while the ankle site was located distal to the crush site. The recording electrodes were placed in the muscles of the foot pad. B–C) Representative CMAP traces recorded from the footpads of WT (B) and Tg (C) mice after ankle stimulation for each time point. By week 4, WT mice already began to show improved CMAP amplitudes while the Tg mice did not. It is only by week 8 that the Tg mice began to show any significant CMAP tracings. D–E) Quantification of CMAP amplitudes in WT (blue, n = 15) and Tg (red, n = 19) mice with the stimulation at the ankle (D) or hip (E). 2 weeks after the crush, neither the WT nor Tg mice showed any improvement of the CMAP amplitudes at either the ankle (D) or hip (E) stimulation sites. Again, at both the ankle and hip, the Tg mice had a delay in the regeneration of axons while the WT mice showed significantly more improvement 4 weeks after the crush. Only at week 8 did the Tg mice begin to catch up with their WT littermates. Points represent the mean ± standard error. * indicates $p < 0.05$. *C. Tallon, E. Rockenstein, E. Masliah, M. H. Farah, Increased BACE1 activity inhibits peripheral nerve regeneration after injury. Neurobiol Dis 106, 147-157 (2017).*

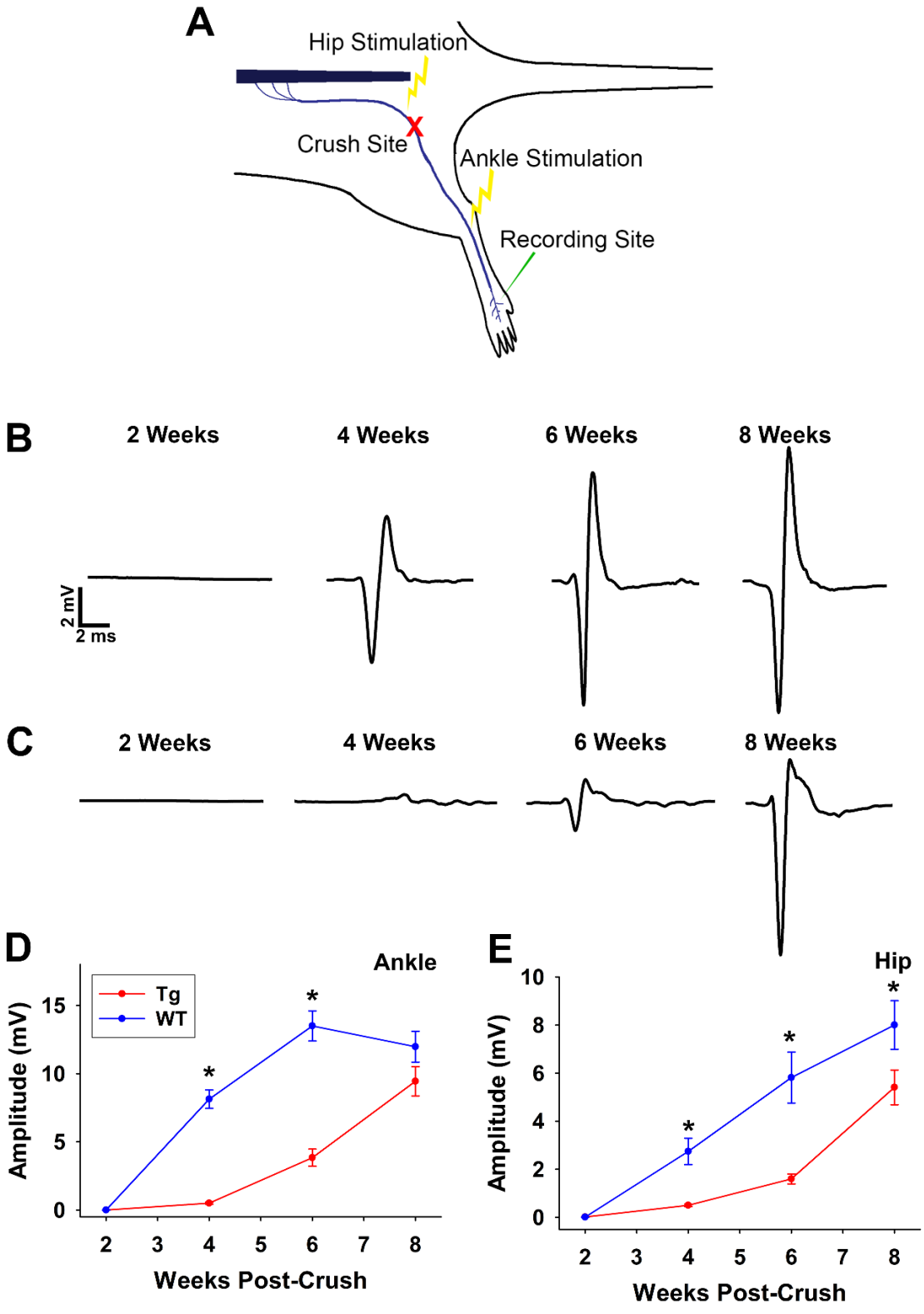
A
Hip Stimulation
Crush Site
Ankle Stimulation
Recording Site
B
2 Weeks
4 Weeks
6 Weeks
8 Weeks
2 mV
2 ms
C
2 Weeks
4 Weeks
6 Weeks
8 Weeks
D
Ankle
Tg
WT
Amplitude (mV)
Weeks Post-Crush
E
Hip
Amplitude (mV)
Weeks Post-Crush

Summary of chapter 2

In this chapter, we determined that neuronal overexpression of BACE1 does not have any statistically significant effects on the peripheral axon morphology in uninjured nerves. Additionally, we were also able to determine that macrophage recruitment and myelin debris clearance early on during the degeneration process was not affected by neuronal overexpression of BACE1, hinting that neuronal BACE1 activity levels may not be responsible for the macrophage recruitment and phagocytosis phenotype seen in BACE1 KO mice. We were also able to confirm our hypothesis that increased BACE1 activity leads to impaired regeneration following a sciatic nerve crush injury. This reduced regeneration capacity was evident both morphologically, by the number of regenerating axons and NMJ reinnervation, as well as functionally in the recovery time of the amplitude of the CMAP in the foot pad muscles.

This data, together with our BACE1 KO studies, supports the overarching hypothesis that BACE1 activity levels inversely influence the efficacy of peripheral nerve regeneration following axonal injury. Having determined this relationship, we next investigated whether we could apply this new understanding as a potential therapy for enhancing regeneration following a nerve crush injury using BACE1 inhibitors.

Chapter 3: Decreased BACE1 activity enhances peripheral nerve regeneration following a nerve crush injury

Introduction to chapter 3

Due to BACE1's role in generating Aβ plaques in AD, many iterations of BACE1 inhibitors have been developed over the years in the hopes of creating a drug that would be effective in slowing or halting the disease progression of AD. Many of the earlier inhibitors were plagued with issues surround difficulties penetrating the blood-brain barrier and various toxicity issues (*160*). Our lab had briefly investigated whether two early BACE1 inhibitors, BACE1 inhibitor IV from Calbiochem (*161*) and WAY 258131 from Wyeth (*175*), could enhance peripheral nerve regeneration following a sciatic nerve crush (*25*). We observed an apparent enhanced debris clearance as well as increased axonal regeneration both in sciatic nerve cross sections and sections of the foot pad.

While this data was encouraging, it gave a very preliminary insight into the potentials of using BACE1 inhibitors to enhance regeneration following a nerve injury. In addition to this, these experiments also used BACE1 inhibitors that never made it to clinical trials. In this chapter, we further explore the efficacy of BACE1 inhibition on enhancing peripheral nerve regeneration following a sciatic nerve crush injury using two more recent BACE1 inhibitors that made it to clinical trials, LY2886721 from Eli Lily and MBI-9 from Merck.

Results

BACE1 inhibitors target BACE1 activity

Before dosing the cells and animals with the BACE1 inhibitors, we first determined that both BACE1 inhibitors, LY2886721 and MBI-9, were able to engage their target and reduce BACE1 activity. One way to monitor whether or not BACE1 activity is reduced is to determine the expression level of full length APP. Full-length APP typically appears as a doublet band around 110-135 kDa. We first tested whether the Eli Lilly BACE1 inhibitor, LY2886721, at a dose of 100mg/kg, was able to reduce BACE1 activity by comparing 3 vehicle treated and 3 inhibitor treated mice (Figure 14 A-B). We saw an increase in the intensity of the band in the brain (vehicle = 0.266±0.0767; inhibitor = 0.956±0.134; p=0.011) and sciatic nerve tissue (vehicle = 0.103±0.0309; inhibitor = 0.502±0.104; p=0.0213) of mice treated with the LY2886721 inhibitor (Figure 14B). We also ensured that the Merck inhibitor, MBI-9, at a dose of 30mg/kg, was able to inhibit BACE1 activity in brain and spinal cord tissue by comparing 4 vehicle treated and 4 inhibitor treated mice (Figure 14 C-D). Again, we saw an increase in the intensity of the full-length bands in the inhibitor treated mice (Figure 14D, brain vehicle = 0.544±0.0447; brain inhibitor = 0.8570±0.0257; brain p=0.000914; spinal cord vehicle = 0.116±0.0127; spinal cord inhibitor = 0.393±0.232; spinal cord p=0.0000434). Based on these observations we were able to conclude that both drugs were inhibiting BACE1 activity levels and proceeded use the inhibitors in subsequent experiments.

Fig. 14. Oral BACE1 inhibitors reduce full length APP.

A) Representative western blot bands from brain and sciatic nerve tissue showing increased full-length APP expression following Eli Lily LY2886721 administration. B) Quantification of normalized full-length APP band intensity from vehicle (blue) and LY2886721 inhibitor (orange) treated brain and sciatic nerve tissue. Band intensity was increased in LY2886721 treated mice indicating that the drug was able to inhibit BACE1 activity. C) Representative blots of full-length APP from the brain and spinal cord of mice treated with vehicle or the Merck MBI-9 inhibitor. D) Quantification of the intensity of full-length APP in the brain and spinal cord of vehicle (blue) and MBI-9 (red) treated mice. Inhibitor treated mice had increase full-length APP indicating that MBI-9 was also able to effectively inhibit BACE1 activity levels. Bars represent the mean ± standard error. * indicates $p < 0.05$.

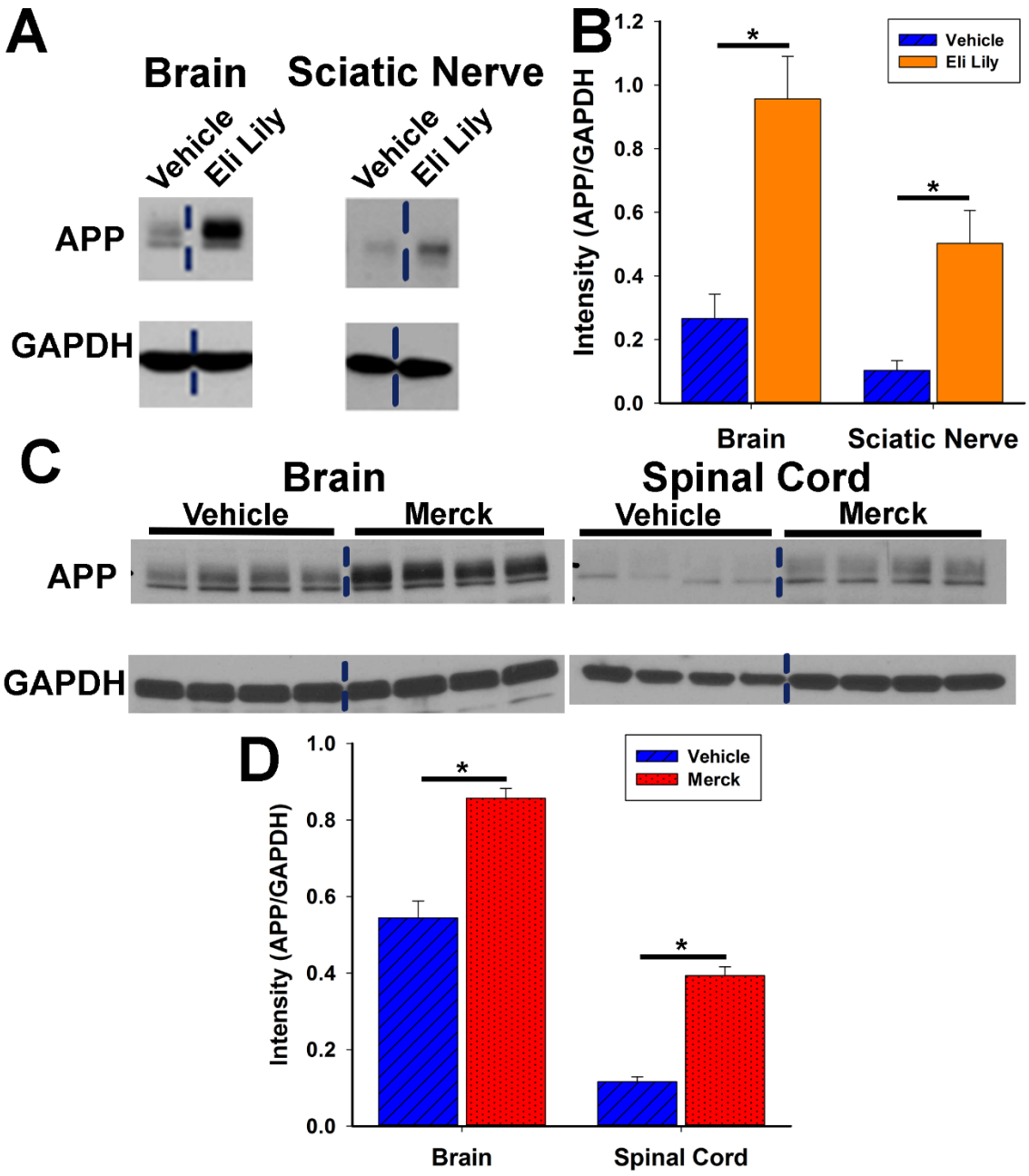
A
Brain
Sciatic Nerve
Vehicle
Eli Lily
Vehicle
Eli Lily
APP
GAPDH
B
Intensity (APP/GAPDH
1.2
1.0
0.8
0.6
0.4
0.2
0.0
*
*
Vehicle
Eli Lily
Brain
Sciatic Nerve
C
Brain
Spinal Cord
Vehicle
Merck
Vehicle
Merck
APP
GAPDH
D
Intensity (APP/GAPDH)
1.0
0.8
0.6
0.4
0.2
0.0
*
*
Vehicle
Merck
Brain
Spinal Cord

BACE1 inhibition enhances neurite branching and outgrowth in vitro

After ensuring that the BACE1 inhibitors were targeting BACE1, we determined whether inhibiting BACE1 activity was able to enhance neurite outgrowth *in vitro*. We collected DRGs from 3 WT C57BL/6J mice and plated the cells on glass coverslips. After allowing the cells to grow for 24h, we gave the cells either DMSO only (vehicle treatment) or 100nM of the LY2886721 BACE1 inhibitor (inhibitor treatment) for 2 days. We then imaged the cells and determined the extent of neurite outgrowth and branching from a total of 100 cells in each condition. Cells that received the inhibitor treatment had visibly more neurite outgrowth and branching than those treated with vehicle only (Figure 15 A and B). We quantified the number of neurite branches extending from the cell soma and found that the inhibitor treated cells had a significantly greater number of neuritic processes growing out of the cell body (Figure 15C). We also found that the length of the longest neurite was greater in cells treated with the inhibitor (Figure 15D). Additionally, there were also more branches along the length of the longest neurite in inhibitor treated cells (Figure 15E). Based on this data, we determined that BACE1 inhibition was able to enhance neurite outgrowth *in vitro*.

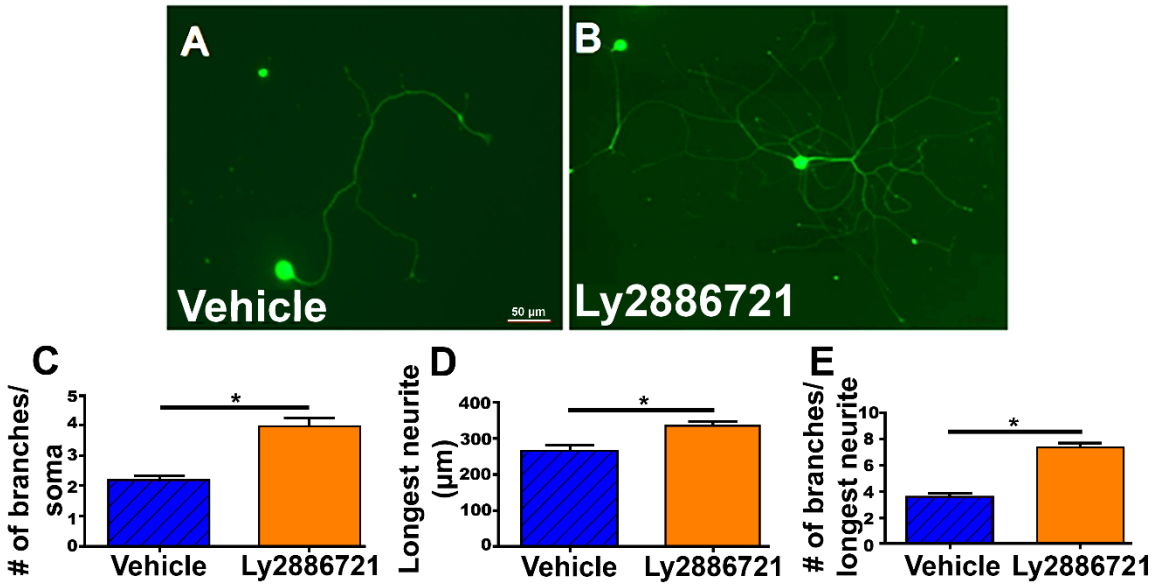

Fig. 15. Cultured adult mouse neurons have enhanced neurite branching after BACE1 inhibitor treatment.

A-B) Representative images from cultured DRG treated with vehicle (A) or a BACE1 inhibitor (B) for 2 days. The inhibitor treated neuron has many more neuritic processes than the vehicle treated neuron. C) Quantification of the number of branches per cell soma with the inhibitor treatment enhanced the number of branches. D) Quantification of the length of the longest neurite. Inhibitor treatment increased the length of the longest neurite. E) Quantification of the number of branches along the longest neurite. Treatment with the BACE1 inhibitor increased the number of branches along the longest neurite. Bars represent the mean ± standard error. * indicates $p < 0.05$. n=100 for each treatment condition.

BACE1 inhibitors do not alter normal, uninjured axon morphology

After determining that BACE1 inhibition was able to increase neurite outgrowth in cultured DRG neurons, we investigated whether BACE1 inhibitors could enhance axonal outgrowth in mouse models of acute axonal injury. Since the LY2886721

inhibitor had liver toxicity issues, we decided to utilize the Merck MBI-9 inhibitor in the mice as it is a more clinically relevant drug that has not shown any liver toxicity issues or other severe side effects in patients (*42*).

Before performing the injury experiments, we first verified whether MBI-9 had any effects on normal axon morphology and physiology. We looked at the morphology and electrophysiology of uninjured sciatic nerves and the morphology of the corresponding gastrocnemius muscle after 2 weeks of inhibitor treatment. When we imaged cross-sections of the uninjured sciatic nerves from both vehicle or inhibitor treated mice, we did not observe any obvious differences between the extent of myelination nor the size or abundance of healthy axons (Figure 16 A and B). We also did not observe any difference in the innervation of the uninjured gastrocnemius muscle in the vehicle and inhibitor treated mice (Figure 16 C-E). The morphology of the uninjured NMJs and the axons innervating them did not appear to differ in shape (Figure 16 C-D). There was also no statistical difference in the percentage of innervated NMJs between vehicle and inhibitor treated mice (Figure 16E; vehicle = 99.49±0.513%, n=3; inhibitor = 100±0%, n=3; $p>0.05$). There was no significant difference between the CMAP amplitudes of the vehicle and inhibitor treated mice (Figure 16F; vehicle = 14.915±1.541 mV, n=12; inhibitor = 16.458±1.344 mV, n=9; $p>0.457$), supporting our earlier observation that there was no difference in the number of healthy axons present in the sciatic nerve. We also did not observe any difference in the latencies of the vehicle and inhibitor treated CMAPs which is indicative of no differences in the extent of myelination between the two conditions (Figure 16G; vehicle = 0.904±0.0396 s, n=12; inhibitor = 0.853±0.0282 s, n=9; $p=0.297$). We concluded that the application of the

BACE1 inhibitor did not alter normal axon morphology, innervation, and nerve physiology.

Fig. 16. BACE1 inhibitors do not alter normal axon morphology and physiology.
A-B) Cross sections of uninjured sciatic nerves in mice treated with either vehicle (A) or a BACE1 inhibitor (B) indicating no difference in the morphology of the axons either in shape and size or myelin thickness. C-D) Representative images of the uninjured gastrocnemius muscle from a vehicle (C) or inhibitor (D) treated mouse. The NMJs (red α-bungarotoxin) looked similar in both treatment conditions as do the axons innervating the NMJs (green NF and SV2). E) Quantification of C and D where there was no difference in the percent of innervated NMJs between vehicle (blue) and inhibitor (red) treated mice. Vehicle and inhibitor n=3. F) Quantification of the amplitudes recorded from the uninjured sciatic nerves in vehicle and inhibitor treated mice. There was no difference between treatments which demonstrated that the number of axons did not differ with inhibitor treatment. G) Quantification of the latencies from uninjured vehicle and inhibitor treated mice. The latencies did not differ between treatment conditions indicating that the myelination of uninjured nerves was not altered by inhibitor treatment. Vehicle n=12 and inhibitor n=9 for E-F. Bars represent the mean ± standard error.

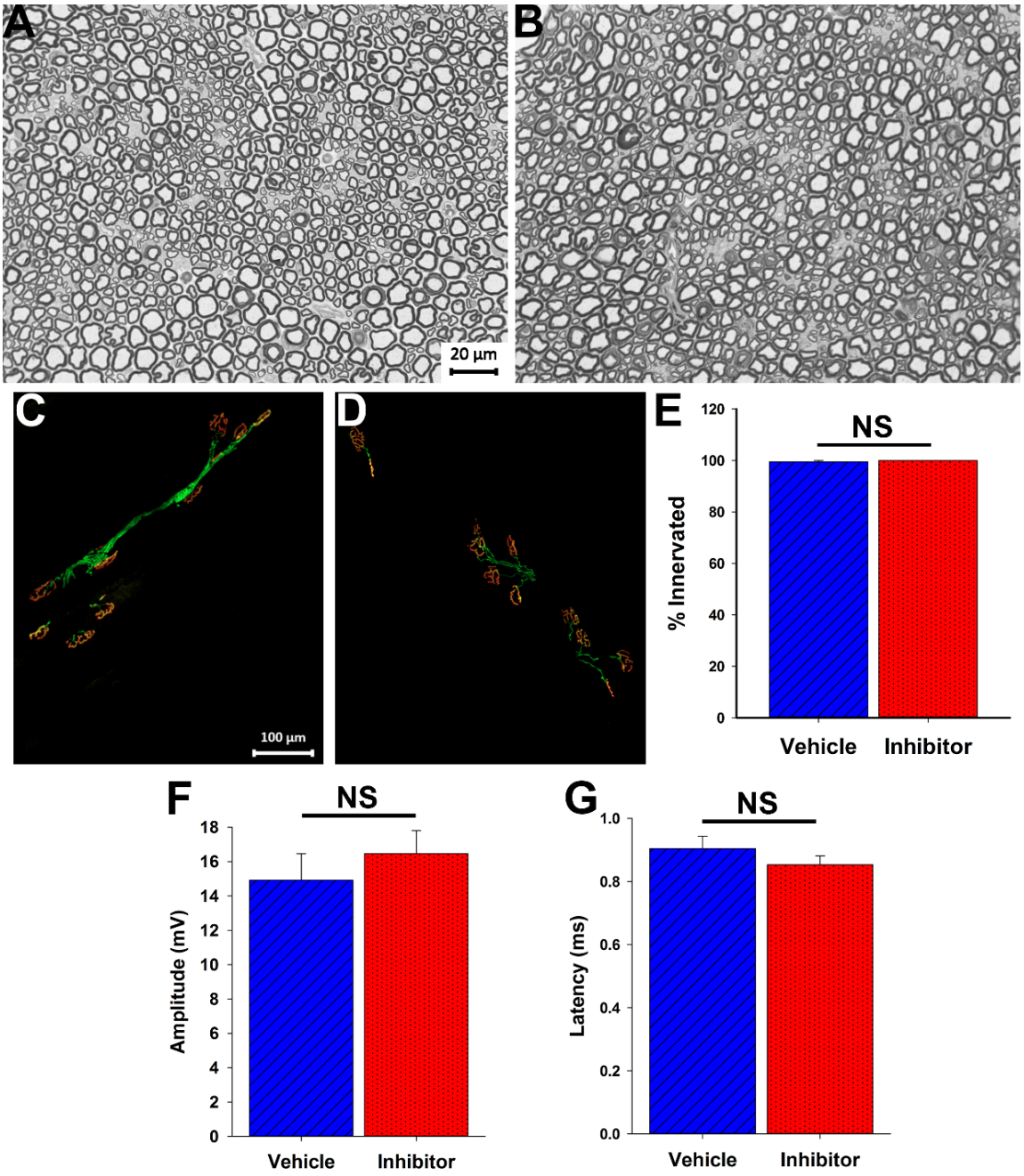
A
B
20 µm
C
D
100 µm
E
NS
% Innervated
120
100
80
60
40
20
0
Vehicle
Inhibitor
F
NS
Amplitude (mV)
18
16
14
12
10
8
6
4
2
0
Vehicle
Inhibitor
G
NS
Latency (ms)
1.0
0.8
0.6
0.4
0.2
0.0
Vehicle
Inhibitor

BACE1 inhibition enhances axon regeneration after a sciatic nerve crush injury

The first type of acute axonal injury model that we wanted to investigate was a sciatic nerve crush. This type of injury completely disconnects the proximal portion of the axon from its distal targets while keeping the basal lamina and Schwann cell tube intact. This type of injury allows for the proximal stump to extend axonal sprouts through the intact Schwann cell tube and be guided towards its appropriate end target.

We performed sciatic nerve crushes on 9 C57BL/6J WT mice and gave 4 mice vehicle food and 5 mice inhibitor food for 2 weeks. We then collected the sciatic nerves and gastrocnemius muscles from these mice and determined the extent of regeneration. Inhibitor treated mice had many more visible regenerating axons in sciatic nerve cross-sections than those treated with vehicle (Figure 17 A and B). After quantifying the regenerating axons, we found that the vehicle treated mice had 1916.75±456.16 regenerating axons while the inhibitor treated mice had significantly more regenerating axons, at 3378.4±353.78 (Figure 17C; p=0.0366).

We next determined whether these faster regenerating axons were reaching the gastrocnemius muscle leading to improved NMJ reinnervation. When we probed the gastrocnemius muscles of the vehicle and inhibitor treated mice, the inhibitor treated mice had visibly better NMJ reinnervation (Figure 17D and E). The inhibitor treated gastrocnemius muscles were 76.64%±7.726 innervated (n=3) while the vehicle treated mice were only 11.55%±6.124 innervated (n=4) (Figure 17F; p=0.00112).

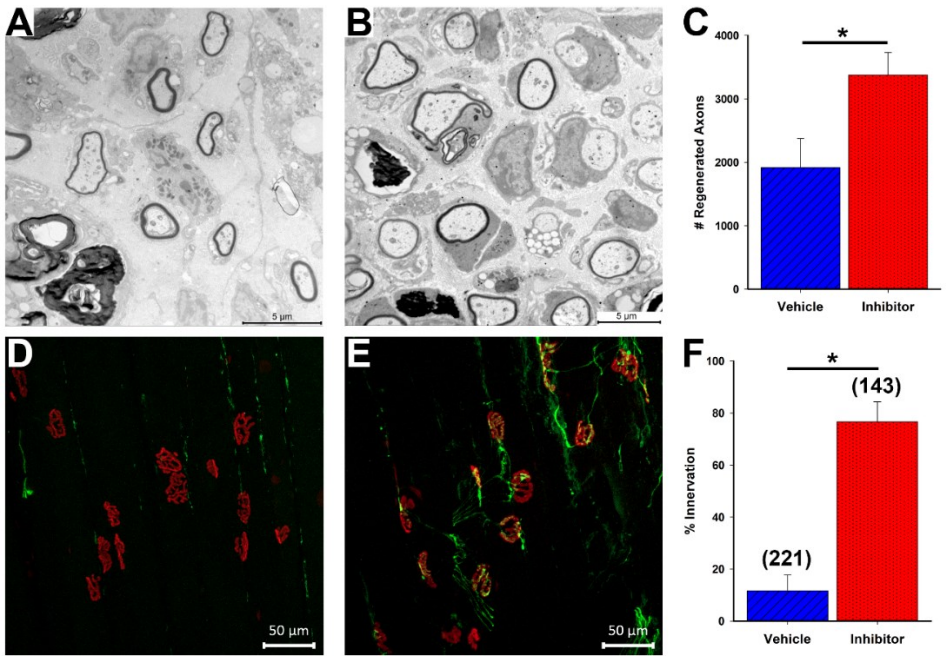

Fig. 17. BACE1 inhibitors enhance axonal regeneration following a sciatic nerve crush.

(A-B) Representative EM images of sciatic nerve cross sections from vehicle (A) and inhibitor (B) treated mice. Inhibitor treated mice have a greater number of regenerating axons compared to the vehicle treated mice. (C) Quantification of the number of regenerated axons in vehicle and inhibitor treated mice. Inhibitor treated mice have significantly more regenerated axons. Vehicle n=4, inhibitor n=5. (D-E) Representative images of sectioned gastrocnemius muscles stained for SV2, NF (both green), and α-BTX (red). The vehicle treated mice (D) have only a few innervated NMJs while the inhibitor treated mice (E) have more innervated NMJs. (F) Quantification of the number of innervated NMJs between vehicle and inhibitor treated mice indicating enhanced innervation after inhibitor treatment. Vehicle n=4, inhibitor n=3. Numbers in parenthesis indicate total number of NMJs counted. Bars represent the mean ± standard error. * indicates $p < 0.05$.

We also determined whether these muscle connections were able to elicit CMAPs in the plantar muscles of the foot pad as this is a good way of observing functional recovery. We crushed the left sciatic nerves of 21 mice and placed 12 on vehicle and 9 on

inhibitor. We then followed the rate of recovery of the CMAP amplitude stimulated at the ankle every 2 weeks over 8 weeks (Figure 18). 2 weeks following the injury, neither the vehicle nor the inhibitor treated mice had any significant recovery of the CMAP amplitude (Figure 18E; vehicle = 0.0602±0.0212 mV; inhibitor = 0.0408±0.0279; p=0.324). At 4 weeks, both the vehicle and inhibitor had an improvement in the amplitude, however, there was no difference between them (Figure 18E; vehicle = 2.867±0.273 mV; inhibitor = 2.344±0.125 mV; p=0.414). We suspected that this may be related to a deficiency in remyelination. Indeed, we saw a longer latency in inhibitor treated mice than vehicle treated at 4 weeks (Figure 18 F; vehicle = 1.688±0.092 ms; inhibitor = 2.219±0.143 ms; p = 0.004). When we examined the shape of the CMAP traces we noticed that the inhibitor treated mice had many more peaks distributed throughout the duration of the CMAP compared to the vehicle treated traces (Figure 18A and B). We then calculated the area under the curve and found that the inhibitor treated mice had a significantly higher area than the vehicle treated mice (Figure 18G; vehicle = 3.111±0.193 mV x ms; inhibitor = 4.164±0.393 mV x ms; p = 0.0153). This most likely indicated that the inhibitor treated mice has a greater number of axons firing than the vehicle treated mice. However, these axons were not able to coherently fire to generate a greater CMAP amplitude and reflects a defect in remyelination related to BACE1's processing of neuregulin 1 and the remyelination of the peripheral nerves (*56, 57*). We decided to halt treatment at 4 weeks to allow for remyelination to occur and potentially improve in the amplitude of inhibitor treated mice. At 6 weeks, the traces of both the vehicle and inhibitor treated mice were firing more synchronously, as seen by the smooth traces in Figures 18C and 18D and that the latencies were no longer significantly

different (Figure 18F; vehicle = 1.291±0.0743; inhibitor = 1.085±0.0533; p=0.0568). At 6 weeks the amplitudes of the inhibitor treated mice were now significantly higher than the vehicle treated mice (Figure 18E; vehicle = 6.898±0.496 mV; inhibitor = 8.709±0.714; p=0.045). We also observed significantly greater amplitudes in the inhibitor treated mice at 8 weeks (Figure 18E; vehicle = 8.335±0.767 mV; inhibitor = 10.732±0.518; p=0.005). Taken together, our data shows that BACE1 inhibitor treatment can enhance sciatic nerve regeneration and muscle reinnervation, as well as improve CMAP amplitude recovery following a complete sciatic nerve crush injury.

Fig. 18. BACE1 inhibition enhances functional repair following a sciatic nerve crush injury. A-B) Representative CMAP traces 4 weeks post injury from vehicle (A) and inhibitor (B) treated mice. The inhibitor treated trace had many small peaks which is evidence of poor myelination impairing the ability of the axons to fire together C-D) Representative traces 6 weeks post injury from vehicle (C) and inhibitor (D) treated mice. After being off the inhibitor for 2 weeks, remyelination occurred and the axons were able to coordinately fire. E) Quantification of the CMAP amplitude recorded every 2 weeks over 8 weeks. Inhibitor treated mice surpassed the vehicle treated mice at 6 weeks and continue to separate at 8 weeks. F) Quantification of the latency from 4 to 8 weeks following injury. At 4 weeks, the latency of inhibitor treated mice was significantly higher than vehicle treated mice. After removing the inhibitor, the latency was no longer significantly different, indicating re-myelination had occurred. G) Quantification of the area under the curve every 2 weeks for 8 weeks. At 4 weeks, the inhibitor treated group had a greater area, reflecting a larger number of axons firing despite not being able to fire together. Points represent the mean ± standard error. * indicates $p < 0.05$. † indicates treatment end point.

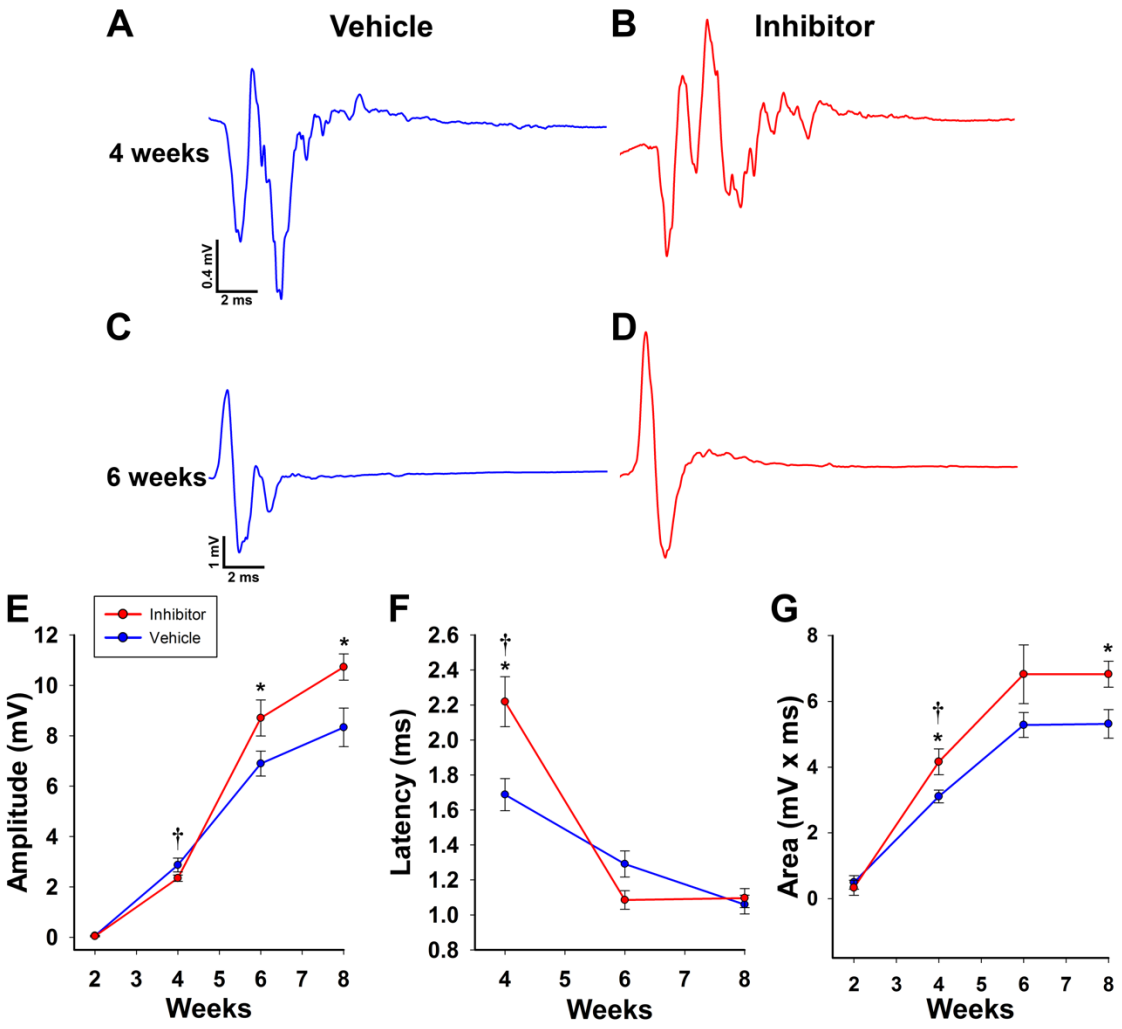

Summary of chapter 3

This chapter provided evidence that determined BACE1 inhibitors are able to effectively enhance axonal regeneration following a sciatic nerve crush injury. We first were able to observe enhanced neurite branching *in vitro* by treating cultured adult DRG neurons with a BACE1 inhibitor. After performing *in vivo* sciatic nerve crush injuries in WT mice, we treated them with a BACE1 inhibitor and monitored the extent of regeneration both morphologically and functionally. BACE1 inhibitor treated mice had a

significantly increased number of regenerating axons as well as an earlier functional recovery time, as evidenced by improved amplitude recordings of the CMAP in the foot pad.

While being able to enhance regeneration following a nerve crush injury can be beneficial to patients, these types of injuries are thought to be less severe, as the endoneurium remains intact and the regenerating axon has a higher chance of successfully reinnervating its target. Nerve crush injuries also do not model the type of axonal reinnervation that would typically occur in cases of peripheral neurodegenerative diseases. Due to these limitations of the crush injury model, we next investigated whether BACE1 inhibitors are beneficial in enhancing regeneration in a more severe model of peripheral nerve injury, a partial nerve transection.

Chapter 4: Axonal sprouting following a partial nerve injury is enhanced by BACE1 inhibition

Introduction to chapter 4

More severe types of peripheral axonal injuries typically involve the disruption of the endoneural tube and the Schwann cells lining the axon. This usually occurs following a partial or complete nerve transection and is also seen in the peripheral nerves of neurodegenerative diseases and neuropathies. Since the proximal and distal portions of the nerve become disconnected, it becomes much harder for the proximal stump to regrow back into the correct Schwann cell tube and become targeted to the proper end organ. In the case of a partial nerve transection, some portion of the nerve is still intact and contacting the proper end organ. These intact axons can respond to the local denervation and send out collateral axonal sprouts, either nodal, pre-terminal, or terminal, to nearby areas of denervation in an attempt to regain partial function. As intact axons typically only send out sprouts to close regions of denervation, it stands to reason that more extensive degeneration may lead to increased instances of axonal sprouting in response to more severe partial nerve injuries. It is also important to be able to trace the beginning and end points of potential axonal sprouts as it can be rather difficult to determine whether an axon is a true sprout or just passing close by to a NMJ. The current model of attempting to sever half of the sciatic nerve is plagued by both of these issues. It is quite difficult to accurately sever the exact same percentage of the sciatic nerve and ensure that you are severing the nerves that travel to the same muscle you want to use for quantification. In addition to these issues with consistency, many of the muscles

innervated by the sciatic nerve are too thick to satisfactorily image the extremely thin axonal sprouts, either due to sectioning limitations or a poor depth of imaging capability in whole mounts. Based on this, we wanted to create a more consistent model for performing partial nerve transections in a nerve-muscle system that can be adequately imaged than what is currently being performed in the sciatic nerve. To do this, we utilized the LTN-CMM system, previously characterized by our group (*111*) and expanded on here, to perform more consistent partial nerve injuries in order to study whether reduced BACE1 activity also has an effect on terminal axonal sprouting in a partial nerve injury model.

Results

Partial nerve transections can be performed in the lateral-thoracic nerve-cutaneous maximus muscle system

In order to carry out a partial nerve injury to study BACE1 inhibition's effect on axonal sprouting, we severed 2 branches of the LTN and turned the ends away from one another to prevent the proximal stump from entering the distal Schwann cell tube. This allowed the remaining intact axons to reinnervate the CMM by sending out axonal sprouts, as diagrammed in Figure 19A. Under normal circumstances, NMJs in the adult mouse are only innervated by a single axon (Figure 19 B). After performing a partial nerve transection of the LTN, we were able to identify regions of the CMM where there was evidence of degenerating axons closely adjacent to intact axons (Figure 19C). These intact axons, theoretically, should have the potential to send out axonal sprouts toward the regions that were undergoing degeneration and lead to reinnervation. Following

axonal injury, NMJs can be multiply innervated as many axonal sprouts can reach the denervated NMJs at the same time before undergoing axonal pruning. NMJs with more than one axon branch that appear to bridge two NMJs or go off to nowhere could also be an innervated NMJ sending out a terminal axonal sprout. Accessing the branches of the LTN and being able to consistently sever the same branches was easier than performing a consistent partial nerve transection in the sciatic nerve.

Fig. 19. Utilizing the LTN-CMM system to perform partial nerve transections.
(A) Schematic drawing showing the location of the LTN branches (red) up near the shoulder (greyed region). The axons of the LTN run caudally down the length of the mouse after entering the CMM up near the shoulder. A partial nerve transection is performed just before the LTN enters the CMM by cutting 2 of the visible branches. The intact axons are then able to send out axonal sprouts in an attempt to reinnervate nearby denervated NMJs (blue). If the denervated NMJ is too far from the intact axon, it remains denervated (black NMJ). (B) A collapsed z-stack image from an uninjured whole mounted CMM transgenically expressing YFP in its neurons. NMJs were stained red with α-bungarotoxin to determine all the NMJs were innervated in the field of view. C) Representative image from a WT mouse 5 days after a partial LTN transection where degenerating axons (white arrows) are adjacent to intact axons (white arrowheads).

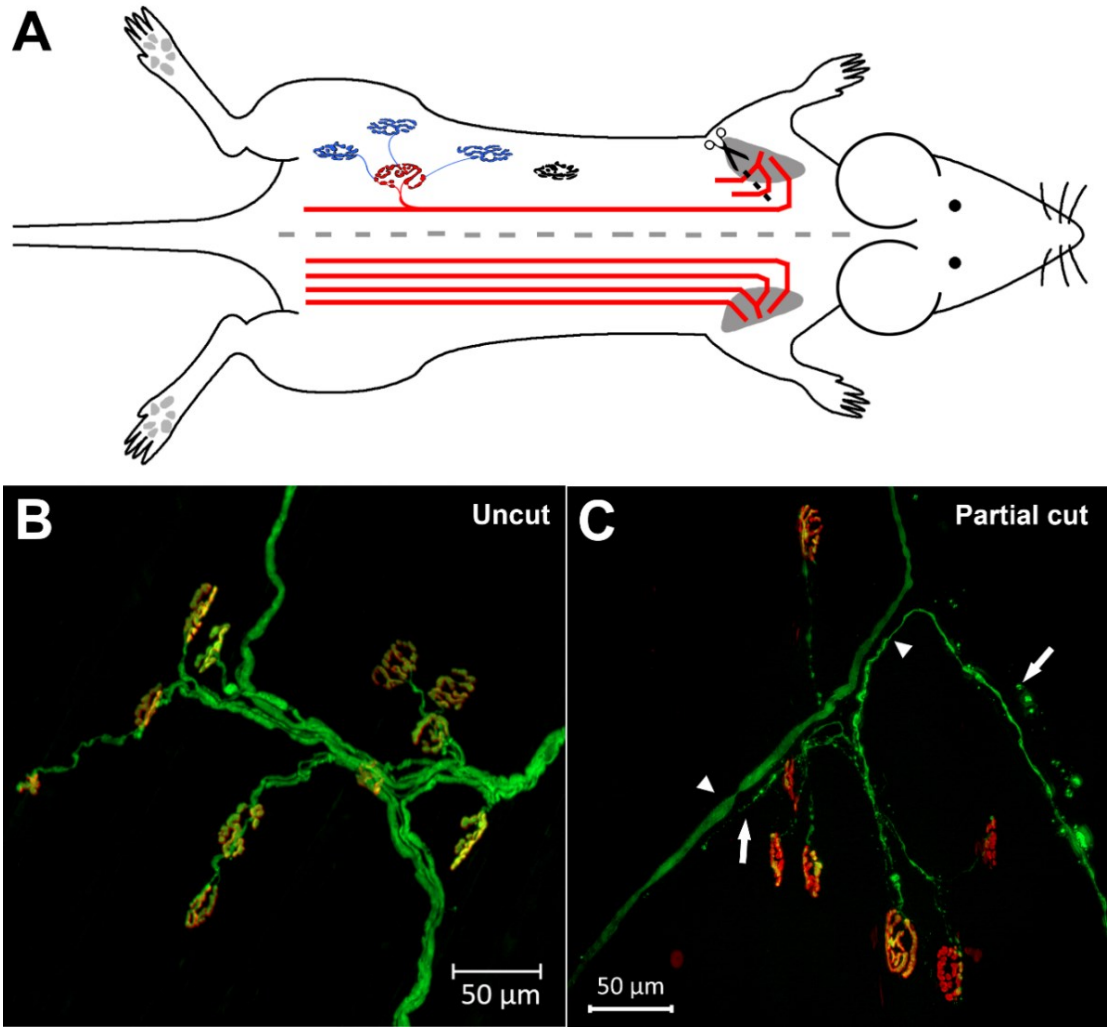

The CMM is a thin muscle exclusively comprised of type II muscle fibers

The following data was published in C. Tallon, K. A. Russell, S. Sakhalkar, N. Andrapallayal, M. H. Farah, Length-dependent axo-terminal degeneration at the neuromuscular synapses of type II muscle in SOD1 mice. Neuroscience 312, 179-189 (2016).

In addition to being an ideal model in which a partial motor nerve transection can be easily and reliably performed, the LTN-CMM system has other benefits for investigating axonal sprouting. In order to investigate axonal sprouting, it is important to be able to trace the origin and destination of axonal sprouts to ensure that the sprouts are

in fact sprouts and not normal axonal branches. Normally, complete images of muscle must be reconstructed from images of sectioned muscle which is often difficult and tedious. This problem can be avoided by being able to whole stain and mount the muscle. This is most easily done in thin muscles and we set out to confirm the CMM as a thin muscle. We collected the CMM from the body by removing the skin off the back of the trunk with the CMM remaining attached to the skin. After staining with Hematoxylin and Eosin, the CMM was identified as a thin layer of muscle closely associated to the dermis of the skin (Fig. 20A, black bar).

In addition to being quite thin, the LTN-CMM system is also a good system to study sprouting from resistant motor fibers. Since fast-fatiguing, α-motor axons innervating type II muscle fibers are very resistant to sprouting in response to Botulinum toxin A administration (*88*), we characterized a system to exclusively study a large type II muscle and its NMJs. To do this, we first confirmed that the LTN–CMM system in the mouse only contained type II muscle. The CMM and soleus muscle were stained for myosin heavy chain type I (A4.840) and type II (My32) to identify muscle fiber types. In the CMM, only type II fibers were present, as evidenced by the uniform staining in the muscle fibers of My32 (Fig. 20B and C). On the other hand, when the soleus muscle was simultaneously stained for type I and type II fiber markers, both were present (Fig. 20D). Since it is well known that the soleus muscle contains both fibers, this indicated that our staining protocol was reliable. Thus, we confirmed that the CMM contains only type II muscle fibers and can confidently be used to specifically study the sprouting properties of type II fibers in response to a partial nerve injury.

Fig. 20. The CMM is exclusively comprised of type II muscle fibers.

(A) Musculoskeletal morphology shown through hematoxylin and eosin staining where the CMM is indicated by a black bar. (B–D) Myosin heavy chain immunostaining of the CMM where type I fibers were labeled with A4.840 (red) and type II fibers were labeled with My32 (green). (B) Low magnification fiber type immunostaining shows the CMM is comprised of only type II fibers. (C) High magnification of B. (D) Control with soleus tissue showing a mix of type I and type II fibers. *C. Tallon, K. A. Russell, S. Sakhalkar, N. Andrapallayal, M. H. Farah, Length-dependent axo-terminal degeneration at the neuromuscular synapses of type II muscle in SOD1 mice. Neuroscience 312, 179-189 (2016)*.

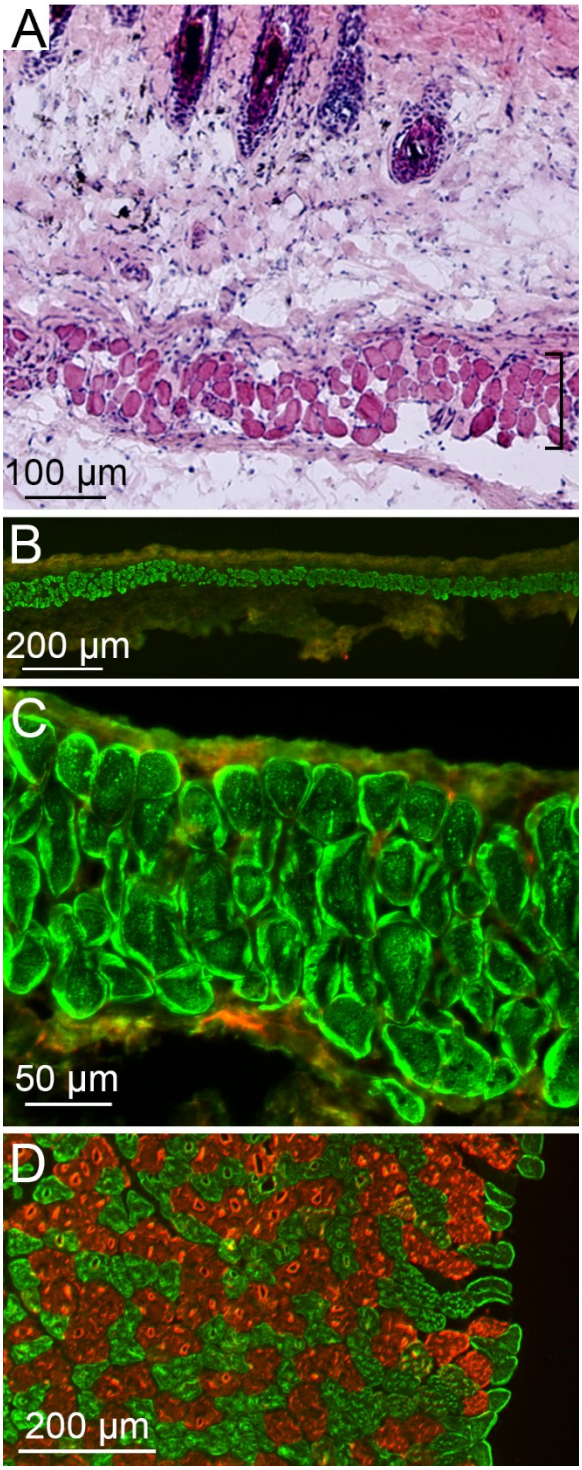
A
100 µm
B
200 µm
C
50 µm
D
200 µm

Whole-mounted LTN–CMM can be stained with antibodies

The following data was published in C. Tallon, K. A. Russell, S. Sakhalkar, N. Andrapallayal, M. H. Farah, Length-dependent axo-terminal degeneration at the neuromuscular synapses of type II muscle in SOD1 mice. Neuroscience 312, 179-189 (2016).

One technical problem with using whole muscle tissue is that many antibodies cannot penetrate deep into the intact tissue, thus requiring sectioning in order to get complete staining. While sectioning allows for easier staining, there is a trade off as it becomes more tedious afterward to reconstruct complete NMJs to determine the extent of axonal sprouting. We stained the CMM with SV2 and S-100 antibodies to visualize the neuronal and glial components of the neuromuscular synapses in whole-mounted tissue. We were able to achieve complete staining with the SV2 antibody as indicated by a complete overlap of the SV2 and α-bungarotoxin (α-btx) staining in the intact CMM of WT mice (Fig. 21A–D). We also observed extensive Schwann cell labeling with the S-100 antibody (Fig. 21E–H). The ability to carry out effective staining in whole tissue provides the LTN–CMM system the unique ability to observe all the components of the neuromuscular synapse in a single preparation.

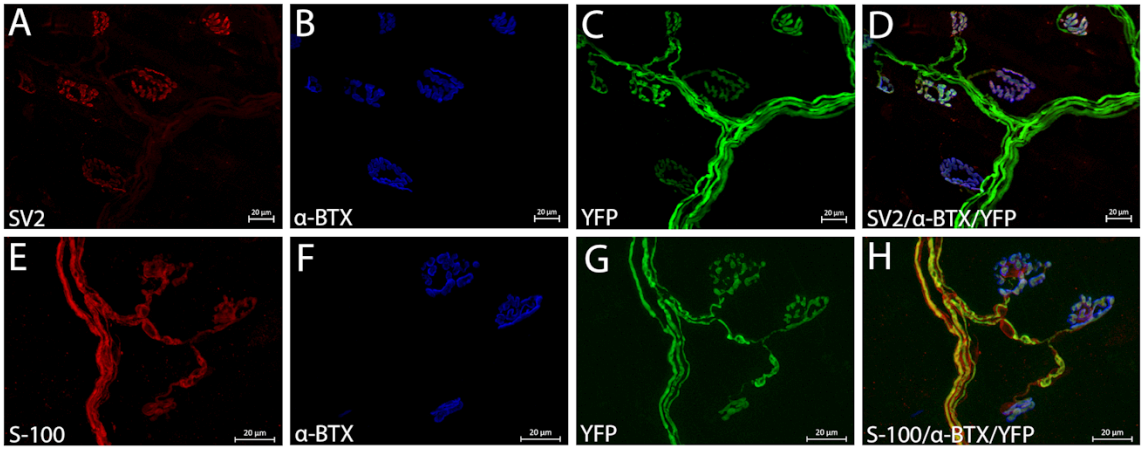

Fig. 21. Reliable antibody staining of the neuromuscular synapse components in the whole, intact CMM.

(A–D) SV2 antibody staining. (A) SV2 staining of the pre-synaptic component of the neuromuscular synapse. (B) α-bungarotoxin staining of the post-synaptic component. (C) YFP expressing motor axons. (D) Overlay of (A–C) showing that all three stains overlap completely and all the terminals have SV2 staining. (E–H) S-100 antibody staining. (E) S-100 staining of Schwann cells. (F) α-bungarotoxin staining of the NMJs. (G) YFP expressing motor axons. (H) Overlay of (E–G) showing that the S-100 staining overlaps both the axons and the NMJs. Both Schwann cells associated with the axon and those at the terminal can be reliably stained. *C. Tallon, K. A. Russell, S. Sakhalkar, N. Andrapallayal, M. H. Farah, Length-dependent axo-terminal degeneration at the neuromuscular synapses of type II muscle in SOD1 mice. Neuroscience 312, 179-189 (2016).*

Reduced BACE1 activity increases axonal sprouting following a partial nerve injury

Following the characterization of a partial nerve transection in the LTN-CMM system, we then set out to investigate how reduced BACE1 activity levels impact axonal sprouting. We first performed a moderate partial nerve transection, leaving two branches

of the LTN intact, in 4 BACE1 KO mice and 4 WT littermates in order to investigate whether a complete loss of BACE1 activity had any effect on axonal sprouting. After 7 days, we collected the CMM to analyze the extent of axonal sprouting. To maximize the likelihood of locating axonal sprouts, images were taken from innervated or partially innervated regions directly adjacent to regions of denervation since axons will only sprout to nearby areas of denervation. For simplicity, only terminal axonal sprouts were scored as those are the easiest to define due to the nature of healthy NMJs only having one axonal input and any additional axonal outputs, either towards another NMJ or empty space, could be scored as a terminal axonal sprout. After examining the images, we observed an increase in the number of NMJs that had at least one terminal axonal sprout in BACE1 KO mice (Figure 22 A and B, white arrows). We analyzed a total of 868 WT and 699 BACE1 KO NMJs and found that there was a significant increase in the percentage of NMJs that had terminal axonal sprouts (Figure 22 C; WT = 6.86 ± 1.49%; KO = 13.37 ± 1.61%; $p = 0.025$). This data provided evidence that a genetic loss of BACE1 activity enhanced terminal axonal sprouting following a partial nerve injury.

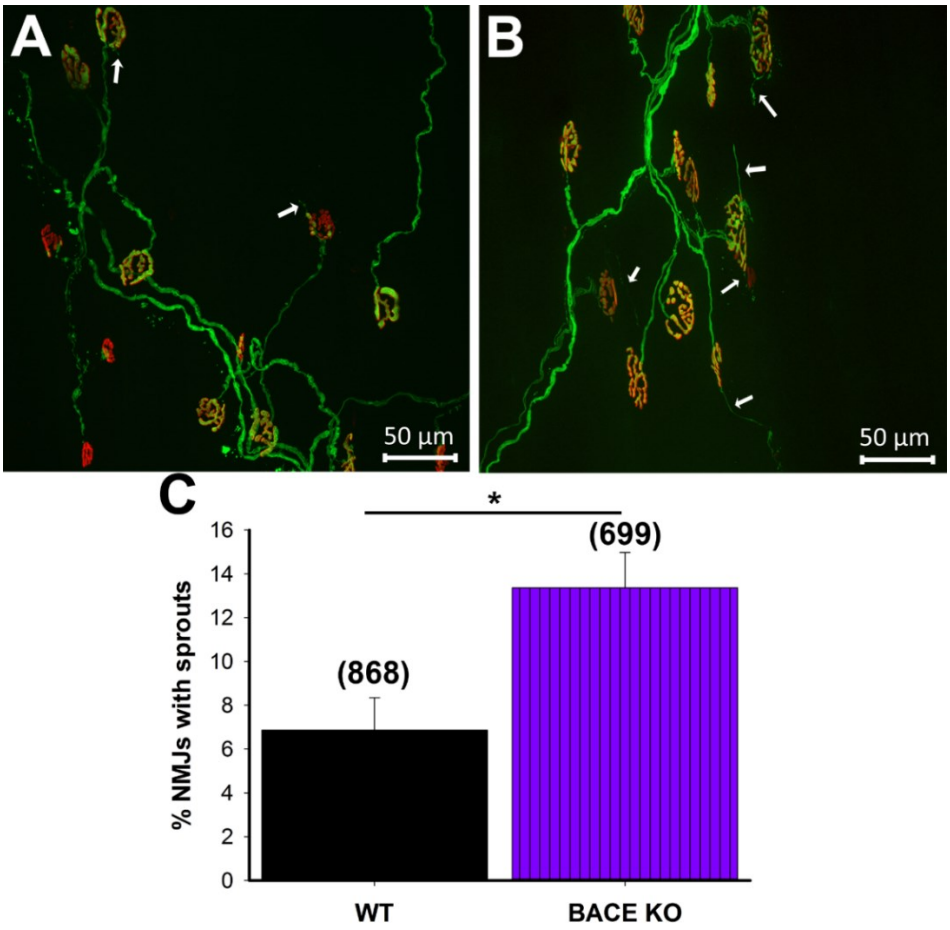

Fig. 22. Genetically knocking out BACE1 enhances axonal sprouting following a partial nerve transection.

A-B) Representative images of terminal axonal sprouts in WT (A) and KO (B) mice 7 days following a partial LTN transection. KO mice have many more NMJs with terminal sprouts as indicated by the white arrows. C) Quantification of the percentage of NMJs that have the presence of a terminal axonal sprout. KO mice have a significantly higher percentage of NMJs with terminal sprouts compared with WT littermates. WT and BACE1 KO n=4. Numbers in parenthesis represent the total number of NMJs counted. * indicates $p < 0.05$. Bars represent mean ± standard error.

We next investigated whether the same principle held true (e.g. enhanced axonal sprouting) with the administration of a BACE1 inhibitor. Again, a partial nerve transection of the LTN was performed, this time leaving only a single branch intact to encourage greater sprouting, in 7 WT mice and gave 3 mice vehicle and 4 mice the inhibitor treatment. The mice were treated for 14 days before collecting the CMM and looking at the extent of terminal axonal sprouting. We then took images from innervated or partially innervated regions directly adjacent to regions of denervation in order to maximize the likelihood of imaging an axonal sprout. As with the BACE1 KO experiment, only terminal axonal sprouts were quantified to ensure that we were counting true axonal sprouts. We observed an increase in the presence of thin axonal sprouts in mice treated with the BACE1 inhibitor when compared with the vehicle treated mice (Figure 23 A and B, white arrows). After quantifying 262 NMJs from the vehicle treated mice and 311 NMJs from the inhibitor treated mice, there was a significant increase in the percentage of NMJs that had terminal axonal sprouts in the inhibitor treated mice when compared with vehicle treated mice (Figure 23C; Vehicle = 14.315 ± 2.763%; Inhibitor = 37.418 ± 2.236%; $p = 0.00122$). This data, together with the BACE1 KO data (from Figure 22), determines that by reducing the activity of BACE1, either genetically or pharmacologically, there is a beneficial impact on the extent of axonal sprouting in response to a partial nerve injury.

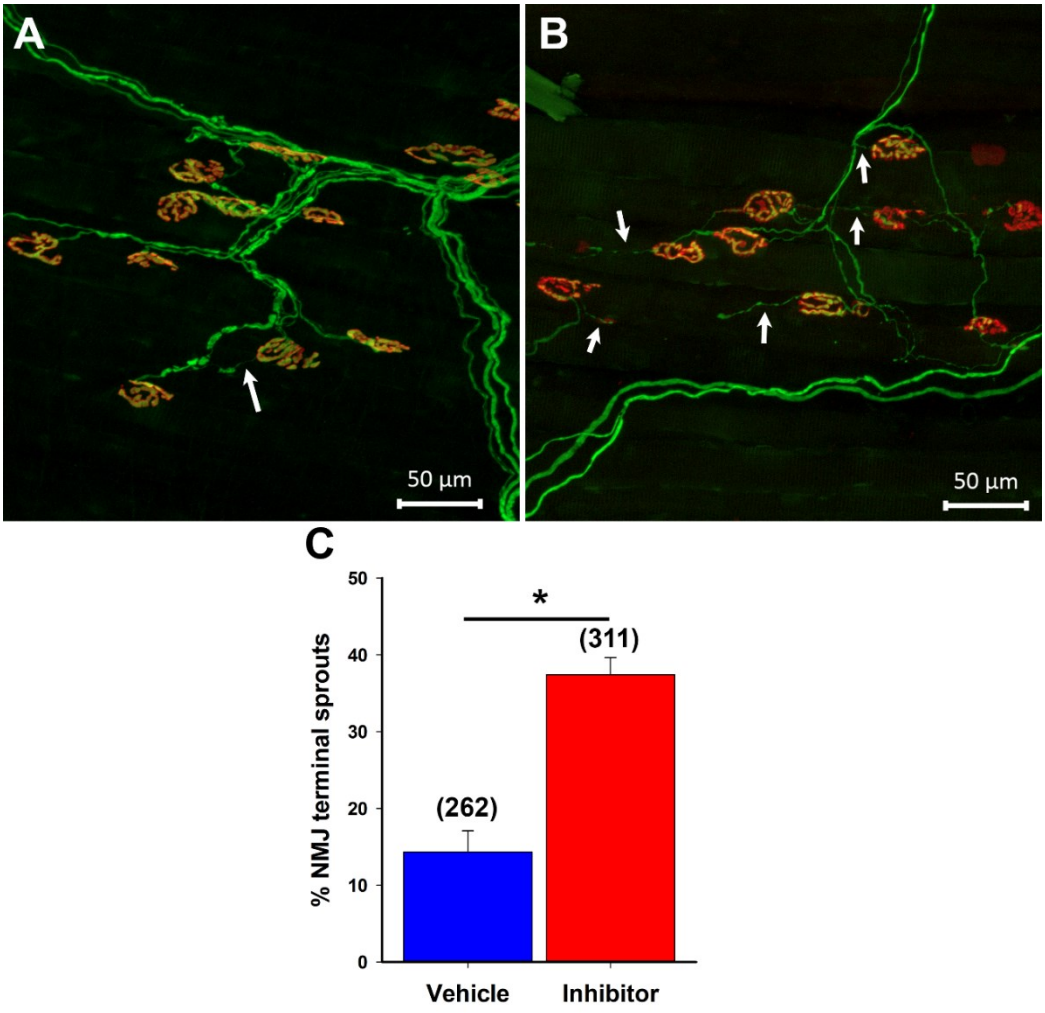

Fig. 23. BACE1 inhibitors enhance terminal axonal sprouting following a partial nerve injury.

A-B) Representative images of a mouse treated with vehicle (A) or inhibitor (B) for 2 weeks following a partial LTN transection. White arrows indicate representative terminal axonal sprouts. C) Quantification of the percentage of NMJs which have a terminal axonal sprout extending out from itself. Inhibitor treated mice have significantly more terminal axonal sprouts than mice treated with the vehicle. Vehicle n=3 and inhibitor n=4. Numbers in parenthesis represent the total number of NMJs counted. * indicates $p < 0.05$. Bars represent mean ± standard error.

Summary of chapter 4

The results presented in this chapter provided evidence that partial nerve transections can be reliable performed in the LTN-CMM system and can be used to study the terminal axonal sprouting response to a partial nerve injury. By severing specific branches of the LTN allowing the same branches to remain intact in each mouse studied, we were more confident in the reliability of our partial nerve transections. We were also able to visualize all the NMJs in the regions imaged and could trace the origin of each axon back to its main branch. After performing a partial nerve transection in both BACE1 KO mice as well as WT mice treated with the MBI-9 BACE1 inhibitor, we observed an increase in the percentage of innervated NMJs with the presence one or more terminal axonal sprouts. This data indicates that reduced BACE1 activity levels are not only able to enhance regeneration from the proximal stump in less severe nerve crush injuries but can also lead to increased axonal sprouting in response to more severe partial nerve transection injuries. This finding is important not only for patients with various types of traumatic peripheral nerve injuries, but may also be a useful mechanism for coaxing surviving axons to sprout and reinnervate denervated target organs in cases of peripheral nerve diseases.

Chapter 5: Monitoring peripheral nerve degeneration in a chronic neurodegenerative disease model

Introduction for chapter 5

Following our finding that BACE1 inhibition can enhance peripheral axon sprouting from intact axons following a partial nerve injury, we next wanted to investigate whether this principle holds true in a neurodegenerative disease model. We settled on the $SOD1^{G93A}$ mouse model of ALS as this model has been very well studied with well documented early distal peripheral axonal degeneration occurring before motor neuron cell death (*131, 132*). That the distal axonopathy precedes neuronal cell death may provide a window to encourage surviving motor axons to send out axonal sprouts to reinnervate areas of denervation and provide some form of prolonged motor function in the early stages of the disease. Prior to the application of a BACE1 inhibitor, we first characterized the degeneration pattern of the LTN in the SOD1 mouse as the LTN-CMM system has never been investigated in the SOD1 mouse. Since the CMM is comprised of only type II motor fibers, as confirmed in the previous chapter, we hypothesized that the axons of the LTN may degenerate even earlier than those in the sciatic nerve because motor fibers innervating type II muscle fibers are more susceptible to degeneration in the SOD1 mouse (*88, 134, 136, 137*). In addition to this, we set out to determine when the earliest detectable signs of degeneration appear in the LTN-CMM system as a way to determine when would be the optimal treatment window for our BACE1 inhibitor studies.

Results

The following data was published in C. Tallon, K. A. Russell, S. Sakhalkar, N. Andrapallayal, M. H. Farah, Length-dependent axo-terminal degeneration at the neuromuscular synapses of type II muscle in SOD1 mice. Neuroscience 312, 179-189 (2016).

Neither axon nor terminal degeneration was detected at 30 days of age

To determine the earliest time point that axon degeneration can be detected in the LTN–CMM system of SOD1 mice, we analyzed them at 30, 60 and 90 days of age. Morphological changes at the NMJs were determined by the extent of denervation of the NMJs by scoring the percentage of presynaptic YFP expression overlapping with the postsynaptic α-BTX staining (Fig. 24B–D). To determine any physiological changes, we measured electrophysiological recordings from 3 different locations on the back (Fig. 24A). We started with the most caudal recording site and moved rostrally, in order to preserve the shorter axons for later recordings at each site.

At the earliest time point investigated, there was no detectable difference between WT mice and the SOD1 mice, both morphologically and physiologically. When we scored the percent of innervated NMJs at the caudal, medial, and rostral regions of the CMM (Fig. 24E), the WT mice had on average 99.9%, 99.4% and 99% innervation respectively ($n = 3$). The SOD1 mice also had no degeneration with 97.1%, 99.4% and 99.7% innervation at the caudal, medial, and rostral regions respectively ($n = 4$). The values in the SOD1 mice were comparable to those seen in the WT indicating that morphological changes had not occurred by P30 ($p > 0.05$). We observed a similar result with the electrophysiological recordings taken at the three sites (Fig. 24F). In the WT mice, CMAP amplitudes on average were 0.27 mA at the caudal region, 0.77 mA at the

medial region, and 2.02 mA at the rostral region (n = 15). The SOD1 mice had similar amplitudes ($p > 0.05$) with the caudal region at 0.34 mA, the medial region at 0.60 mA and the rostral region at 1.90 mA (n = 17). The latencies at each region were also similar between the WT and SOD1 mice (data not shown).

Fig. 24. No evidence of axonal degeneration in 30-day-old SOD1 mice.

(A) Schematic diagram of our electrophysiology setup. LTN stimulation is near the shoulder (green) while the active (red) and the reference (black) recording electrodes are placed 6 mm on either side of the midline (dashed gray line). The three data collection sites are indicated by roman numerals with the caudal site measured 6 mm (I), the medial site measured 24 mm (II), and the rostral site measured 36 mm (III) anterior to the baseline (blue line). Representative CMAP recordings are shown below with their corresponding site denoted by the roman numerals. (B–D) Example of fully innervated NMJs in a 30-day-old WT mouse. (B) YFP positively labeled motor axons and terminals from YFP transgenic mouse. (C) α-BTX labeled NMJs. (D) Merged image of B and C showing all NMJs are innervated by the complete overlap of YFP and α-bungarotoxin staining. (E) There was no significant difference in the percentage of innervated NMJs at each of the collection site for 30-day-old SOD1 (red, n = 4) and WT (blue, n = 3) mice (bars represent mean ± standard error). Numbers in parenthesis indicate the total number of NMJs counted. (F) CMAP amplitudes at each collection site were not significantly different for 30-day-old SOD1 (n = 17) and WT (n = 15) mice (points represent mean ± standard error). *C. Tallon, K. A. Russell, S. Sakhalkar, N. Andrapallayal, M. H. Farah, Length-dependent axo-terminal degeneration at the neuromuscular synapses of type II muscle in SOD1 mice. Neuroscience 312, 179-189 (2016).*

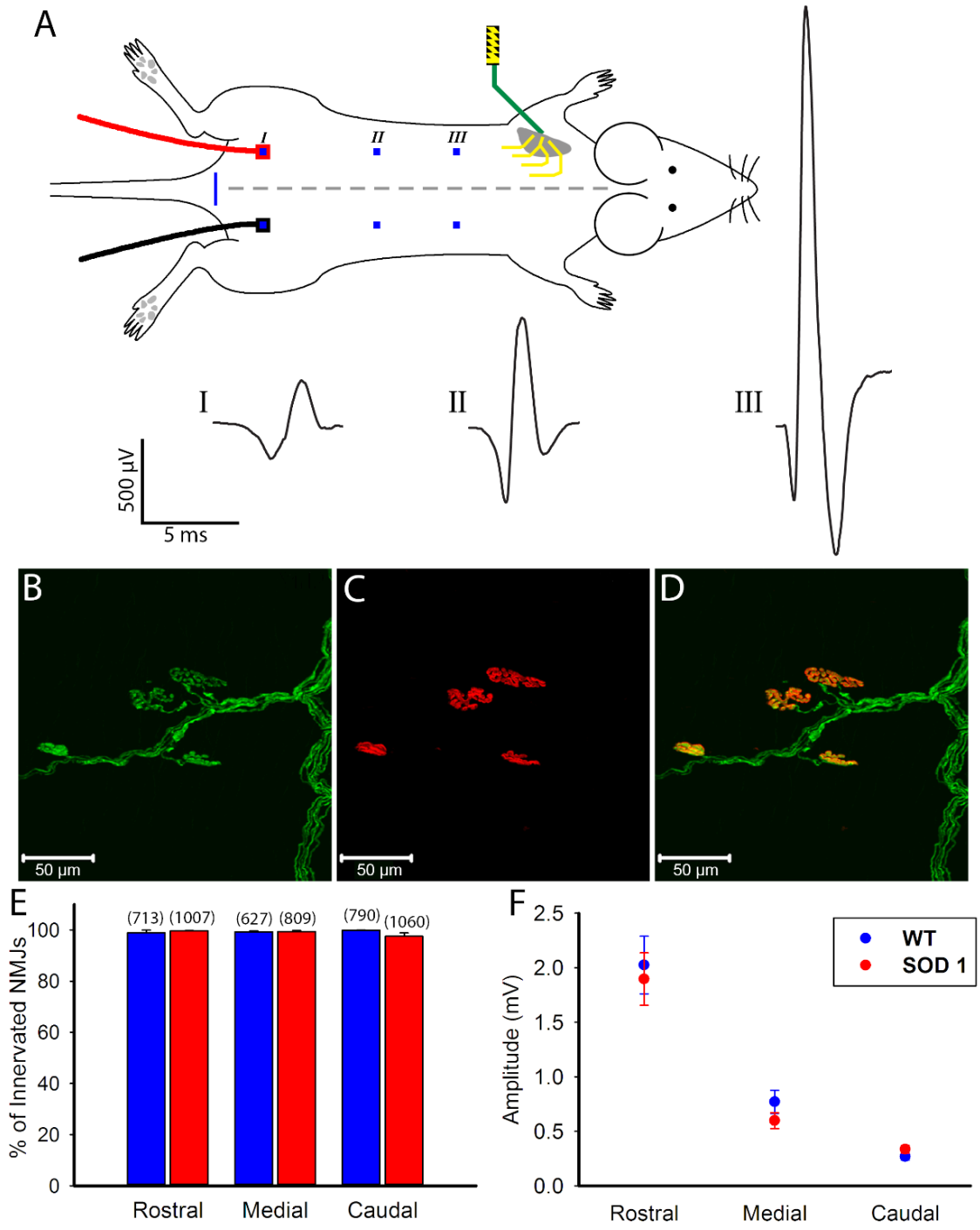
A
I
II
III
I
II
III
500 µV
5 ms
B
C
D
50 µm
50 µm
50 µm
E
% of Innervated NMJs
100
80
60
40
20
0
(713) (1007)
(627) (809)
(790) (1060)
Rostral
Medial
Caudal
F
Amplitude (mV)
2.5
2.0
1.5
1.0
0.5
0.0
WT
SOD 1
Rostral
Medial
Caudal

Marked degeneration appears at the caudal region by 60 and 90 days

When we examined 60-day-old mice, we observed evidence of degeneration in the SOD1 mice compared with the WT mice. The largest difference in NMJ innervation was seen at the caudal site, with an average of only 44.5% of the NMJs being innervated in the SOD1 mice compared with 97.9% innervation in the WT mice (Fig. 25A–C; SOD1 $n = 3$; WT $n = 4$; $p = 0.0093$). There was also a slight decrease in the number of innervated NMJs at the medial region of the back with 77.8% innervation in the SOD1 mice compared with 98.7% in the WT mice ($p > 0.05$). At the rostral site, there was no significant difference between the WT and the SOD1 mice (97.1% and 95.8% respectively; $p > 0.05$). Examining the neurophysiological changes in the SOD1 mice at 60 days revealed a decrease in the amplitudes of the CMAP at both the caudal (Fig. 25D; WT amplitude = 0.36 mA, SOD1 amplitude = 0.16 mA; WT $n = 21$, SOD1 $n = 17$; $p = 0.00031$) and medial sites (Fig. 25D; WT amplitude = 0.79 mA, SOD1 amplitude = 0.50 mA; $p = 0.029$). There was no significant difference in the amplitudes at the rostral site, in agreement with the lack of denervation seen at the rostral region (Fig. 25D; WT amplitude = 1.39 mA, SOD1 amplitude = 1.63; $p > 0.05$).

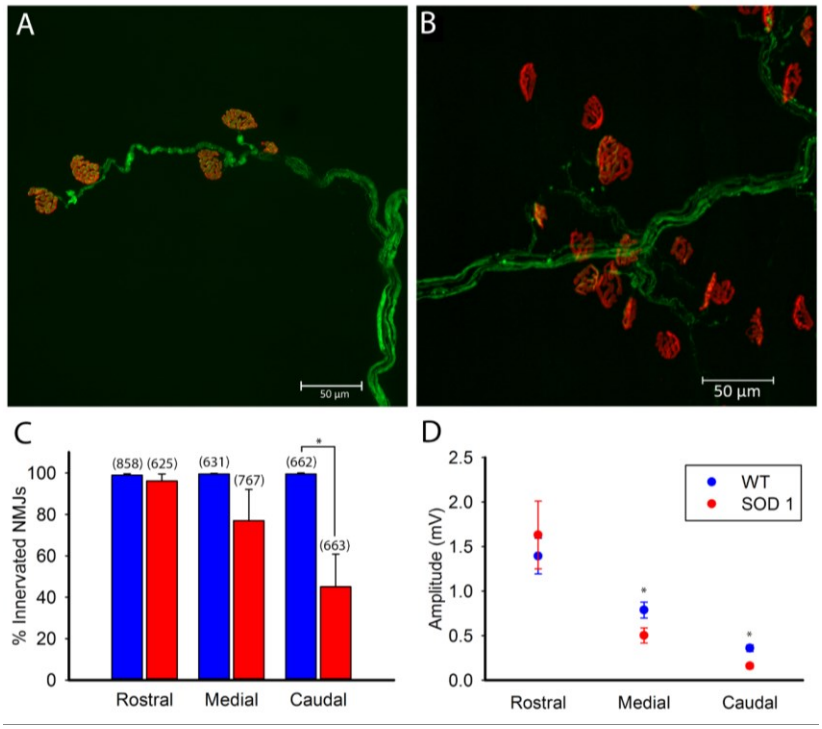

Fig. 25. Axonal degeneration is evident by 60 days in SOD1 mice at the caudal site but not the rostral site.

(A, B) A morphological comparison of the caudal site from 60-day-old WT mice (A) and 60-day-old SOD1 mice (B) showing far more denervated NMJs in the SOD1 mice than the WT. YFP expressing axons are shown in green and α-bungarotoxin labeled NMJs are in red. (C) A quantification of the percentage of innervated NMJs between 60-day-old WT mice (blue, n = 4) and SOD1 mice (red, n = 3). The caudal region has the greatest decline in innervation while the rostral region remains relatively intact. Bars represent mean ± standard error. Numbers in parenthesis indicate the total number of NMJs counted. (D) CMAP amplitudes at the caudal and medial regions in SOD1 mice (n = 17) showed a significant decline in amplitude when compared to WT mice (n = 21). Points represent mean ± standard error. ∗ indicates $p < 0.05$. *C. Tallon, K. A. Russell, S. Sakhalkar, N. Andrapallayal, M. H. Farah, Length-dependent axo-terminal degeneration at the neuromuscular synapses of type II muscle in SOD1 mice. Neuroscience 312, 179-189 (2016).*

At 90 days of age, we observed further degeneration of the LTN axons. The caudal site of the SOD1 mice showed an even greater decrease in innervation with only 24.3% innervated compared to 88.4% in the WT (Fig. 26A, B, E; SOD1 n = 4, WT n = 3; $p = 0.00091$). The medial region of the SOD1 mice was only 55.3% innervated while the WT mice had 90.7% innervation (Fig. 26E; $p = 0.0050$). It was only at 90 days that degeneration in the SOD1 mice was apparent at the rostral site (Fig. 26C, D, E). Only 59.8% of the NMJs were innervated in the SOD1 mice while the WT mice had 93.9% innervation (Fig. 26E; $p = 0.029$). When we compared the CMAP amplitudes of WT and SOD1 mice, there was a further decrease in the amplitudes at the caudal site with the SOD1 mice at 0.13 mA compared to the WT amplitude of 0.27 mA (Fig. 26F; WT n = 19, SOD1 n = 19; $p = 0.013$). The medial site also continued to decline, with the SOD1 amplitude at 0.37 mA while the WT remained normal at 0.75 mA (Fig. 26F; $p = 0.020$). The amplitude at the rostral site in the SOD1 mice was 1.66 mA which was slightly below the WT amplitude at 2.13 mA (Fig. 26F; $p > 0.05$).

Fig. 26. Axonal degeneration is apparent at the rostral site at 90 days of age in SOD1 mice. (A, B) Representative images at the caudal site of WT mice (A) and SOD1 mice (B) show increased degeneration with extensive denervation in the SOD1 mice while the WT remain fully innervated. YFP expressing axons are shown in green and α-bungarotoxin labeled NMJs are in red. (C, D) Representative images at the rostral site of WT mice (C) and SOD1 mice (D) show degeneration at the rostral site in SOD1 mice while the WT is intact. (E) Quantification of the percentage of innervated NMJs in 90-day-old mice showing increased denervation at the caudal region and medial sites and significant degeneration appearing at the rostral region in SOD1 mice (red, n = 4) compared with WT mice (blue, n = 4). Bars represent mean ± standard error. Numbers in parenthesis indicate the total number of NMJs counted. (F) CMAP amplitudes are significantly reduced at the caudal and medial regions in SOD1 mice (n = 19) at 90 days when compared with WT mice (n = 19). The rostral region also shows a slight decrease in SOD1 mice but it did not reach significance. Points represent mean ± standard error. ∗ indicates $p < 0.05$. *C. Tallon, K. A. Russell, S. Sakhalkar, N. Andrapallayal, M. H. Farah, Length-dependent axo-terminal degeneration at the neuromuscular synapses of type II muscle in SOD1 mice. Neuroscience 312, 179-189 (2016).*

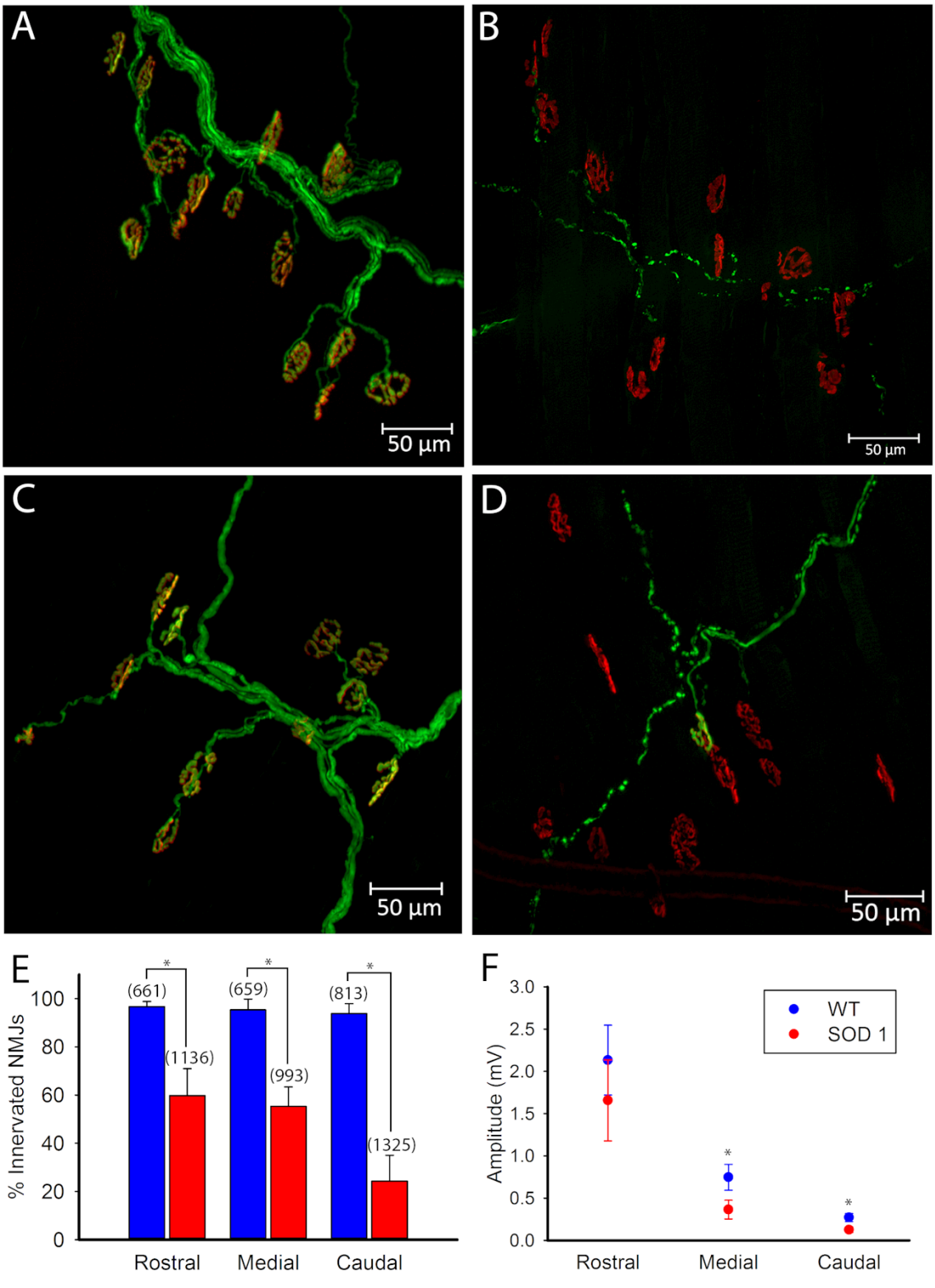
A
50 µm
B
50 µm
C
50 µm
D
50 µm
E
% Innervated NMJs
100
80
60
40
20
0
(661)
(1136)
(659)
(993)
(813)
(1325)
*
Rostral
Medial
Caudal
F
Amplitude (mV)
3.0
2.5
2.0
1.5
1.0
0.5
0.0
WT
SOD 1
Rostral
Medial
Caudal

Physiological changes at the distal LTN occurs earlier than the sciatic nerve

We next compared the time course of the physiological changes in the LTN–CMM system with the time course in the sciatic nerve of SOD1 mice. Similarly to the LTN–CMM, the sciatic nerve did not show any difference in the CMAP amplitude between the WT (n = 6) and SOD1 (n = 6) mice at 30 days of age at both the proximal and distal stimulation sites (Fig. 27B; $p > 0.05$). When we examined P60 mice, there was again no significant difference in amplitude between the WT (n = 7) and SOD1 (n = 8) mice at both sites (Fig. 27C; $p > 0.05$). This differs from what was observed in the LTN–CMM system as there was a significant decrease in the CMAP amplitude at the caudal site by 60 days, whereas in the sciatic nerve there was no decrease in the amplitudes at either stimulating site. Only at 90 days were we able to detect a significant decrease in the CMAP amplitudes in the sciatic nerve for both the distal ($p = 0.050$) and proximal stimulation sites ($p = 0.003$) (Fig. 27D; WT n = 18, SOD1 n = 19). The ability to detect degeneration earlier in the LTN–CMM system makes it a more robust and attractive model to study the earliest time point of degeneration in the SOD1 mice.

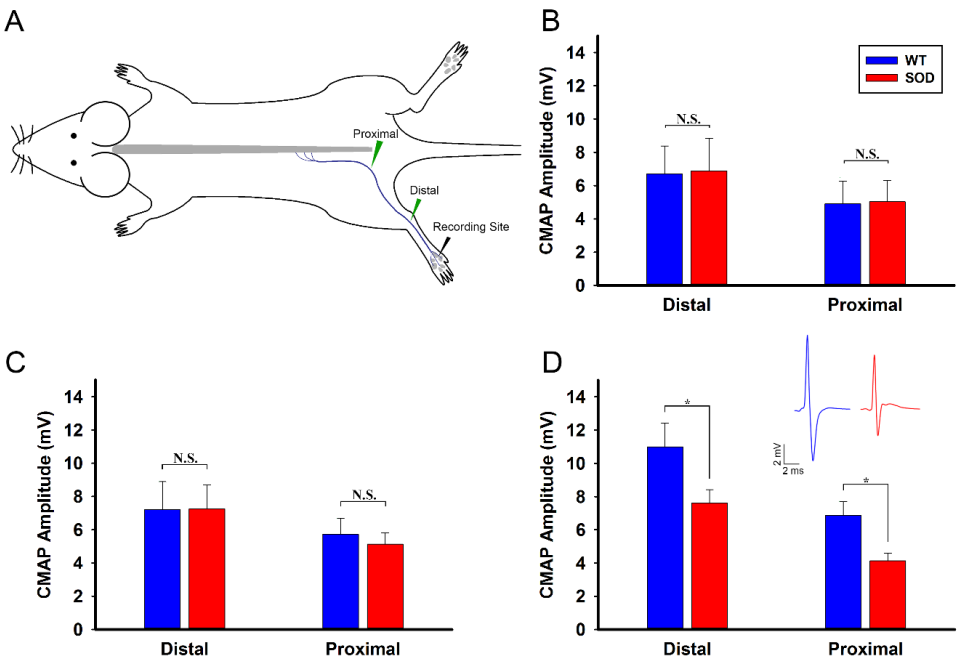

Fig. 27. The sciatic nerve shows a decrease in CMAP amplitude at 90 days.

(A) Schematic diagram showing electrode placements for the left sciatic nerve recordings. The recording electrodes were placed in the foot pad as indicated by the black electrode. The sciatic nerve was stimulated separately at each of the green electrodes with the proximal or distal stimulation sites labeled. The proximal site was located 31 mm from the recording electrodes and the distal site was 12 mm from the recording electrodes. (B) At 30 days old, SOD1 mice (red, n = 6) show no significant difference in recordings for both the distal and proximal stimulating sites when compared with WT mice (blue, n = 6). (C) Again, at 60 days of age, SOD1 mice (red, n = 8) do not show any significant difference from the WT mice (blue, n = 7). (D) Only at 90 days of age do SOD1 mice show a significant decline in the CMAP amplitudes when stimulated at either the distal or proximal sites. The inset shows representative traces at the proximal site in WT mice (blue, n = 18) and SOD1 mice (red, n = 19) at 90 days old. Bars represent mean ± standard error. ∗ indicates $p < 0.05$. *C. Tallon, K. A. Russell, S. Sakhalkar, N. Andrapallayal, M. H. Farah, Length-dependent axo-terminal degeneration at the neuromuscular synapses of type II muscle in SOD1 mice. Neuroscience 312, 179-189 (2016).*

Limited sprouting of the surviving LTN axons

Next, we searched for evidence of axonal sprouting from the surviving axons in the SOD1 mice. To do this, we used the same preparations as those used to characterize the extent of NMJ denervation and looked for the presence of extremely thin terminal sprouts. Terminal sprouting was not robust in the 30-day-old mice, as was expected given the lack of degeneration seen in Fig. 24. We detected some sprouting at the caudal and medial sites in both the 60- and 90-day-old SOD1 mice (Fig. 28). Figs. 28A–C show an image of two terminal sprouts in a 60-day-old SOD1 mouse as indicated by the white arrows in Fig. 28C. While there was evidence of sprouting, there was a very limited sprouting at 60 days (Fig. 28D, red bars, n = 5). At the caudal region only 0.35% of NMJs had a terminal sprout and the medial region had 0.42%. There were no sprouts detected at the rostral region as there was no denervation observed to initiate the sprouting machinery. At 90 days, when the degeneration was more extensive, there was an increase in the percentage of NMJs with terminal sprouts (Fig. 28D, blue bars, n = 6). The caudal, medial, and rostral regions had 1.47%, 1.0%, and 0.54% of NMJs with terminal sprouts respectively. Despite this increase, the extent of sprouting is still very limited and cannot keep up with the degenerative process. The presence of these sprouts, however limited, does indicate that type II fibers do have the capacity for some limited regeneration in the SOD1 mouse model. With the advantage of being able to whole mount the intact CMM, we were able to image the origin of the sprouts and easily determine whether it was a terminal sprout or not. The LTN–CMM system provides a unique model to selectively investigate potential strategies for axonal protection and enhancing regeneration of type II motor fibers in SOD1 mouse models.

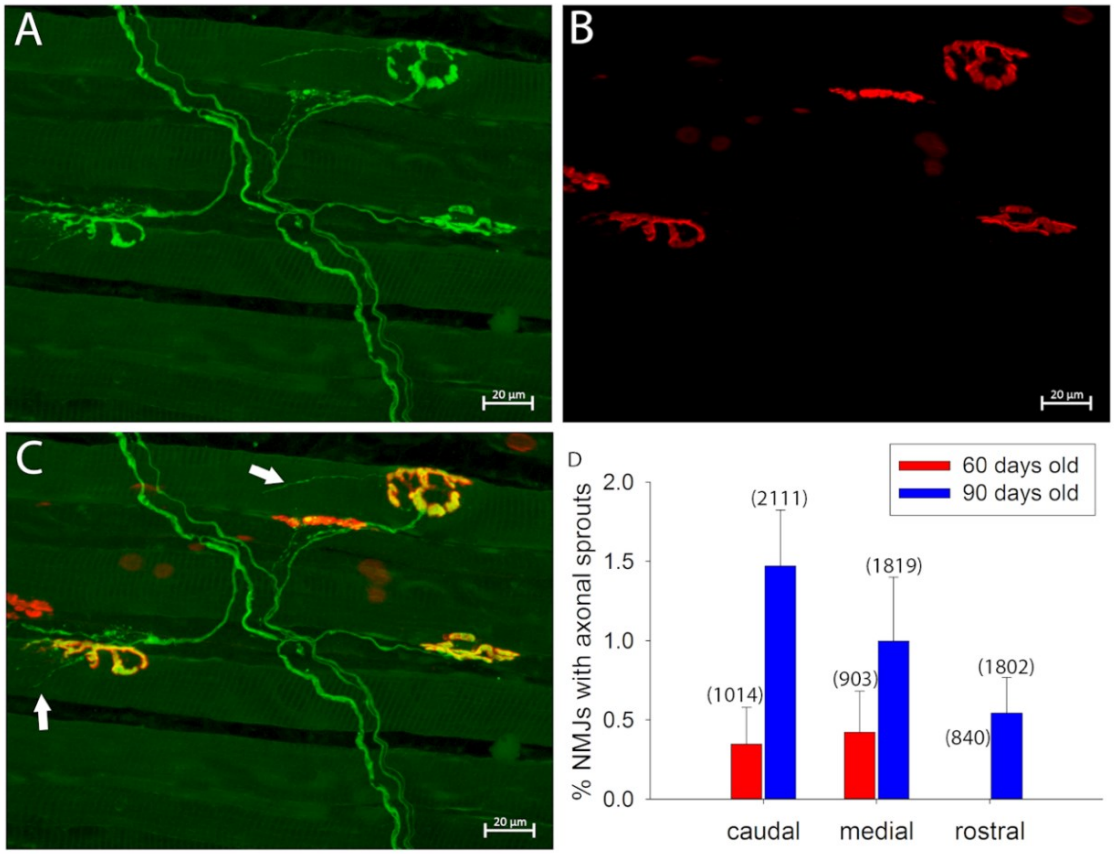

Fig. 28. SOD1 mice show very limited axonal sprouting.

(A–C) Representative images of sprouting in a 60-day-old SOD1 mouse (A) YFP labeled motor axons and presynaptic terminals. (B) α-bungarotoxin labeled NMJs. (C) Combined images of (A) and (B) showing that the medial region in an SOD1 mouse has the capacity for axonal sprouting with terminal sprouts indicated by white arrows. (D) Quantification of the percentage of NMJs with terminal sprouts at the three regions (caudal, medial, and rostral). 60-day-old mice are shown in red (n = 5). Ninety-day-old mice are shown in blue (n = 6). Numbers in parenthesis indicate the number of NMJs counted. Bars represent mean ± standard error. *C. Tallon, K. A. Russell, S. Sakhalkar, N. Andrapallayal, M. H. Farah, Length-dependent axo-terminal degeneration at the neuromuscular synapses of type II muscle in SOD1 mice. Neuroscience 312, 179-189 (2016).*

Summary of chapter 5

In this chapter, we identified a length dependent degeneration pattern of the LTN in the SOD1^{G93A} mouse model of ALS. The longest axons reaching the caudal region of the CMM were the first to show evidence of denervation by 2 months of age. As the mice aged, the degeneration moved further up the CMM towards the shorter axons in the rostral region. We determined that the earliest time point of detectable denervation occurred around 2 months of age, which was 1 month earlier than the window of detectable denervation in the sciatic nerve system. We were also able to identify evidence of a very limited amount of terminal axonal sprouts from the surviving axons at 2 and 3 months of age. Based on this data, we determined that the optimal treatment window for BACE1 inhibitors would be to begin treatment when the mice are 1 month old, before significant degeneration is detected, in order to maximize the effects the inhibitors may have on reinnervation.

Chapter 6: BACE1 inhibitors as potential therapeutics to enhance peripheral nerve regeneration in the ALS mouse model

Introduction

Following our characterization of the LTN-CMM system in the SOD1^{G93A} mouse model of ALS, we were able to determine that the optimal time to begin the BACE1 inhibitor treatment was when the mice were 1 month of age. This time point allowed us to start treatment before any significant denervation was detected in the CMM and would therefore provide the greatest chance of exerting any effect on the extent of innervation. In order to monitor whether the BACE1 inhibitors were having any effect on NMJ innervation, we used the same end point analyses used to determine the degeneration profile, namely the percent of innervated NMJs and the amplitude of the CMAP along the CMM. In addition to determining whether there was any effect on the level of innervation in these mice, we also explored whether BACE1 inhibitors would be able to enhance the limited terminal sprouting identified in the previous chapter. Based on our findings in the partial nerve transection study with the BACE1 inhibitor administration, we hypothesize that we will also find an increased level of sprouting in the BACE1 inhibitor treated SOD1 mice. We also set out to investigate a possible mechanism for how BACE1 inhibition may be influencing expression levels of the cell adhesion molecule CHL1, a RAG that is also cleaved by BACE1.

Results

BACE1 inhibitors improve muscle innervation and electrophysiological values in an ALS mouse model after 1 month of treatment

After determining the progression of axonal degeneration in the early stages of disease in the $SOD1^{G93A}$ mouse model of ALS (*112*), we were able to use this data as a way of determining a dosage schedule for the BACE1 inhibitors. At 1 month of age, the mice did not have much degeneration, as evident by the complete innervation of the CMM. By 2 months, we saw degeneration beginning to occur in the longest LTN axons innervating the region closest to the tail. Based on this observation, we began treating the mice with either the vehicle or inhibitor at 1 month of age, before degeneration becomes apparent. We then allowed the mice to continue eating the vehicle or inhibitor food for another month before performing electrophysiological recordings at the caudal region of the CMM and then collecting the CMM for morphological analysis.

We performed these experiments with the more clinically relevant MBI-9 BACE1 inhibitor. After imaging the CMM from vehicle and inhibitor treated mice, it was apparent that there was a difference in the extent of innervation between the two conditions. At the caudal region, where the longest axons were reaching, the vehicle treated mice appeared to have fewer innervated NMJs than the inhibitor treated mice (Figure 29 A and B). Following quantification of the percentage of completely innervated NMJs in the vehicle and inhibitor treated mice, we observed a significantly greater percentage of innervated NMJs in the inhibitor treated mice compared to those with vehicle (Figure 29C; Vehicle = 56.40±0.378%, n=3; Inhibitor = 87.27±0.797%, n=3; p = 3.98E-6). The inhibitor treated mice still had fewer innervated NMJs than the WT mice,

however (Figure 29C; WT = 100%, n=3; p = 8.96E-5). At the medial region, we did not observe any significant difference between the vehicle and inhibitor treated mice, most likely due to there being only minimal degeneration present (Figure 29C; Vehicle = 92.519±3.231%; Inhibitor = 96.187±2.515%; p = 0.421). When we recorded the caudal CMAP amplitudes in vehicle and inhibitor treated mice we saw significantly greater amplitudes in the inhibitor treated mice than the vehicle treated mice (Figure 29 D and E; p = 0.0103). The vehicle treated mice had an amplitude of 0.916 ± 0.0636mV (n=23) while the inhibitor treated mice had an amplitude of 1.238 ± 0.091mV (n=23). Despite there being a deficit in the percentage of innervation between the inhibitor treated SOD1 mice and the WT mice, the innervation that was present in the inhibitor treated mice was sufficient to bring their amplitudes to a similar value as those of the WT mice (WT = 1.108 ± 0.0608mV, n=25; p = 0.225).

Fig. 29. 1 month MBI-9 BACE1 inhibitor treatment improves morphological and physiological repair in SOD1 mice.

(A-B) Representative images of the CMM from the caudal section of a mouse treated for 1 month with vehicle (A) and the Merck inhibitor (B). Axons labeled green and NMJs labelled with red α-BTX. (C) Quantification after 1 month of treatment of the percentage of NMJs that are fully innervated in uninjured WT (black, n=3), vehicle treated SOD1 (blue striped, n=3), and inhibitor treated SOD1 mice (red dotted, n=3). At the caudal region, while the SOD1 treated with inhibitor had significantly fewer innervated NMJs compared to uninjured WT mice, there was a large, significant improvement in innervation from vehicle treated SOD1 mice. At the medial region, the disease had not progressed far enough for a significant reduction in innervation with either vehicle treatment or inhibitor treatment. Numbers in parenthesis represent total number of NMJs counted. WT n=; vehicle n=; inhibitor n= (D) Representative traces of CMAP recordings at the caudal site from vehicle treated SOD1 mice (blue) and inhibitor treated SOD1 mice (red). (E) Quantification of the average CMAPs recorded from WT mice (black), vehicle treated SOD1 mice (blue striped), and inhibitor treated SOD1 mice (red dotted). Inhibitor treatment significantly enhanced CMAP recordings when compared with vehicle treated SOD1 mice. There was no significant difference in CMAP recordings between inhibitor treated SOD1 mice and WT mice. WT n=25, vehicle n=23, and inhibitor n=23. Bars represent mean ± standard error. * indicates $p < 0.05$.

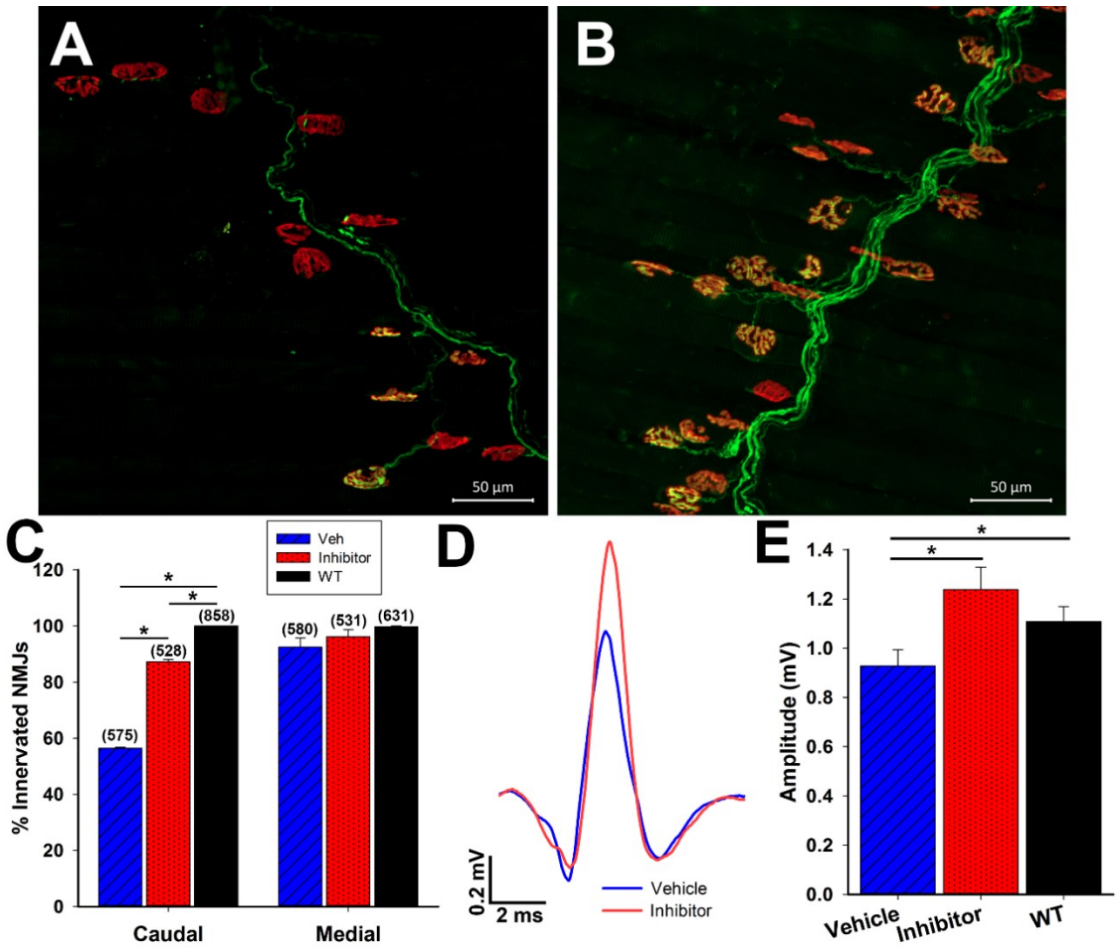

In addition to the MBI-9 BACE1 inhibitor, we also wanted to carry out these experiments with a second BACE1 inhibitor to rule out the differences being due to the drug specifically and not general BACE1 inhibition. We followed the same dosing schedule with the LY2886721 BACE1 inhibitor and once again monitored the extent of innervation of the CMM as well as the CMAP amplitudes in mice treated with the LY2886721 inhibitor and compared it to the vehicle treated mice. Like the MBI-9 inhibitor, there was a significant increase in the percentage of innervated NMJs in the inhibitor treated mice compared to the vehicle treated mice (Figure 30A; vehicle = 56.40±0.378%, n=3; Inhibitor = 81.901±5.562%, n=3; p = 0.0102). We also observed an

improvement in the CMAP amplitudes of the inhibitor treated mice compared with the vehicle treated mice (Figure 30B; Vehicle = 0.339±0.0538 mV, n=12; Inhibitor = 0.530±0.0619 mV, n=14; p = 0.017). Together with the MBI-9 data, we determined that pharmacologically inhibiting BACE1 for 1 month led to increased NMJ innervation in the SOD1^{G93A} ALS mouse model. This improved NMJ innervation is also reflected in the CMAP amplitudes recorded from inhibitor treated mice.

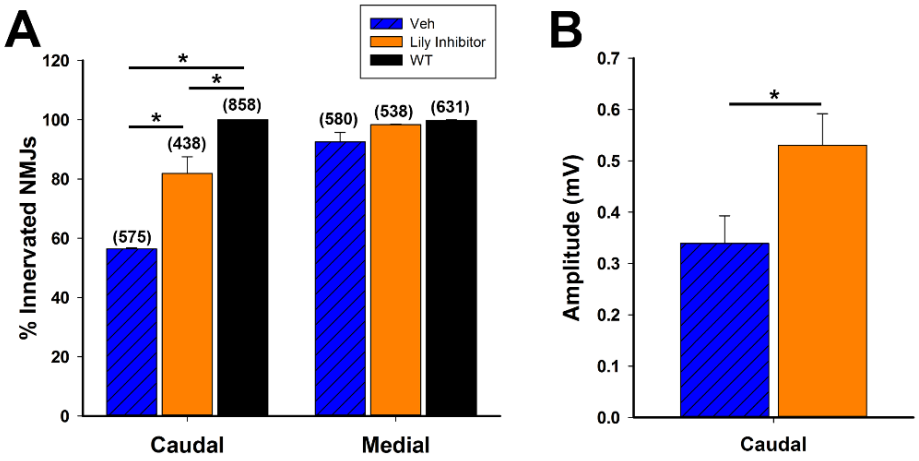

Fig. 30. 1 Month of LY2886721 BACE1 inhibitor treatment enhances morphological and electrophysiological values in SOD1 mice.

A) Quantification of the percentage of innervated NMJ from WT (black, n=3), vehicle treated SOD1 mice (blue, n=3), or LY2886721 treated SOD1 mice (orange, n=3). LY2886721 treatment greatly increased NMJ innervation compared to vehicle. B) Quantification of the CMAP amplitudes recorded from vehicle and inhibitor treated mice. LY2886721 treatment improved the amplitudes of the CMAPs recorded at the caudal site compared with the vehicle treated mice. Vehicle n=12 and inhibitor n=14. Bars represent mean ± standard error. * indicates $p < 0.05$.

BACE1 inhibitor treatment only improves morphological repair after 2 months of treatment

After determining that BACE1 inhibition is able to improve both morphological and physiological function following 1 month of treatment, we next extended the treatment window and determined whether there was any improvement following 2 months of treatment. Like the 1 month treatment, we began treating the mice with the MBI-9 BACE1 inhibitor at 30 days of age and allowed them to continue on the treatment for 2 months before performing electrophysiological recordings and collecting the CMM for morphological analysis. Qualitative observations indicated that the BACE1 inhibitor treated mice had an increased number of innervated NMJs when compared with the vehicle treated mice (Figure 31 A and B). Following quantification (Figure 31C), the inhibitor treated mice had significantly higher innervation than the vehicle treated mice at the caudal (vehicle 35.57±6.614%, n=6; Inhibitor = 53.45±4.823%, n=7; p = 0.0477), medial (vehicle 43.89±5.23%, n=6; Inhibitor = 69.25±6.136%, n=7; p = 0.0104), and rostral region (vehicle 62.28±6.714%, n=6; Inhibitor = 83.41±2.826%, n=7; p = 0.0107). Despite the increased innervation with the inhibitor treatment, the disease progression appears to have continued with lower innervation percentages compared to the inhibitor treated values after 1 month of treatment. The further progression of the disease is also reflected in the electrophysiological analysis of the CMAP amplitude after 2 months of treatment (Figure 31 D – F). While the caudal region following 1 month of treatment showed a significant increase in the amplitude, after 2 months of treatment we were only able to observe a very weak trend at both the caudal (Figure 31D; Vehicle 0.398±0.0345 mV, n=34; Inhibitor = 0.457±0.0526 mV, n=36; p = 0.668) and medial (Figure 31E;

Vehicle 1.838±0.199 mV, n=34; Inhibitor = 2.12±0.216 mV, n=36; p = 0.335) region of the CMM. At the rostral region, there was virtually no difference between the inhibitor and vehicle treated mice (Figure 31F; Vehicle 6.713±0.548 mV, n=34; Inhibitor = 6.589±0.509 mV, n=36; p = 0.925). We hypothesize that this loss of significance following 2 months of treatment may be due to the disease process overwhelming the repair process.

Fig. 31. 2 month Merck BACE1 inhibitor treatment improves morphological repair but not functional repair.

(A-B) Representative images of the CMM from the caudal section of a mouse treated for 2 months with vehicle (A) and the Merck inhibitor (B). Axons labelled green and NMJs labelled with red α-BTX. (C) Quantification after 2 months of treatment of the percentage of NMJs that are fully innervated in uninjured WT (black, n=3), vehicle treated SOD1 (blue striped, n=6), and inhibitor treated SOD1 mice (red dotted, n=7). At this stage, the disease has progressed far enough to be able to detect a significant drop in innervation at all three locations along the CMM in vehicle treated SOD1 mice. Inhibitor treated mice had significantly more innervated NMJs compared with the vehicle treated mice. Numbers in parenthesis represent total number of NMJs counted. (D-F) Quantification of the CMAP recordings in vehicle treated SOD1 (blue striped, n=34), and inhibitor treated SOD1 mice (red dotted, n=36) at the caudal (D), medial (E), and rostral sites (F). There was no significant difference between the vehicle and inhibitor treated mice at all three regions however, there is a very weak trend with the inhibitor having a small improvement in amplitude at both the caudal (D) and medial regions (E). Bars represent mean ± standard error. * indicates $p < 0.05$.

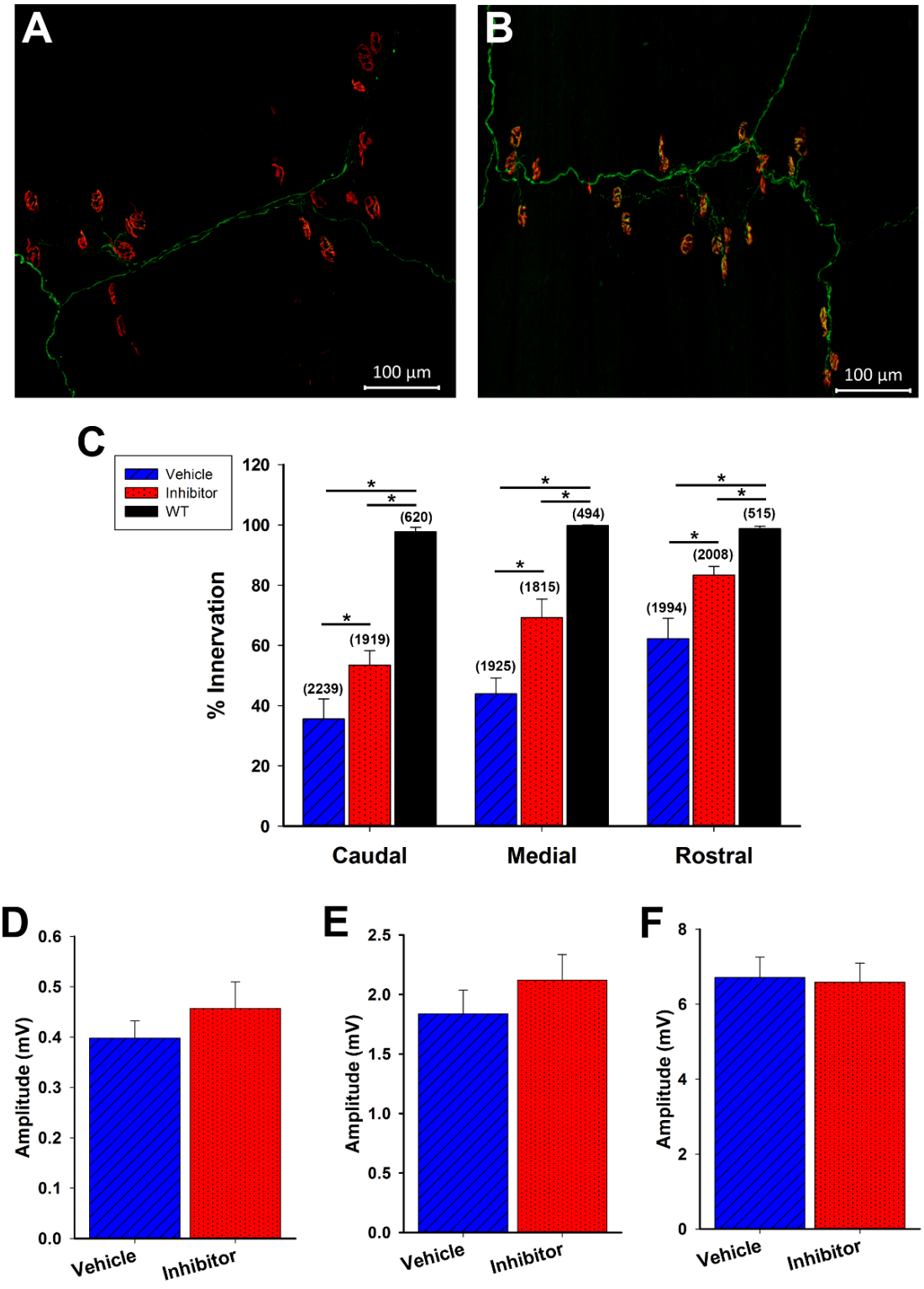
A
100 µm
B
100 µm
C
Vehicle
Inhibitor
WT
% Innervation
120
100
80
60
40
20
0
(2239)
(1919)
(620)
(1925)
(1815)
(494)
(1994)
(2008)
(515)
*
Caudal
Medial
Rostral
D
Amplitude (mV)
0.6
0.5
0.4
0.3
0.2
0.1
0.0
Vehicle
Inhibitor
E
Amplitude (mV)
2.5
2.0
1.5
1.0
0.5
0.0
Vehicle
Inhibitor
F
Amplitude (mV)
8
6
4
2
0
Vehicle
Inhibitor

Axonal sprouting is enhanced by reducing BACE1 activity

To further understand whether this increased innervation following BACE1 inhibition in the SOD1 mouse was due to a neuroprotective effect or increased reinnervation, we investigated the extent of terminal axonal sprouting. As determined earlier, the extent of axonal sprouting in SOD1 mouse at 60 days of age was extremely minimal (*112*). We observed very few sprouts in both vehicle and inhibitor treated mice however it appeared to be slightly easier to capture an image of sprouts in the inhibitor treated mice compared (Figure 32 A-B). More mice need to be studied in order to definitively conclude that one month of inhibitor treatment enhances axonal sprouting.

By the time the mice are 3 months of age, the extent of axonal sprouting has increased and it is easier to capture images of axonal sprouts. Figures 32C and D showcase representative images from vehicle treated and inhibitor treated caudal regions, respectively. There were many more visible terminal axonal sprouts in the inhibitor treated mice compared to vehicle treated mice, as indicated by the white arrows. Following quantification, there was a significant increase in the percentage of NMJs with the presence of one or more terminal axonal sprouts (Figure 32E; Vehicle 3.52±0.989%, n=6; Inhibitor = 9.29±1.976%, n=6; $p = 0.026$). Based on this finding that terminal axonal sprouting was increased following BACE1 inhibitor treatment in the SOD1 mouse, we believe that the increased innervation is due to enhanced axonal reinnervation and is not due to a neuroprotective effect.

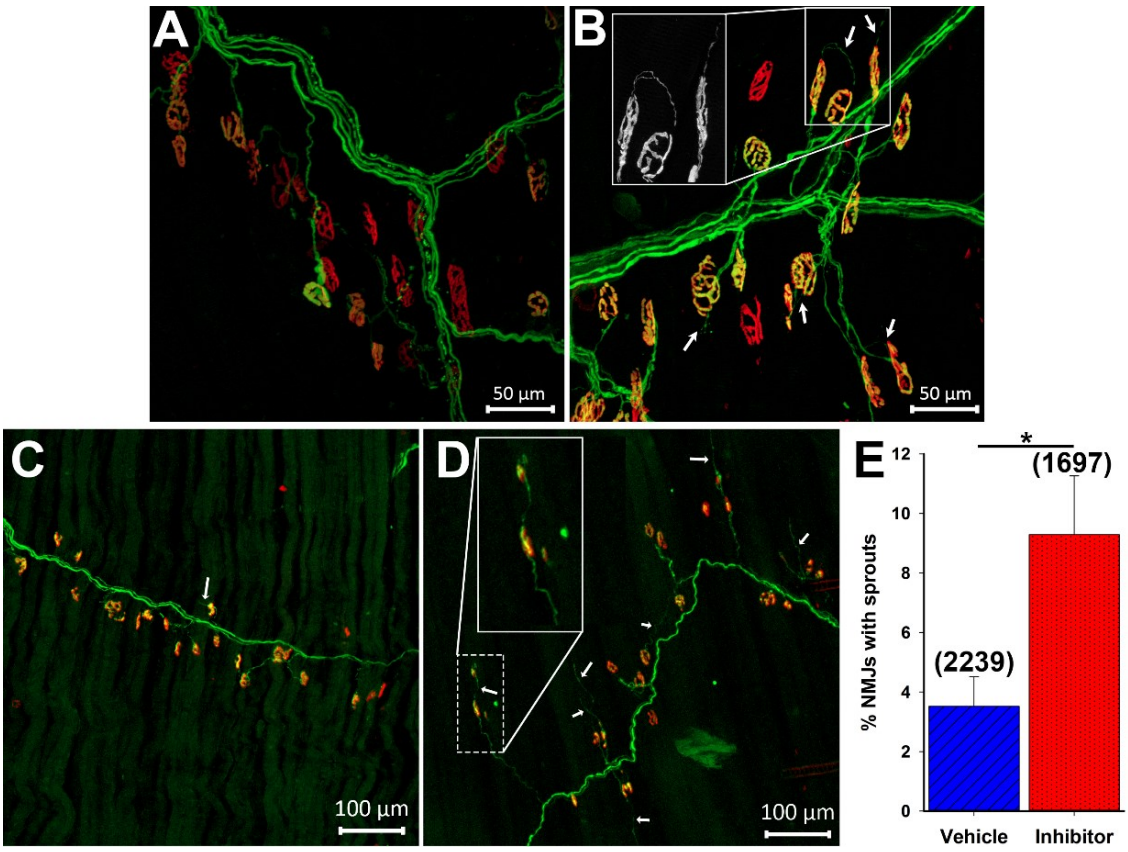

Fig. 32. BACE1 inhibition enhances axonal sprouting in disease.

(A-B) Representative sprouting images of SOD1 mice treated for 1 month with vehicle (A) or the inhibitor (B). Axons are labeled green and NMJs are labeled red. White arrows point to terminal axonal sprouts. Inset shows magnified terminal axonal sprout. (C-D) Representative sprouting images of SOD1 mice treated for 2 months with vehicle (C) or the inhibitor (D). Inset shows magnified terminal-to-terminal axonal sprout. (E) Quantification of the percentage of NMJs with terminal sprouts after 2 months of treatment. Mice treated with BACE1 inhibitors (n=6) have an increased percentage of NMJs with terminal axonal sprouts compared to vehicle treated mice (n=6). Numbers in parenthesis represent total number of NMJs counted. Bars represent mean ± standard error. * indicates $p < 0.05$.

L1/CHL1 expression levels are increased in SOD1^{G93A} mice following BACE1 inhibition

After determining that BACE1 inhibitors increase NMJ innervation in the early stages of disease in the SOD1 mouse, most likely via enhanced axonal sprouting, we next explored a potential molecular mechanism for how this phenomenon was occurring. Since BACE1 is a fairly promiscuous enzyme, we decided to narrow our initial investigation to a logical, well-known candidate. In order for axons to sprout and be guided towards a target they need to interact with the supporting Schwann cell tubes. We therefore hypothesized that BACE1 may be modulating expression levels of neuronal adhesion molecules as a way of controlling this axon-Schwann cell interaction. Previously, CHL1, a neuronal cell-cell adhesion molecule, had been identified and verified as a known substrate of BACE1 (*49*). We decided to investigate whether the levels of full-length CHL1 was altered in SOD1 mice treated with a BACE1 inhibitor. After collecting the spinal cord and processing the tissue for Western blot analysis, we observed a significant increase in the normalized intensity of the inhibitor treated bands compared with the vehicle treated bands (Figure 33A and B; Vehicle = 0.868±0.0419, n=4; inhibitor = 1.032±0.216, n=4; p=0.0149). We believe that this data lends some support to our hypothesis that BACE1 activity levels modulate expression levels of full-length adhesion molecules as a way of regulating axonal outgrowth. While fairly preliminary, we plan on continuing this hypothesis and further validating it in future experiments.

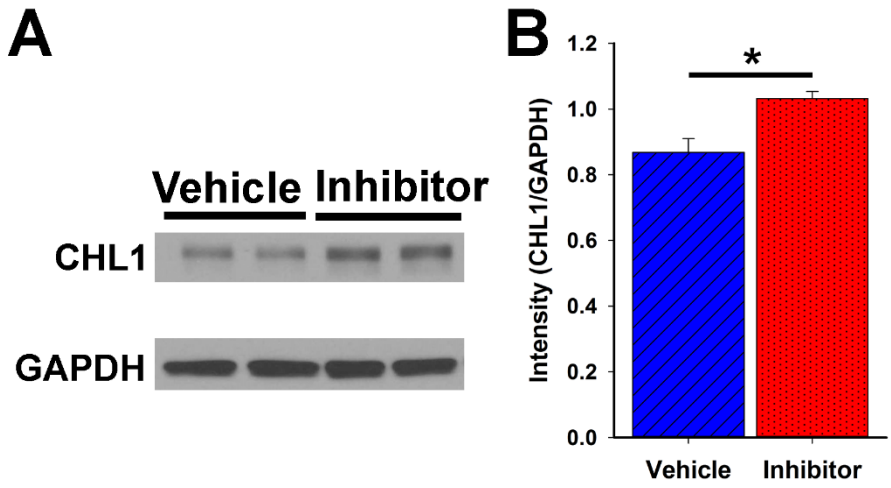

Fig. 33. BACE1 inhibition alters L1/CHL1 expression levels in SOD1 mice.

(A) Representative Western blot of spinal cord tissue collected from SOD1^{G93A} mice following 1 month of either vehicle or BACE1 inhibitor treatment. GAPDH was used as a loading control for normalization calculations. (B) Quantification of the Western blots following normalization of the CHL1 band intensity to the GAPDH band intensity. BACE1 inhibitor treatment led to a significant increase in the intensity of the CHL1 bands. Bars represent mean ± standard error. * indicates $p < 0.05$.

Summary of chapter 6

Based on the data presented in this chapter, we determined that pharmacological inhibition of BACE1 was able to improve NMJ innervation and CMAP amplitudes in the SOD1 mice after 1 month of treatment. When we extended the treatment time to 2 months, we still observed improved NMJ innervation, however, a significant improvement of the CMAP amplitude was lost. This lack of functional improvement may be attributed to the progression of the disease already beginning to overwhelm the repair process or the motor unit size may be too large due to the progressive loss of viable axons

available for sprouting. Indeed, we did see an increased percentage of NMJs which had terminal sprouts after 2 months of treatment, indicating that the greater percentage of innervated NMJ may be in part due to increased axonal sprouting from intact axons. We were also able to detect a significant increase in the expression level of full length CHL1, providing early evidence that CHL1 processing by BACE1 may be a mechanism by which axons are able to regulate the extent of axonal regeneration and sprouting that occurs as a result of peripheral nerve injuries.

Chapter 7: Conclusions

Overall, this dissertation set out to explore 3 major questions pertaining to how BACE1 activity levels are related to peripheral nerve regeneration. The first was whether neuronal BACE1 overexpression led to impaired axonal regeneration, in contrast to improved regeneration observed in BACE1 KO mice. The second was to determine if BACE1 inhibitors can enhance peripheral nerve regeneration and axonal sprouting following acute nerve injuries. Finally, the third question was to identify if BACE1 inhibitors could improve early regeneration in the $SOD1^{G93A}$ mouse model of ALS. In the first portion of the data presented here, we were able to show that transgenic mice that overexpress human BACE1 in their neurons do have impaired axonal regeneration following a sciatic nerve crush, without any differences in macrophage recruitment and axonal debris clearance. Together with the BACE1 KO studies conducted earlier, we can conclude that BACE1 activity levels do inversely influence peripheral nerve regeneration. We were then able to take this relationship and apply it as a way of therapeutically enhancing peripheral nerve regeneration and sprouting in both a nerve crush and a partial nerve transection injury model by administering BACE1 inhibitors following injury. In addition to enhancing peripheral nerve repair following acute injuries, we also demonstrated that BACE1 inhibitor treatment can improve NMJ innervation in the early stages of disease in an ALS mouse model. These major findings have many implications beyond their therapeutic potential and also provide insight into how we can model peripheral nerve injuries, ways that the repair machinery is able to regulate peripheral nerve regeneration, and possible insights into ways that disease and aging may further complicate axonal regeneration. The implications of these major

findings, as well as other potential conclusions that may be considered as a result of these findings, are discussed in greater detail below.

Increased BACE1 activity levels are detrimental to peripheral nerve repair

We had previously shown that knocking out BACE1 enhances regeneration following a sciatic nerve crush (*25*). Taken together with the results outlined in chapter 2, it would seem that BACE1 activity levels are involved in regulating the activation or inhibition of the repair process in neurons after injury. Based on what we have observed, there is an inverse relationship between the levels of BACE1 expression and the effectiveness of peripheral nerve regeneration. When BACE1 activity levels are high, peripheral nerves have a reduced regeneration response. Since a crucial component to whether or not the peripheral nervous system is effective at repairing itself after injury is the time it takes the axons to reach their target (*9*), having an excessive amount of BACE1 present could be detrimental to the recovery process. In fact, it may be interesting to explore endogenous BACE1 activity levels in animals that have different rates of axonal growth and explore whether there is any correlation between the level of BACE1 expression following injury and the rate of axonal growth. That this data identifies high levels of BACE1 activity as being detrimental to peripheral nerve regeneration, it suggests that administering a BACE1 inhibitor to patients after suffering a peripheral nerve injury could help improve their functional recovery. Fortunately, BACE1 inhibitors are currently being heavily investigated for safety and efficacy by numerous pharmaceutical companies with regards to AD and would therefore be a very

attractive route to explore in terms of therapeutically improving peripheral nerve regeneration (*42, 164, 176*). We were able to exploit this interest in developing BACE1 inhibitors and obtained multiple drugs to use in my studies regarding potential therapeutics for treating peripheral nerve injuries.

Potential BACE1 mechanisms

In addition to understanding how BACE1 activity levels influence peripheral nerve regeneration following a peripheral nerve injury, the use of mice that selectively overexpressed BACE1 in their neurons provided interesting insight into whether the changes in regeneration due to BACE1 expression levels could be isolated to the neuron alone or whether the changes required altered expression levels in the supporting cells as well. The results presented in chapter 2 indicated that BACE1 overexpression within the neuron is sufficient to impair regeneration without altered levels in macrophages or Schwann cells. However, a peripheral axon injured by trauma or disease is always in close contact with a Schwann cell membrane and that interaction is required for regrowth. Two substrates of BACE1, L1 and CHL1 (*49, 159*), might be the neuronal molecules that BACE1 acts through in regulating peripheral axon regeneration. CHL1 promotes neurite outgrowth in culture and possibly does so in vivo through Schwann cell–regenerating axon interaction (*98, 177*). L1 also promotes the outgrowth of cultured dorsal root ganglion neurites on co-cultured Schwann cells (*178, 179*). By potentially increasing their cleavage, the BACE1 Tg axons may have less interaction with Schwann cell tubes. Conversely, it may be hypothesized that reducing BACE1 expression may lead to increased levels of full length L1/CHL1 on regenerating axons, which could potentially

enhance the interactions between Schwann cells and axons, leading to enhanced outgrowth. Further studies need to be conducted in order to rule out whether the regeneration deficits in BACE1 Tg mice are solely due to a neuronal component or whether it is based on the interactions between the Schwann cell and axon involved in the regenerative process. It would also be beneficial to carry out nerve injury experiments in conditional KO mice that specifically lack BACE1 in neurons, Schwann cells, or macrophages separately to further tease out the individual roles of each cell type.

BACE1 activity levels may be further complicating repair in disease and ageing

The finding of reduced regeneration in BACE1 Tg mice also has interesting implications for other neurodegenerative diseases, especially AD. It is now well known that BACE1 activity is required for the generation of Aβ peptides present in the plaques found in AD (*15, 39, 41, 180*). In AD brains, elevated levels of BACE1 have been identified in addition to the amyloid beta plaques (*181-183*). In mice overexpressing human BACE1, neurodegeneration was apparent by 6 months of age, with or without the presence of plaques, suggesting that the formation of plaques may not be necessary for neurodegeneration (*44*). The increased neurodegeneration seen in these mice coupled with our finding that BACE1 overexpression leads to impaired regeneration supports BACE1 inhibitors as a potential therapy for AD. The benefits would be two-fold: Firstly, inhibiting BACE1 would reduce the neurodegeneration occurring. Secondly, lowering BACE1 activity levels could help to improve axon regeneration.

These findings may also shed some light on to the mechanisms underlying poorer regenerative repair seen with aging peripheral nerves (*14, 184-188*). While studies on BACE1 activity levels in the aging peripheral nervous system have not been performed, an increase in BACE1 activity has been seen in aging mouse, monkey and human brains (*189*). This increase in activity has been hypothesized as a potential reason why AD is a disease of aging, since increased BACE1 activity leads to increased Aβ production (*189*). The findings in outlined in chapter 2 indicate that an increase in BACE1 expression and activity leads to impaired axonal repair. If the increased BACE1 activity associated with aging, as seen in the central nervous system (*181-183*), holds true in the peripheral nervous system, this may be a potential mechanism underlying reduced axonal repair in elderly patients. This has clinical significance as it may also be beneficial to provide elderly patients with a BACE1 inhibitor after undergoing nerve damage to help improve repair and recovery.

The LTN-CMM system is useful for studying peripheral nerve repair following acute nerve trauma and in neurodegenerative diseases

In order to accurately study whether BACE1 inhibitors would have an impact on peripheral nerve regeneration, we wanted to develop a system that would provide an easy way to consistently perform a partial nerve transection and easily trace the origin and end point of axonal sprouts. In chapter 4, we were able to show that the LTN-CMM system is a good model for performing partial nerve transection injuries and monitoring the sprouting response following BACE1 inhibitor treatment. The LTN innervates only a single muscle, the CMM, and has a nicely conserved branching pattern that can be easily

accessed before it enters the CMM. This branching pattern made the CMM advantageous over the sciatic nerve because it allowed greater control over the percentage of axons that were left intact and is a much simpler surgery to perform than trying to access the ventral roots to perform a more constant sciatic nerve injury. We were also able to trace axonal sprouts in detail throughout the CMM which allowed for accurate quantification of the extent of axonal sprouting. Due to the anatomy of how the CMM is innervated by the LTN and the sensory nerve, it is possible to remove a large portion of the sensory nerves, making it easier to image the motor axons and its axonal sprouts. The CMM is also a very thin muscle and is easy to whole mount and stain, providing the ability to visualize all the axons innervating all the NMJs as well as the extremely thin axonal sprouts. Imaging axonal sprouts is very challenging in thicker muscle whole mounts and an even greater challenge in muscle sections as they must be reconstructed in order to accurately quantify an axonal projection as a terminal sprout.

In chapter 5 we were able to show that the LTN-CMM system is also a good candidate for monitoring changes in the SOD1^{G93A} ALS mouse model. By using the LTN–CMM system, it allowed us to observe that the longer axons in the caudal region showed more extensive degeneration at 60 days of age, while the shorter rostral region only had moderate degeneration at 90 days. This degeneration was detected by both the extent of NMJ denervation as well as a functional decline using electrophysiological recordings of the CMAP. Fischer et al. (*132*) showed that the degeneration in the SOD1 mouse model begins in the periphery, long before it is observed at the level of the spinal cord. While this study was instrumental in understanding that ALS is a peripheral neuropathy, it did not study in depth how the length of the peripheral axons affects their

susceptibility for degeneration. They sectioned the gastrocnemius, soleus and tibialis muscles to determine the extent of degeneration. Each of these muscles is innervated by nerves of similar length in the mouse. The data presented in chapter 5 fills in this gap by providing evidence that the longer the axon, the earlier it degenerates. The ability to study length-dependent degeneration in peripheral axons is easier to perform in the LTN–CMM system as axons of different lengths can be studied within the same muscle preparation. This is much easier than having to look at different muscles to generate a large difference in axon length. We were also able to record electrophysiological data from three different lengths within the same muscle to generate more information about how there is a length-dependent functional decline. Using the CMM also allows for the entire muscle to be stained and whole mounted. By being able to collect all of this information from a single muscle, the LTN–CMM system is a much simpler system to study length-dependent degeneration.

Another characteristic that makes the LTN-CMM system so attractive for studying axonal regeneration and sprouting is that it is a type II muscle. Motor fibers that innervate fast-fatigable, type IIb muscle fibers have a lower capacity for sprouting in response to Botulinum A toxin induced sprouting compared to slow twitch, type I fibers (*88*). We were able detect a low level of axonal sprouting from the LTN in WT mice following a partial nerve transection. While the sprouting is very limited, the presence of a basal capacity for axonal sprouting provides an interesting system to determine whether compounds can enhance this sprouting capacity and potentially improve repair outcomes. Additionally, the LTN-CMM system could be used to explore whether BACE1 inhibition could be used to coax these sprouting resistant motor fibers to sprout under an even more

hostile sprouting environment. In SOD1 mice, it has been shown that there is a limited amount of intrinsic sprouting in the early stages of the disease. As the disease progresses, this capacity for sprouting gets overwhelmed and cannot keep up with the rate of degeneration (*87*). Due to the LTN–CMM system being made up of only sprouting resistant, type II motor fibers, we first examined the extent of sprouting in the SOD1 mouse in order to determine whether this limited sprouting could be detected. While there was some evidence of a few sprouts in some of the SOD1 mice, most of these sprouts did not seem to be directed toward areas of denervation in particular. If a compound could be used to enhance sprouting in the LTN-CMM system, it may be able to improve reinnervation in the early stages of the disease and possibly lead to prolonged motor function.

Another reason for using the LTN-CMM system to study disease progression and potential therapeutics is that previous studies have shown that each muscle fiber type is affected differently, with type IIb being the most susceptible to denervation in the SOD1 mouse (*88, 134, 137, 169*). The varying time points of degeneration in the different types of motor fibers confound the investigation of the effect of axon length on degeneration, as various regions have unique motor fiber type makeups. If one region consists of more type IIb fibers, then it may show greater degeneration compared to a longer region consisting of more type I fibers. The LTN–CMM system eliminates any possible confusion with the different degeneration profiles of different motor fiber types as it only consists of type II fibers, which we verified in this study. This eliminates the variable of different fiber types and allows for a more consistent study of how the length of the axon affects its susceptibility to degeneration. Based on our findings, the degeneration of fast

fatiguing, α-motor axons innervating type II muscle fibers is a length-dependent process in the SOD1 mouse model.

In order to study how axon length affects degeneration susceptibility at the earliest stages of disease, we used SOD1G93A mice on the C57BL/6J background. The C57BL/6J SOD1 mice show clinical symptoms on average around 110 days and die around 150 days (*129, 138-141*), while those on a mixed background show clinical symptoms starting at around 90 days and die by 130 days (*86, 131, 132, 135, 138*). The BL/6J background is advantageous in studying earlier degeneration because the later onset of clinical symptoms allows for more time to study the time course of degeneration in these long axons. We observed that there is extensive degeneration almost 2 months prior to the onset of clinical symptoms in the BL/6J SOD1 mice. The early time point of the LTN degeneration is advantageous since it allows for a quicker investigation of degeneration of the type II motor synapses well before the onset of symptoms. Also, using the LTN–CMM model in the C57BL/6J backgrounds gives a few more weeks of studying degeneration before the onset of clinical symptoms and may be a better system to study early intervention therapies.

BACE1 inhibitors as a therapy for traumatic peripheral nerve injuries

Using the knowledge that too much BACE1 activity levels were detrimental to axonal regeneration and genetically knocking out BACE1 led to improved regeneration following a nerve crush injury, we explored whether BACE1 inhibitors would be able to enhance regeneration as well. After giving WT mice a BACE1 inhibitor, the extent of regeneration following a sciatic nerve crush was significantly increased compared to

mice that did not receive any treatment. This enhanced regeneration was seen both in the number of regenerating axons and extent of NMJ innervation, as well as in the recovery rate of the amplitude of the CMAP. We did notice, however, that the recovery of the CMAP amplitude was not different between vehicle and inhibitor treated mice halfway through the experiment, after 4 weeks of treatment following the injury. What we did observe was that the area under the curve of the CMAP traces in the inhibitor treated mice was greater than the vehicle treated mice. This was an interesting finding and we hypothesize that this difference was due to myelination issues surrounding BACE1 inhibition. While there may have been more axons firing, because the myelination of these axons was impaired, they were unable to fire in a cohesive manner allowing the fewer, but better myelinated, vehicle treated axons to fire with a similar amplitude. We then removed the inhibitor treatment and recorded the CMAPs again 2 weeks later and found that the inhibitor treated mice were now able to fire together and generate a greater amplitude. This finding raises a question about how BACE1 inhibitors should be used to treat peripheral nerve injuries. While BACE1 inhibition was able to increase the number of regenerating axons, functional recovery was impaired, most likely due to myelination issues. For optimal recovery, it would be most beneficial to provide patients with BACE1 inhibitors as soon as possible following injury in order to maximize the effects that BACE1 inhibition has on enhancing regeneration and then removing the treatment to allow for proper remyelination to occur. Another possibility that needs to be addressed is whether these BACE1 inhibitors are also able to increase macrophage influx and debris clearance following injury as we saw with an earlier experimental BACE1 inhibitor as this may be contributing to the observation of enhanced regeneration (*25*).

In addition to enhancing regeneration of the proximal stump following a nerve crush injury, reduced BACE1 activity, by both genetic and pharmacological intervention, was able to induce increased terminal axonal sprouting in a partial nerve transection injury. This is important because partial nerve transections are a more severe injury due to the disconnect between the proximal stump and distal portion of the axon and the regenerating axon has difficulty entering the correct tube. By enhancing sprouting at the level of the muscle, the muscle has a chance at getting reinnervated earlier than waiting for the proximal stump to make it down to the muscle, if it even succeeds. This is also important for transections of very long axons as the rate of regeneration is incredible slow and collateral sprouting can reinnervate the muscle before any degeneration of the muscle occurs due to a lack of neuronal input. We were also able to observe many terminal-to-terminal sprouts in BACE1 inhibitor treated mice. This implies that these terminal sprouts were actually finding denervated NMJs and reinnervating them and not just wandering off without reinnervating anything.

Another important finding was that there weren't any issues with the morphology and functionality of uninjured nerves in mice treated with or without the inhibitor. This indicates that reducing BACE1 after the peripheral nerves have had a chance to become fully developed doesn't appear to have the issues with hypomyelination that is seen in the complete BACE1 KO mice. Additionally, mice where neuregulin was conditionally knocked out in the adult also do not show any issues with the maintenance of myelin in uninjured axons (*190*). This is good for BACE1 inhibitor treatment of peripheral nerve injuries as there appears to be no negative effect on normal nerve morphology and would therefore not have any unintentional decline in normal motor and sensory function.

Early treatment with BACE1 inhibitors improves CMM innervation in an ALS mouse model

In addition to determining whether BACE1 inhibitors were useful for enhancing peripheral nerve regeneration in traumatic nerve injuries, we also explored whether these inhibitors could improve reinnervation of the CMM in the SOD1^{G93A} mouse model of ALS. After treating one month old mice with the inhibitor for either one or two months, there was an increased percentage of innervated NMJs as well as a functional improvement following the one-month inhibitor treatment. After two months of treatment there was no longer a significant functional difference despite seeing improved NMJ innervation. This may be due to the extent of the disease overwhelming the repair process and at that point the neurons themselves may be too sick to fire in any meaningful way. Another possibility could be that the size of the motor units has become too large for the neurons to be able to support and therefore leads to impaired firing capacity. A third possibility could be due to BACE1's impairment on remyelination and the axons may be having difficulty firing together, like what we observed after 4 weeks of treatment following a sciatic nerve crush injury. However, just observing the CMAP traces did not indicate any substantial difference in the firing cohesiveness nor were there any differences in the latencies, ruling this out as a possible reason for the loss of significance.

In addition to improved NMJ innervation, we were also able to observe an increase in the extent of axonal sprouting in these mice following BACE1 inhibitor treatment. This is a similar observation as the one that we detected in the partial nerve injury model following BACE1 inhibitor treatment and further supports the hypothesis

that BACE1 activity levels influence peripheral nerve regeneration by enhancing axonal outgrowth, both from the proximal stump and via collateral sprouting from neighboring axons. That there was enhanced axonal sprouting evident in the treated SOD1 mice also supported the hypothesis that the improved innervation seen with BACE1 inhibition is due to enhanced reinnervation and not a neuroprotective effect. This finding indicates that BACE1 inhibitors may be beneficial in other neurodegenerative diseases that have a peripheral neuropathy, such as CMT or diabetic peripheral neuropathies. This is further supported by our finding that BACE1 inhibitors also improve regeneration and sprouting in two different traumatic nerve injury models. In addition to the improved innervation being caused by enhanced collateral sprouting, we cannot exclude the possibility that some regeneration may be due to the retraction bulbs being encouraged to regenerate back towards its NMJ as we have not studied this phenomenon. This may be possible as we demonstrated that the proximal stump of a nerve crush injury was able to regenerate back out following BACE1 inhibitor treatment and a similar mechanism may also be at work in the SOD1 mouse. In order to conclude this however, further studies would need to be conducted to identify sprouts growing out of retraction bulbs as it is not as easy to determine as terminal sprouts.

This study provided encouraging findings in terms of using BACE1 inhibitors as a way to enhance axonal sprouting in the case of partial peripheral nerve injury due to a chronic disease providing the neurons remain sufficiently viable. We were able to demonstrate that there is enhanced reinnervation due at least in part to increased collateral sprouting in the early stages of the disease. Further studies need to be conducted in order to more definitely determine whether there are meaningful functional

improvements, such as improved grip strength and performance on a rotarod apparatus. Additional studies would also need to be conducted to determine whether there is any benefit to survival in these mice following BACE1 inhibitor treatment. Another interesting future study would be to utilize an ALS mouse model which has a slowly progressing disease process as this may be able to further demonstrate the benefits of BACE1 inhibitors as there is an even greater window of opportunity for treatment before the disease progression overwhelms the repair process. It may also be interesting to provide BACE1 inhibitors together with Riluzole and determine whether both treatments together can improve the modest effect that Riluzole has on survival for ALS patients.

Final conclusion

The studies outlined in this dissertation provided further insight into the mechanisms that peripheral nerves are able to control the extent of regeneration. We further supported the hypothesis that BACE1 negatively influences peripheral nerve regeneration. We were able to demonstrate that BACE1 inhibitors are a promising novel treatment not only for acute traumatic peripheral nerve injuries, but also in the context of a chronic disease model. These preclinical results hold a lot of promise for the development of a long needed therapeutic for enhancing peripheral nerve regeneration.

Chapter 8: Methods

Animals

All experiments and animal care procedures were conducted in accordance with the guidelines of the Johns Hopkins University Committee on the Use and Care of Animals. Mice associated with this study were housed in a facility at Johns Hopkins University. Animal numbers used in each experiment were determined based on previous experience (*25, 126, 170, 172*). For all the experiments performed there was no significant difference between male and female mice and therefore the data was pooled together according to genotype.

BACE1 overexpression experiments

A total of 36 WT and 40 BACE1 transgenic (Tg) mice were used in this study. The transgenic mice were graciously provided by Dr. Eliezer Masliah at UCSD. All mice were between 3 and 4 months of age at the time of the experiment. The transgenic mice were engineered to over-express the human BACE1 protein in neurons (*44*) and their control littermates were designated as wild type.

BACE1 KO experiments

A total of 4 WT and 4 BACE1 KO mice were used in this study. All breeding mice were obtained from Jackson Labs (Bar Harbor, Maine, USA). Yellow fluorescent protein (YFP)-transgenic mice (B6.Cg-Tg(Thy1-YFP)16Jrs/J), in which all the motor axons express YFP fluorescence (*191*), were bred with BACE1 KO mice crossed 10 times to the B6 background, that were generously donated by Dr. Alena Savonenko at

Johns Hopkins, to generate KO mice expressing YFP in all their axons. Mice were 3-4 months old at the time of experiments.

Injury experiments in WT mice

WT type mice on the B6 background were obtained from existing breeding cages from our lab. For the inhibitor studies following a sciatic nerve crush, a total of 53 mice were used, with 29 on the vehicle and 24 on the inhibitor treatment. For the partial nerve transection studies, WT mice expressing YFP on the B6 background from Jackson Labs were used (B6.Cg-Tg(Thy1-YFP)16Jrs/J). A total of 10 mice were used, with 3 on the vehicle and 4 on the inhibitor treatment. 3 YFP mice were used to determine the reliability of a partial nerve transection in the LTN-CMM system. 3 non-YFP B6 mouse were used to perform the staining and muscle type characterization experiments of the LTN-CMM.

SOD1 experiments

All breeding mice were obtained from Jackson Labs (Bar Harbor, Maine, USA). Yellow fluorescent protein (YFP)-transgenic mice (B6.Cg-Tg(Thy1-YFP)16Jrs/J), in which all the motor axons express YFP fluorescence (*191*), were bred with SOD1 transgenic mice (B6.Cg-Tg(SOD1*G93A)1Gur/J) (*129*), which express a G93A mutant form of human SOD1 and exhibit an ALS-like phenotype. Both lines used in this study were in the C57BL/6J genetic background. Progeny from breeding pairs were genotyped and grouped into SOD1-transgene carrying mice (SOD1) and wild type littermates (WT). During the 3-month course of the studies, the SOD1 mice showed no signs of disease, no weight loss and no gait abnormality.

For the degeneration studies, a total of 73 wild type (WT) and 72 SOD1 mice were used. Mice were between 1-3 months of age. For the inhibitor studies a total of 142 SOD1 mice were used, with 69 on vehicle and 73 on inhibitor treatment. Mice were between 2-3 months of age at the time of the experiments. Control littermates were designated as WT.

Mouse perfusion

Before perfusion, LTN or sciatic nerve electrophysiological experiments were carried out and when necessary, the hair was removed from the dorsal portion of the trunk of the body and legs with electric clippers to prepare for CMM dissection. Mice were then deeply anesthetized with 10% chloral hydrate (Sigma–Aldrich, St. Louis, MO, USA) and killed by transcardial perfusion with 1 X phosphate-buffered saline (PBS) (Life Technologies, Carlsbad, CA, USA) followed by 2% paraformaldehyde (PFA) (Electron Microscopy Sciences, Hatfield, PA, USA) in 1 X PBS at room temperature. 2% PFA was decided on in order to reduce background fluorescence when imaging. For the CMM dissection, the remaining hair was removed from the back of the body with an over the counter chemical depilatory. The skin, with the CMM attached, was removed from the back of the body and post-fixed in 2% paraformaldehyde for up to 16 h and before being transferred to PBS for long term storage at 4 °C. Both injured and uninjured sciatic nerves were removed and post-fixed overnight at room temperature for light microscopy in 2% PFA and electron microscopy in 2% PFA/2% gluteraldehyde. Both the left and right gastrocnemius muscles were removed from the perfused mice and post-fixed in 2% PFA overnight at room temperature.

Tissue processing for light and electron microscopy

For semi-thin sections, sciatic nerves were post-fixed at room temperature overnight in 2% PFA/2% gluteraldehyde followed by OsO4 and embedded in Epon (all from Electron Microscopy Sciences). The nerves were then cross sectioned at a 1 μm thickness and stained for toluidine blue before being examined under light microscopy. For ultra-structural analyses, nerves were processed as described previously (*25*). Briefly, 70 nm thin sections were obtained and stained for citrate/uranyl acetate. Electron micrographs were acquired using a Zeiss Libra transmission electron microscope (Zeiss, Germany). Sciatic nerves used for early regeneration and degeneration analyses were post-fixed overnight at room temperature in 2% PFA in 1 X PBS before being transferred to 1 X PBS and stored at 4 °C. Nerves were cyroprotected in 30% sucrose (Thermo Fisher Scientific, Waltham, MA, USA) in 1 X PBS overnight before being immersed and quick-frozen in Tissue-TEK (Electron Microscopy Sciences), and sectioned longitudinally at a 20 μm thickness using a cryostat (Microm HM 505E, International Medical Equipment, MI, USA). Sciatic nerves used for the 15 days post crush neurofilament study were processed in the same way before being cross-sectioned at a 20 μm thickness using the same cryostat. Following dissection, gastrocnemius muscles were cryoprotected in 30% sucrose in 1 x PBS overnight. The gastrocnemius muscles were then frozen using dry ice and 50 μm thick sections were cut using a microtome (Microm MH450, Thermo Fisher Scientific). For muscle type analysis samples of the CMM from each recording site were collected immediately after recording, flash-frozen with liquid nitrogen and stored at −80 °C. Soleus muscles were obtained and prepared in a similar manner. Tissues were then immersed in TissueTek (Electron Microscopy

Sciences) and cryosectioned at a thickness of 20 μm before both H&E and fiber type staining protocols were performed.

Nerve injury protocols

Sciatic nerve crush

The mice were anesthetized using 2–3% isoflurane (Isosol, Vedco, MO, USA) and the hair on their left thigh was shaved off using an electric clipper. A small incision was made along the thigh and the sciatic nerve was exposed. The left sciatic nerve of all the mice were crushed at mid-thigh level, just below the sciatic notch, by pinching the nerve between tweezers for 30 s before suturing the wound closed. The nerves were then monitored electrophysiologically through the progression of regeneration for eight weeks, taking measurements every 2 weeks. For the inhibitor studies, mice were taken off the drug at 4 weeks to allow optimal remyelination to occur. For morphological analysis, the crush sites were marked by 11–0 sutures during surgery and the sciatic nerves were removed 3, 10, and 14 days after the crush. Sciatic nerves were collected above and below the crush site for the early regeneration marker studies at 3 days. For the 10 and 14 day regeneration analysis, 2 mm long nerves segments that were 3 mm distal to the marked injury site were collected for toluidine blue staining and EM processing. The remaining portion of the nerves were saved for neurofilament analysis.

Sciatic nerve transection

The mice were anesthetized and prepared as described for sciatic nerve crushes. Again, a small incision was made along the thigh to expose the sciatic nerve. The sciatic nerve was then completely cut and the distal stump was turned away from the proximal

stump to prevent regeneration before suturing the wound closed. The distal stumps were collected 5 days later and processed for nerve degeneration analysis.

Partial LTN transection

WT and BACE1 KO mice were anesthetized using 2–3% isoflurane and the hair was removed from the left shoulder using electric clippers. A small incision was made along the shoulder blade and the branches of the LTN were exposed. Two of the branches were completely cut and the ends were turned away from each other to prevent the proximal stump from reaching the distal portion. The wound was then closed and mice were perfused 7, 14 and 21 days later for further analysis of axonal sprouting in the LTN-CMM.

DRG primary culture

12 mm coverslips were coated with Poly-L-Lysine (Sigma) for 30 mins at 37℃ before coating with 10mg/ml laminin (Millipore-Sigma) overnight at 37℃. DRGs were isolated from 3 WT mice between 2-4 months of age. To obtain DRGs, mice were anesthetized by isoflurane before being decapitated and exposing the spinal column. DRGs were collected from the lumbar region on both sides and immediately placed in a dish of ice cold L-15 dissection medium. Any extraneous axonal processes were quickly removed from the DRGs and then they were mechanically teased apart under a dissection scope. 10mg/ml of collagenase (ThermoFisher) was used to further break down the cells at 37℃ for 45 mins, with mild agitation every 10 mins. The collagenase was then aspirated and a mixture of 0.25% Trypsin (ThermoFisher) and 0.5mg/ml of DNase

(Millipore-Sigma) was added for 15 mins at 37°C. The cells were triturated and then strained through a 40μm pore filter before plating at a density of $5x10^4$ cells/well.

Electrophysiology protocols

Sciatic nerve electrophysiology

To assess the speed and degree of recovery, we performed electrophysiological recordings of the CMAP from crushed nerves every other week for 8 weeks using an Evidence 3102evo EMG system (Schreiber & Tholen Medizintechnik, Stade, Germany). The recording electrode was placed in the plantar muscle of the foot pad and the sciatic nerve was stimulated at two locations. The hip stimulating site was located proximal to the injury at the sciatic notch, approximately 30 mm from the recording site. The ankle stimulating site was located distal to the injury at the ankle, approximately 10 mm from the recording site. A diagram of the electrode placements is shown in Fig. 10A. The recordings were performed in an anesthetized mouse using isoflurane and the crushed sciatic nerve was stimulated at the hip or ankle by very short (< 0.2 milliseconds) electrical impulses. The skeletal muscle in the foot pad innervated by this nerve generated a CMAP after regenerated axons re-innervated the muscle. The amplitude level and latency of the response at the muscle were analyzed as readouts for the degree of functional recovery. The traces of the CMAPs in Figs. 10B-C, 16C and 22A-D were generated by exporting the values from the Evidence software into SigmaPlot (Systat Software Inc., CA, USA) to create a line graph representing the CMAP traces. Uncrushed nerves were recorded from the right side to determine baseline values.

LTN–CMM electrophysiology

Mice were anesthetized using 2–3% isoflurane and the hair on their backs was removed by shaving with electric clippers. CMAPs were recorded from the LTN–CMM at three sites along the CMM using an Evidence 3102evo EMG system. In order to accurately determine each testing site, an easily identifiable baseline site between the second and third caudal vertebrae was established by palpating for the muscle mass on top of the third caudal vertebrae. Testing sites were marked 6, 24, and 36 mm anterior to the baseline site, with the recording and reference electrodes placed 6 mm on either side of the animal's midline. Two small incisions were made at the most caudal testing site and both the active and reference recording electrodes were placed just beneath the skin. A diagram of the experimental set up is shown in Fig. 13A. The grounding electrode was placed beneath the skin on the animal's side away from the recording and stimulating electrodes. An incision was made just below the left shoulder blade and the LTN was exposed proximal to where the nerve enters the CMM. Using a hooked electrode, the middle branch of LTN was isolated and stimulated (0.05 ms, 1 Hz). Stimulation was optimized with respect to both polarity (preferred polarity yielding the shortest CMAP latency) and intensity (supramax stimulation defined as 3 mA above the amount of current required for the size and shape of the CMAP to remain unchanged). CMAPs from the LTN–CMM system were then recorded and amplitudes and latencies were analyzed as measures of neuromuscular function. Repetitive stimulation schedules (optimized stimulation at 1, 5, and 10 Hz) were used to ensure stable electrode positioning. After testing was completed at the caudal site, the active and reference recording electrodes were cleaned and the electrophysiology procedure was repeated moving up toward the

head at the medial and then the rostral testing sites. The traces of the CMAPs in Figs. 13A and 24D were generated by exporting the values from the Evidence software into SigmaPlot to create a line graph representing the CMAP traces.

Tissue staining

Table 1. Antibodies used for tissue staining.

1° Antibody	Target	Company	Dilution
Neurofilament H (NF)	Axonal marker	Millipore	1:500
Synaptic vesicle 2 (SV2)	Presynaptic terminal	DSHB	1:250
Myelin basic protein (MBP)	Myelin sheath	Millipore	1:1000
CD68	Macrophages	Serotec	1:1000
GAP-43	Early regeneration marker	Millipore	1:1000
SCG10	Early regeneration marker	Novus	1:2000
α-bungarotoxin-AF647 conjugate	Postsynaptic NMJ	Life Technologies	1:500
S-100	Schwann cells	Sigma-Aldrich	1:250
Type I myosin heavy chain (A4.840)	Type I muscle cells	DSHB	1:250
Type II myosin heavy chain (My32)	Type II muscle cells	Thermo Fisher	1:500
Neurofilament 200	Axonal marker	Sigma	1:500
Tuj1	Neuronal marker	Covance	1:1000

Cultured DRG neurons

Cultured DRGs on glass coverslips were fixed for 1 hour with 2% PFA in 1 X PBS at room temperature. Cells were then washed in PBS before being permeabilized and blocked by 5% goat serum (Jackson labs)/0.3% Triton (Sigma-Aldrich) in 1 X PBS for 1h at room temperature. The cells were then stained with either a Tuj1 or NF-200 primary Ab in blocking solution overnight at 4°C. After thorough washing, the cells were

then stained with appropriate secondary antibodies conjugated to AlexaFluor 488 before being mounted on slides in ProLong Gold mounting medium with DAPI (Life Technologies).

Sciatic nerve staining

Sciatic nerve sections affixed to slides were permeabilized and blocked by 5% goat serum (Jackson labs)/0.3% Triton (Sigma-Aldrich) in 1 X PBS for 1h at room temperature. The cross-sections were stained with a primary antibody against NF and the longitudinal sections stained with an anti-GAP43, anti-SCG10, anti-MBP, or anti-CD68 antibody at 4°C overnight. The samples were then washed in PBS for 5 minutes 3 times before the appropriate Alexa Fluor conjugated secondary antibody was added for 1 hour at room temperature. The samples were again washed and then mounted in prolong gold mounting reagent with DAPI (Life Technologies) and cover-slipped.

Gastrocnemius muscle staining

Free floating gastrocnemius muscle tissue sections were permeabilized and blocked by 5% goat serum (Jackson labs)/0.3% Triton (Sigma-Aldrich) in 1 X PBS for 1h at room temperature. The sections were stained with primary antibodies against NF H and SV2 at 4°C overnight. The samples were then washed in PBS for 5 minutes 3 times before appropriate Alexa Flour conjugated secondary antibodies were added together with α-BTX Alexa Fluor 647 for 1 hour at room temperature. The samples were again washed and then mounted in prolong gold mounting reagent (Life Technologies) and cover-slipped.

LTN–CMM staining

LTN-CMMs were collected for analysis for the partial nerve transection studies in BACE1 KO mice and inhibitor treated WT mice as well as for the SOD1 degeneration and regeneration studies. Before staining, the connective tissue covering the CMM was carefully dissected off of the whole back while leaving the skin intact. The back was then cut in half along the midline and one side from the SOD1 mice was randomly selected for staining. For the partial nerve transection studies the left side of the back was selected. The muscle was permeabilized for 1 h at room temperature in a solution of 1% Triton X and 5% dimethyl sulfoxide (DMSO) (Sigma–Aldrich) in 1× PBS. They were then stained with α-bungarotoxin conjugated to Alexa Fluor 647 (Life Technologies) at room temperature for 3 h. The back halves were then whole mounted onto slides using ProLong Diamond Antifade mounting medium (Life Technologies). CMM tissue from WT mice were also blocked in the same permeabilization solution with 5% goat serum (Jackson ImmunoResearch Laboratories Inc., West Grove, PA, USA). I blocked the tissue with Mouse on Mouse blocking reagent then stained the whole CMM from WT mice for SV2 and Schwann cells (S-100) to identify endogenously expressed markers of the neuromuscular synapse.

Muscle type staining

Dissected CMMs were washed and a standard H&E staining protocol was followed (Thermo Fisher, Halethorpe, MD, USA). For fiber typing, samples were permeabilized in a solution of 0.3% Triton X (Sigma–Aldrich) in 1× PBS, blocked with a Mouse on Mouse blocking reagent (Vector Labs, Burlingame, CA, USA), and then

labeled with antibodies to identify type I myosin heavy chain (A4.840) and type II myosin heavy chain (My32).

Regeneration analysis

Sciatic nerve regeneration

In order to count all of the regenerated axons, 63X oil-immersion bright field images of toluidine blue stained sciatic nerve cross-sections were tiled to obtain the complete area of the nerves using as Axio Imager fluorescence microscope (Zeiss, Germany). Axons which had evidence of very thin myelin sheaths were scored as a regenerated axon and the total number of regenerated axons was scored for the entire nerve. Each mouse was assigned a random number and the genotype or treatment status of each mouse was unknown at the time of quantification. The results were then unblinded and statistical analysis was performed before calculating the average and SEM.

Early regeneration analysis

After staining longitudinal sections of 3 days post crush sciatic nerves for GAP43, the entire length of the nerves were imaged using a Zeiss LSM 800 confocal microscope by tiling 20X images together. The crush site was identified by staining for CD68 positive macrophages which congregate at the site of injury by 3 days (data not shown). The length of the longest GAP43 positive axon was quantified by tracing the nerve in Image J software (NIH) from the middle of the crush site to the end and then the length of the line was measured. Each mouse was assigned a random number and the genotype was unknown at the time of quantification. The results were then unblinded and each genotype was averaged before performing statistical analysis.

Macrophage quantification

20 μm longitudinal sections of sciatic nerves stained for CD68, a macrophage marker, were used for macrophage quantification. The nerves were imaged using a Zeiss LSM 800 confocal microscope at a magnification of 20X to generate 3D z-stacks. The number of CD68 positive macrophages were counted and the macrophage density was then determined by taking into account the total volume of the image. Each mouse was assigned a random number and the genotype was unknown at the time of quantification. The samples were then unblinded and statistical analysis was performed before calculating the average and SEM.

NMJ reinnervation

LTN–CMM imaging was done by imaging whole-mounted back halves with a 20X objective using an Axio Imager fluorescence microscope with an Apotome apparatus (Zeiss) and two laser scanning confocal microscopes (LSM 510 and LSM 800, Zeiss). The backs were imaged at three different locations along the CMM corresponding to the caudal, medial and rostral regions used for the electrophysiological experiments (6, 24, and 36 mm from the baseline respectively). Stained and mounted gastrocnemius muscle sections were imaged at 20X on a LSM 800 Zeiss microscope. Z-stacks were taken for each image and were flattened with the ZEN software (Zeiss). The gamma and brightness was raised on the images in order to visualize axons with low YFP expression. Approximately 100-150 NMJs were imaged at each CMM site and gastrocnemius per mouse. To determine the extent of innervation, NMJs were counted and scored as either completely innervated or fully denervated. Complete innervation was counted as a total overlap of the pre-synaptic and post-synaptic staining comparable to control mice. Fully

denervated NMJs were counted as no overlapping of the pre-synaptic and post-synaptic staining. The number of innervated NMJs was then divided by the total number of NMJs to determine the percentage of innervation. Each mouse was assigned a random number and the genotype was unknown at the time of quantification. The samples were then unblinded and statistical analysis was performed before calculating the average and SEM.

Axonal sprouting

Axonal sprouting in the SOD1 models was analyzed using the same images from the NMJ innervation analysis. For the partial nerve injury, images were taken in regions adjacent to areas of denervation. I scored thin, YFP-positive axons which innervated a NMJ that already had another axon innervating it as an axonal sprout. Extra-terminal axonal sprouts were specifically characterized as a thin axon sprouting from a terminal bouton that either did or did not make a connection with another NMJ. To calculate the percentage of terminal axonal sprouts I counted the number of extra-terminal sprouts and divided by the total number of NMJs.

Western Blot

Fresh, unfixed sciatic nerves and brains were collected from mice and the protein was extracted by homogenizing in a glass-made micro-homogenizer in extraction buffer (T-PER® tissue protein extraction reagent, Thermo Fisher Scientific, MA, USA) containing a protease inhibitor mixture. Protein concentration was determined using a Micro BCA™ Protein Assay Kit as per the manufacturer's instructions (Thermo Fisher Scientific). Protein was loaded onto a Novex WedgeWell 8–16% Tris-Glycine gel or a 4-20% Tris-Glycine gel (both from Invitrogen, CA, USA) and transferred to nitrocellulose

membrane (Invitrogen). The blots were then blocked with 5% milk (Bio-Rad, CA) or 5% donkey serum (Millipore) and stained overnight at 4 °C with an anti-BACE1 (*39*), anti-APP (Millipore), or anti-CHL1 (R&D Systems, Minneapolis MN) primary antibody. The blots were then washed 3 times for 5 minutes in TBST before adding appropriate HRP conjugated secondary antibodies for 1 h at room temperature. The blots were washed again and then visualized on film using Amersham ECL detection reagent (GE Healthcare, UK). The blots were stripped and re-stained for loading controls using an anti-GAPDH-HRP conjugated antibody (Sigma-Aldrich) for 1 h at room temperature before being visualized in the same way as the other antibodies.

Statistical analysis

Each mouse was randomly assigned a number and the specific genotype of each mouse was unknown at the time of data collection and analysis for all experiments performed in order to ensure blinded analysis. Power analyses were performed, together with previous experience, to determine sample sizes. All statistical analyses were performed using a Student's *t*-test. Where the data failed to pass the normalization test, the Mann-Whitney Rank Sum Test was performed. All data analysis was performed using SigmaPlot software and any value of $p < 0.05$ was scored as statistically significant. All graphed data are presented as mean ± SEM.

References

1. G. Stoll, C. Y. Li, B. D. Trapp, J. W. Griffin, Expression of NGF-receptors during immune-mediated and lysolecithin-induced demyelination of the peripheral nervous system. *J Neurocytol* **22**, 1022-1029 (1993).
2. B. S. Mietto, K. Mostacada, A. M. Martinez, Neurotrauma and inflammation: CNS and PNS responses. *Mediators Inflamm* **2015**, 251204 (2015).
3. R. Martini, S. Fischer, R. Lopez-Vales, S. David, Interactions between Schwann cells and macrophages in injury and inherited demyelinating disease. *Glia* **56**, 1566-1577 (2008).
4. W. Bruck, The role of macrophages in Wallerian degeneration. *Brain Pathol* **7**, 741-752 (1997).
5. K. A. Kigerl *et al.*, Identification of two distinct macrophage subsets with divergent effects causing either neurotoxicity or regeneration in the injured mouse spinal cord. *J Neurosci* **29**, 13435-13444 (2009).
6. A. R. Ferguson *et al.*, Cell death after spinal cord injury is exacerbated by rapid TNF alpha-induced trafficking of GluR2-lacking AMPARs to the plasma membrane. *J Neurosci* **28**, 11391-11400 (2008).
7. R. George, J. W. Griffin, Delayed macrophage responses and myelin clearance during Wallerian degeneration in the central nervous system: the dorsal radiculotomy model. *Exp Neurol* **129**, 225-236 (1994).
8. D. Toy, U. Namgung, Role of glial cells in axonal regeneration. *Exp Neurobiol* **22**, 68-76 (2013).
9. J. W. Griffin, B. Pan, M. A. Polley, P. N. Hoffman, M. H. Farah, Measuring nerve regeneration in the mouse. *Exp Neurol* **223**, 60-71 (2010).
10. J. W. Fawcett, R. J. Keynes, Peripheral nerve regeneration. *Annu Rev Neurosci* **13**, 43-60 (1990).
11. E. A. Huebner, S. M. Strittmatter, Axon regeneration in the peripheral and central nervous systems. *Results Probl Cell Differ* **48**, 339-351 (2009).

12. R. Seijffers, C. D. Mills, C. J. Woolf, ATF3 increases the intrinsic growth state of DRG neurons to enhance peripheral nerve regeneration. *J Neurosci* **27**, 7911-7920 (2007).

13. T. Gordon, A. W. English, Strategies to promote peripheral nerve regeneration: electrical stimulation and/or exercise. *Eur J Neurosci* **43**, 336-350 (2016).

14. M. W. Painter *et al.*, Diminished Schwann cell repair responses underlie age-associated impaired axonal regeneration. *Neuron* **83**, 331-343 (2014).

15. R. Vassar *et al.*, Beta-secretase cleavage of Alzheimer's amyloid precursor protein by the transmembrane aspartic protease BACE. *Science* **286**, 735-741 (1999).

16. R. Yan *et al.*, Membrane-anchored aspartyl protease with Alzheimer's disease beta-secretase activity. *Nature* **402**, 533-537 (1999).

17. S. Sinha *et al.*, Purification and cloning of amyloid precursor protein beta-secretase from human brain. *Nature* **402**, 537-540 (1999).

18. M. L. Hemming, J. E. Elias, S. P. Gygi, D. J. Selkoe, Identification of beta-secretase (BACE1) substrates using quantitative proteomics. *PLoS One* **4**, e8477 (2009).

19. M. Pigoni *et al.*, Seizure protein 6 and its homolog seizure 6-like protein are physiological substrates of BACE1 in neurons. *Mol Neurodegener* **11**, 67 (2016).

20. P. H. Kuhn *et al.*, Regulated intramembrane proteolysis of the interleukin-1 receptor II by alpha-, beta-, and gamma-secretase. *J Biol Chem* **282**, 11982-11995 (2007).

21. L. Zhou *et al.*, The neural cell adhesion molecules L1 and CHL1 are cleaved by BACE1 protease in vivo. *J Biol Chem* **287**, 25927-25940 (2012).

22. M. Willem *et al.*, Control of peripheral nerve myelination by the beta-secretase BACE1. *Science* **314**, 664-666 (2006).

23. X. Hu *et al.*, Bace1 modulates myelination in the central and peripheral nervous system. *Nat Neurosci* **9**, 1520-1525 (2006).

24. L. Liu *et al.*, Increased TNFR1 expression and signaling in injured peripheral nerves of mice with reduced BACE1 activity. *Neurobiol Dis* **93**, 21-27 (2016).

25. M. H. Farah *et al.*, Reduced BACE1 activity enhances clearance of myelin debris and regeneration of axons in the injured peripheral nervous system. *J Neurosci* **31**, 5744-5754 (2011).

26. M. H. Farah, BACE1 influences debris clearance and axonal regeneration in injured peripheral nerve. *J Peripher Nerv Syst* **17 Suppl 3**, 30-33 (2012).

27. H. J. Seddon, A Classification of Nerve Injuries. *Br Med J* **2**, 237-239 (1942).

28. S. Sunderland, A classification of peripheral nerve injuries producing loss of function. *Brain* **74**, 491-516 (1951).

29. W. A. Palispis, R. Gupta, Surgical repair in humans after traumatic nerve injury provides limited functional neural regeneration in adults. *Exp Neurol* **290**, 106-114 (2017).

30. S. L. Cole, R. Vassar, The Basic Biology of BACE1: A Key Therapeutic Target for Alzheimer's Disease. *Curr Genomics* **8**, 509-530 (2007).

31. U. Bodendorf, F. Fischer, D. Bodian, G. Multhaup, P. Paganetti, A splice variant of beta-secretase deficient in the amyloidogenic processing of the amyloid precursor protein. *J Biol Chem* **276**, 12019-12023 (2001).

32. R. Ehehalt *et al.*, Splice variants of the beta-site APP-cleaving enzyme BACE1 in human brain and pancreas. *Biochem Biophys Res Commun* **293**, 30-37 (2002).

33. R. Yan, P. Han, H. Miao, P. Greengard, H. Xu, The transmembrane domain of the Alzheimer's beta-secretase (BACE1) determines its late Golgi localization and access to beta -amyloid precursor protein (APP) substrate. *J Biol Chem* **276**, 36788-36796 (2001).

34. H. Shimizu *et al.*, Crystal structure of an active form of BACE1, an enzyme responsible for amyloid beta protein production. *Mol Cell Biol* **28**, 3663-3671 (2008).

35. C. Haass, A. Capell, M. Citron, D. B. Teplow, D. J. Selkoe, The vacuolar H(+)-ATPase inhibitor bafilomycin A1 differentially affects proteolytic processing of mutant and wild-type beta-amyloid precursor protein. *J Biol Chem* **270**, 6186-6192 (1995).

36. E. H. Koo, S. L. Squazzo, Evidence that production and release of amyloid beta-protein involves the endocytic pathway. *J Biol Chem* **269**, 17386-17389 (1994).

37. G. Thinakaran, D. B. Teplow, R. Siman, B. Greenberg, S. S. Sisodia, Metabolism of the "Swedish" amyloid precursor protein variant in neuro2a (N2a) cells. Evidence that cleavage at the "beta-secretase" site occurs in the golgi apparatus. *J Biol Chem* **271**, 9390-9397 (1996).

38. P. C. Kandalepas, R. Vassar, Identification and biology of β-secretase. *J Neurochem* **120 Suppl 1**, 55-61 (2012).

39. H. Cai *et al.*, BACE1 is the major beta-secretase for generation of Abeta peptides by neurons. *Nat Neurosci* **4**, 233-234 (2001).

40. S. L. Roberds *et al.*, BACE knockout mice are healthy despite lacking the primary beta-secretase activity in brain: implications for Alzheimer's disease therapeutics. *Hum Mol Genet* **10**, 1317-1324 (2001).

41. Y. Luo *et al.*, Mice deficient in BACE1, the Alzheimer's beta-secretase, have normal phenotype and abolished beta-amyloid generation. *Nat Neurosci* **4**, 231-232 (2001).

42. M. E. Kennedy *et al.*, The BACE1 inhibitor verubecestat (MK-8931) reduces CNS β-amyloid in animal models and in Alzheimer's disease patients. *Sci Transl Med* **8**, 363ra150 (2016).

43. U. Bodendorf *et al.*, Expression of human beta-secretase in the mouse brain increases the steady-state level of beta-amyloid. *J Neurochem* **80**, 799-806 (2002).

44. E. Rockenstein *et al.*, High beta-secretase activity elicits neurodegeneration in transgenic mice despite reductions in amyloid-beta levels: implications for the treatment of Alzheimer disease. *J Biol Chem* **280**, 32957-32967 (2005).

45. P. C. May *et al.*, The potent BACE1 inhibitor LY2886721 elicits robust central Abeta pharmacodynamic responses in mice, dogs, and humans. *J Neurosci* **35**, 1199-1210 (2015).

46. S. Sankaranarayanan *et al.*, In vivo beta-secretase 1 inhibition leads to brain Abeta lowering and increased alpha-secretase processing of amyloid precursor protein without effect on neuregulin-1. *J Pharmacol Exp Ther* **324**, 957-969 (2008).

47. W. P. Chang *et al.*, Beta-secretase inhibitor GRL-8234 rescues age-related cognitive decline in APP transgenic mice. *FASEB J* **25**, 775-784 (2011).

48. G. Cebers *et al.*, AZD3293: Pharmacokinetic and Pharmacodynamic Effects in Healthy Subjects and Patients with Alzheimer's Disease. *J Alzheimers Dis* **55**, 1039-1053 (2017).

49. L. Zhou *et al.*, The neural cell adhesion molecules L1 and CHL1 are cleaved by BACE1 protease in vivo. *J Biol Chem* **287**, 25927-25940 (2012).

50. J. Zhang *et al.*, Sez-6 may play an important role in neurite outgrowth through the PKCgamma signaling pathways. *Z Naturforsch C* **66**, 614-620 (2011).

51. M. T. Gersbacher, D. Y. Kim, R. Bhattacharyya, D. M. Kovacs, Identification of BACE1 cleavage sites in human voltage-gated sodium channel beta 2 subunit. *Mol Neurodegener* **5**, 61 (2010).

52. S. F. Lichtenthaler *et al.*, The cell adhesion protein P-selectin glycoprotein ligand-1 is a substrate for the aspartyl protease BACE1. *J Biol Chem* **278**, 48713-48719 (2003).

53. S. Kitazume *et al.*, Alzheimer's beta-secretase, beta-site amyloid precursor protein-cleaving enzyme, is responsible for cleavage secretion of a Golgi-resident sialyltransferase. *Proc Natl Acad Sci U S A* **98**, 13554-13559 (2001).

54. X. Hu *et al.*, Genetic deletion of BACE1 in mice affects remyelination of sciatic nerves. *FASEB J* **22**, 2970-2980 (2008).

55. V. Velanac *et al.*, Bace1 processing of NRG1 type III produces a myelin-inducing signal but is not essential for the stimulation of myelination. *Glia* **60**, 203-217 (2012).

56. C. Taveggia *et al.*, Neuregulin-1 type III determines the ensheathment fate of axons. *Neuron* **47**, 681-694 (2005).

57. G. V. Michailov *et al.*, Axonal neuregulin-1 regulates myelin sheath thickness. *Science* **304**, 700-703 (2004).

58. R. La Marca *et al.*, TACE (ADAM17) inhibits Schwann cell myelination. *Nat Neurosci* **14**, 857-865 (2011).

59. B. Hitt *et al.*, β-Site amyloid precursor protein (APP)-cleaving enzyme 1 (BACE1)-deficient mice exhibit a close homolog of L1 (CHL1) loss-of-function phenotype involving axon guidance defects. *J Biol Chem* **287**, 38408-38425 (2012).

60. P. H. Kuhn *et al.*, Secretome protein enrichment identifies physiological BACE1 protease substrates in neurons. *EMBO J* **31**, 3157-3168 (2012).

61. M. Montag-Sallaz, M. Schachner, D. Montag, Misguided axonal projections, neural cell adhesion molecule 180 mRNA upregulation, and altered behavior in mice deficient for the close homolog of L1. *Mol Cell Biol* **22**, 7967-7981 (2002).

62. M. Pratte, G. Rougon, M. Schachner, M. Jamon, Mice deficient for the close homologue of the neural adhesion cell L1 (CHL1) display alterations in emotional reactivity and motor coordination. *Behav Brain Res* **147**, 31-39 (2003).

63. K. Sakurai, O. Migita, M. Toru, T. Arinami, An association between a missense polymorphism in the close homologue of L1 (CHL1, CALL) gene and schizophrenia. *Mol Psychiatry* **7**, 412-415 (2002).

64. S. Weller, J. Gärtner, Genetic and clinical aspects of X-linked hydrocephalus (L1 disease): Mutations in the L1CAM gene. *Hum Mutat* **18**, 1-12 (2001).

65. A. Kurumaji, H. Nomoto, T. Okano, M. Toru, An association study between polymorphism of L1CAM gene and schizophrenia in a Japanese sample. *Am J Med Genet* **105**, 99-104 (2001).

66. Q. Y. Chen *et al.*, Case-control association study of the close homologue of L1 (CHL1) gene and schizophrenia in the Chinese population. *Schizophr Res* **73**, 269-274 (2005).

67. M. Traka, J. L. Dupree, B. Popko, D. Karagogeos, The neuronal adhesion protein TAG-1 is expressed by Schwann cells and oligodendrocytes and is localized to the juxtaparanodal region of myelinated fibers. *J Neurosci* **22**, 3016-3024 (2002).

68. M. Yamamoto, A. M. Boyer, J. E. Crandall, M. Edwards, H. Tanaka, Distribution of stage-specific neurite-associated proteins in the developing murine nervous system recognized by a monoclonal antibody. *J Neurosci* **6**, 3576-3594 (1986).

69. M. A. Wolman *et al.*, Transient axonal glycoprotein-1 (TAG-1) and laminin-alpha1 regulate dynamic growth cone behaviors and initial axon direction in vivo. *Neural Dev* **3**, 6 (2008).

70. S. Soares *et al.*, Neuronal and glial expression of the adhesion molecule TAG-1 is regulated after peripheral nerve lesion or central neurodegeneration of adult nervous system. *Eur J Neurosci* **21**, 1169-1180 (2005).

71. V. Gautam, C. D'Avanzo, M. Hebisch, D. M. Kovacs, D. Y. Kim, BACE1 activity regulates cell surface contactin-2 levels. *Mol Neurodegener* **9**, 4 (2014).

72. J. M. Gunnersen *et al.*, Sez-6 proteins affect dendritic arborization patterns and excitability of cortical pyramidal neurons. *Neuron* **56**, 621-639 (2007).

73. J. Walter, Fishing for function--distinct roles of Bace1 and Bace2 in Zebrafish development. *J Neurochem* **127**, 435-437 (2013).

74. B. D. Bennett *et al.*, Expression analysis of BACE2 in brain and peripheral tissues. *J Biol Chem* **275**, 20647-20651 (2000).

75. S. Casas *et al.*, BACE2 plays a role in the insulin receptor trafficking in pancreatic ß-cells. *Am J Physiol Endocrinol Metab* **299**, E1087-1095 (2010).

76. R. Yan, J. B. Munzner, M. E. Shuck, M. J. Bienkowski, BACE2 functions as an alternative alpha-secretase in cells. *J Biol Chem* **276**, 34019-34027 (2001).

77. M. Farzan, C. E. Schnitzler, N. Vasilieva, D. Leung, H. Choe, BACE2, a beta -secretase homolog, cleaves at the beta site and within the amyloid-beta region of the amyloid-beta precursor protein. *Proc Natl Acad Sci U S A* **97**, 9712-9717 (2000).

78. F. van Bebber, A. Hruscha, M. Willem, B. Schmid, C. Haass, Loss of Bace2 in zebrafish affects melanocyte migration and is distinct from Bace1 knock out phenotypes. *J Neurochem* **127**, 471-481 (2013).

79. D. R. Shimshek *et al.*, Pharmacological BACE1 and BACE2 inhibition induces hair depigmentation by inhibiting PMEL17 processing in mice. *Sci Rep* **6**, 21917 (2016).

80. T. Gordon, G. H. Borschel, The use of the rat as a model for studying peripheral nerve regeneration and sprouting after complete and partial nerve injuries. *Exp Neurol* **287**, 331-347 (2017).

81. C. J. Woolf *et al.*, Denervation of the motor endplate results in the rapid expression by terminal Schwann cells of the growth-associated protein GAP-43. *J Neurosci* **12**, 3999-4010 (1992).

82. M. L. Reynolds, C. J. Woolf, Terminal Schwann cells elaborate extensive processes following denervation of the motor endplate. *J Neurocytol* **21**, 50-66 (1992).

83. H. Kang, L. Tian, W. Thompson, Terminal Schwann cells guide the reinnervation of muscle after nerve injury. *J Neurocytol* **32**, 975-985 (2003).

84. H. Kang, L. Tian, M. Mikesh, J. W. Lichtman, W. J. Thompson, Terminal Schwann cells participate in neuromuscular synapse remodeling during reinnervation following nerve injury. *J Neurosci* **34**, 6323-6333 (2014).

85. M. C. Brown, R. L. Holland, W. G. Hopkins, Motor nerve sprouting. *Annu Rev Neurosci* **4**, 17-42 (1981).

86. J. Hegedus, C. T. Putman, N. Tyreman, T. Gordon, Preferential motor unit loss in the SOD1 G93A transgenic mouse model of amyotrophic lateral sclerosis. *The Journal of physiology* **586**, 3337-3351 (2008).

87. T. Gordon, J. Hegedus, S. L. Tam, Adaptive and maladaptive motor axonal sprouting in aging and motoneuron disease. *Neurol Res* **26**, 174-185 (2004).

88. D. Frey *et al.*, Early and selective loss of neuromuscular synapse subtypes with low sprouting competence in motoneuron diseases. *J Neurosci* **20**, 2534-2542 (2000).

89. M. A. Ariano, R. B. Armstrong, V. R. Edgerton, Hindlimb muscle fiber populations of five mammals. *J Histochem Cytochem* **21**, 51-55 (1973).

90. C. H. Ma *et al.*, Accelerating axonal growth promotes motor recovery after peripheral nerve injury in mice. *J Clin Invest* **121**, 4332-4347 (2011).

91. H. Lindå, M. K. Sköld, T. Ochsmann, Activating transcription factor 3, a useful marker for regenerative response after nerve root injury. *Front Neurol* **2**, 30 (2011).

92. G. Raivich *et al.*, The AP-1 transcription factor c-Jun is required for efficient axonal regeneration. *Neuron* **43**, 57-67 (2004).

93. F. W. Schwaiger *et al.*, Peripheral but not central axotomy induces changes in Janus kinases (JAK) and signal transducers and activators of transcription (STAT). *Eur J Neurosci* **12**, 1165-1176 (2000).

94. R. Y. Liu, W. D. Snider, Different signaling pathways mediate regenerative versus developmental sensory axon growth. *J Neurosci* **21**, RC164 (2001).

95. M. Kanje, A. Skottner, J. Sjöberg, G. Lundborg, Insulin-like growth factor I (IGF-I) stimulates regeneration of the rat sciatic nerve. *Brain Res* **486**, 396-398 (1989).

96. G. W. Glazner, S. Lupien, J. A. Miller, D. N. Ishii, Insulin-like growth factor II increases the rate of sciatic nerve regeneration in rats. *Neuroscience* **54**, 791-797 (1993).

97. H. Hammarberg, F. Piehl, M. Risling, S. Cullheim, Differential regulation of trophic factor receptor mRNAs in spinal motoneurons after sciatic nerve transection and ventral root avulsion in the rat. *J Comp Neurol* **426**, 587-601 (2000).

98. Y. Zhang *et al.*, Expression of CHL1 and L1 by neurons and glia following sciatic nerve and dorsal root injury. *Mol Cell Neurosci* **16**, 71-86 (2000).

99. J. H. Skene, M. Willard, Characteristics of growth-associated polypeptides in regenerating toad retinal ganglion cell axons. *J Neurosci* **1**, 419-426 (1981).

100. H. M. Bomze, K. R. Bulsara, B. J. Iskandar, P. Caroni, J. H. Skene, Spinal axon regeneration evoked by replacing two growth cone proteins in adult neurons. *Nat Neurosci* **4**, 38-43 (2001).

101. D. Frey, T. Laux, L. Xu, C. Schneider, P. Caroni, Shared and unique roles of CAP23 and GAP43 in actin regulation, neurite outgrowth, and anatomical plasticity. *J Cell Biol* **149**, 1443-1454 (2000).

102. A. Valero-Cabré, K. Tsironis, E. Skouras, X. Navarro, W. F. Neiss, Peripheral and spinal motor reorganization after nerve injury and repair. *J Neurotrauma* **21**, 95-108 (2004).

103. C. Tallon, E. Rockenstein, E. Masliah, M. H. Farah, Increased BACE1 activity inhibits peripheral nerve regeneration after injury. *Neurobiol Dis* **106**, 147-157 (2017).

104. A. R. Bauder, T. A. Ferguson, Reproducible mouse sciatic nerve crush and subsequent assessment of regeneration by whole mount muscle analysis. *J Vis Exp*, (2012).

105. C. K. Magill *et al.*, Reinnervation of the tibialis anterior following sciatic nerve crush injury: a confocal microscopic study in transgenic mice. *Exp Neurol* **207**, 64-74 (2007).

106. R. D. Madison, S. J. Archibald, T. M. Brushart, Reinnervation accuracy of the rat femoral nerve by motor and sensory neurons. *J Neurosci* **16**, 5698-5703 (1996).

107. T. M. Brushart, Motor axons preferentially reinnervate motor pathways. *J Neurosci* **13**, 2730-2738 (1993).

108. A. B. Malmberg, A. I. Basbaum, Partial sciatic nerve injury in the mouse as a model of neuropathic pain: behavioral and neuroanatomical correlates. *Pain* **76**, 215-222 (1998).

109. T. Lindenlaub, C. Sommer, Partial sciatic nerve transection as a model of neuropathic pain: a qualitative and quantitative neuropathological study. *Pain* **89**, 97-106 (2000).

110. L. Li, C. J. Xian, J. H. Zhong, X. F. Zhou, Effect of lumbar 5 ventral root transection on pain behaviors: a novel rat model for neuropathic pain without axotomy of primary sensory neurons. *Exp Neurol* **175**, 23-34 (2002).

111. B. Pan *et al.*, The lateral thoracic nerve and the cutaneous maximus muscle--a novel in vivo model system for nerve degeneration and regeneration studies. *Exp Neurol* **236**, 6-18 (2012).

112. C. Tallon, K. A. Russell, S. Sakhalkar, N. Andrapallayal, M. H. Farah, Length-dependent axo-terminal degeneration at the neuromuscular synapses of type II muscle in SOD1 mice. *Neuroscience* **312**, 179-189 (2016).

113. A. Patzkó, M. E. Shy, Update on Charcot-Marie-Tooth disease. *Curr Neurol Neurosci Rep* **11**, 78-88 (2011).

114. K. A. Nave, M. W. Sereda, H. Ehrenreich, Mechanisms of disease: inherited demyelinating neuropathies--from basic to clinical research. *Nat Clin Pract Neurol* **3**, 453-464 (2007).

115. L. Gutmann, M. Shy, Update on Charcot-Marie-Tooth disease. *Curr Opin Neurol* **28**, 462-467 (2015).

116. D. Bouhy, V. Timmerman, Animal models and therapeutic prospects for Charcot-Marie-Tooth disease. *Ann Neurol* **74**, 391-396 (2013).

117. U. Suter *et al.*, A leucine-to-proline mutation in the putative first transmembrane domain of the 22-kDa peripheral myelin protein in the trembler-J mouse. *Proc Natl Acad Sci U S A* **89**, 4382-4386 (1992).

118. R. E. Madrid, A. Lofgren, J. Baets, V. Timmerman, Biopsy in a patient with PMP22 exon 2 mutation recapitulates pathology of Trembler-J mouse. *Neuromuscul Disord* **23**, 345-348 (2013).

119. A. N. Scurry *et al.*, Structural and Functional Abnormalities of the Neuromuscular Junction in the Trembler-J Homozygote Mouse Model of Congenital Hypomyelinating Neuropathy. *J Neuropathol Exp Neurol* **75**, 334-346 (2016).

120. M. Polydefkis, P. Hauer, J. W. Griffin, J. C. McArthur, Skin biopsy as a tool to assess distal small fiber innervation in diabetic neuropathy. *Diabetes Technol Ther* **3**, 23-28 (2001).

121. M. Polydefkis, J. W. Griffin, J. McArthur, New insights into diabetic polyneuropathy. *JAMA* **290**, 1371-1376 (2003).

122. M. Polydefkis *et al.*, The time course of epidermal nerve fibre regeneration: studies in normal controls and in people with diabetes, with and without neuropathy. *Brain* **127**, 1606-1615 (2004).

123. N. E. Cameron, S. E. Eaton, M. A. Cotter, S. Tesfaye, Vascular factors and metabolic interactions in the pathogenesis of diabetic neuropathy. *Diabetologia* **44**, 1973-1988 (2001).

124. K. Juster-Switlyk, A. G. Smith, Updates in diabetic peripheral neuropathy. *F1000Res* **5**, (2016).

125. P. D. O'Brien, S. A. Sakowski, E. L. Feldman, Mouse models of diabetic neuropathy. *ILAR J* **54**, 259-272 (2014).

126. Y. Liu *et al.*, Sensory and autonomic function and structure in footpads of a diabetic mouse model. *Sci Rep* **7**, 41401 (2017).

127. D. W. Cleveland, J. D. Rothstein, From Charcot to Lou Gehrig: deciphering selective motor neuron death in ALS. *Nature reviews. Neuroscience* **2**, 806-819 (2001).

128. D. R. Rosen, Mutations in Cu/Zn superoxide dismutase gene are associated with familial amyotrophic lateral sclerosis. *Nature* **364**, 362 (1993).

129. M. E. Gurney *et al.*, Motor neuron degeneration in mice that express a human Cu,Zn superoxide dismutase mutation. *Science* **264**, 1772-1775 (1994).

130. P. C. Wong *et al.*, An adverse property of a familial ALS-linked SOD1 mutation causes motor neuron disease characterized by vacuolar degeneration of mitochondria. *Neuron* **14**, 1105-1116 (1995).

131. M. Azzouz *et al.*, Progressive motor neuron impairment in an animal model of familial amyotrophic lateral sclerosis. *Muscle Nerve* **20**, 45-51 (1997).

132. L. R. Fischer *et al.*, Amyotrophic lateral sclerosis is a distal axonopathy: evidence in mice and man. *Exp Neurol* **185**, 232-240 (2004).

133. A. M. Schaefer, J. R. Sanes, J. W. Lichtman, A compensatory subpopulation of motor neurons in a mouse model of amyotrophic lateral sclerosis. *J Comp Neurol* **490**, 209-219 (2005).

134. S. Pun, A. F. Santos, S. Saxena, L. Xu, P. Caroni, Selective vulnerability and pruning of phasic motoneuron axons in motoneuron disease alleviated by CNTF. *Nat Neurosci* **9**, 408-419 (2006).

135. J. Hegedus, C. T. Putman, T. Gordon, Time course of preferential motor unit loss in the SOD1 G93A mouse model of amyotrophic lateral sclerosis. *Neurobiol Dis* **28**, 154-164 (2007).

136. S. Saxena, E. Cabuy, P. Caroni, A role for motoneuron subtype-selective ER stress in disease manifestations of FALS mice. *Nat Neurosci* **12**, 627-636 (2009).

137. S. Saxena *et al.*, Neuroprotection through excitability and mTOR required in ALS motoneurons to delay disease and extend survival. *Neuron* **80**, 80-96 (2013).

138. T. D. Heiman-Patterson *et al.*, Background and gender effects on survival in the TgN(SOD1-G93A)1Gur mouse model of ALS. *J Neurol Sci* **236**, 1-7 (2005).

139. A. Y. Chiu *et al.*, Age-dependent penetrance of disease in a transgenic mouse model of familial amyotrophic lateral sclerosis. *Molecular and cellular neurosciences* **6**, 349-362 (1995).

140. G. Dobrowolny *et al.*, Muscle expression of a local Igf-1 isoform protects motor neurons in an ALS mouse model. *J Cell Biol* **168**, 193-199 (2005).

141. C. M. Wooley *et al.*, Gait analysis detects early changes in transgenic SOD1(G93A) mice. *Muscle Nerve* **32**, 43-50 (2005).

142. B. Zhang, P. Tu, F. Abtahian, J. Q. Trojanowski, V. M. Lee, Neurofilaments and orthograde transport are reduced in ventral root axons of transgenic mice that express human SOD1 with a G93A mutation. *J Cell Biol* **139**, 1307-1315 (1997).

143. M. E. Gurney *et al.*, Motor neuron degeneration in mice that express a human Cu,Zn superoxide dismutase mutation. *Science* **264**, 1772-1775 (1994).

144. A. H. Williams *et al.*, MicroRNA-206 delays ALS progression and promotes regeneration of neuromuscular synapses in mice. *Science* **326**, 1549-1554 (2009).

145. C. E. Schmidt, J. B. Leach, Neural tissue engineering: strategies for repair and regeneration. *Annu Rev Biomed Eng* **5**, 293-347 (2003).

146. A. Hoke, Mechanisms of Disease: what factors limit the success of peripheral nerve regeneration in humans? *Nat Clin Pract Neurol* **2**, 448-454 (2006).

147. T. Gordon, N. Tyreman, M. A. Raji, The basis for diminished functional recovery after delayed peripheral nerve repair. *J Neurosci* **31**, 5325-5334 (2011).

148. P. Wu *et al.*, Key changes in denervated muscles and their impact on regeneration and reinnervation. *Neural Regen Res* **9**, 1796-1809 (2014).

149. A. Höke, A (heat) shock to the system promotes peripheral nerve regeneration. *J Clin Invest* **121**, 4231-4234 (2011).

150. F. K. Sanders, D. Whitteridge, Conduction velocity and myelin thickness in regenerating nerve fibres. *J Physiol* **105**, 152-174 (1946).

151. E. Verdu, D. Ceballos, J. J. Vilches, X. Navarro, Influence of aging on peripheral nerve function and regeneration. *J Peripher Nerv Syst* **5**, 191-208 (2000).

152. M. Y. Lin, G. Manzano, R. Gupta, Nerve allografts and conduits in peripheral nerve repair. *Hand Clin* **29**, 331-348 (2013).

153. C. Xu *et al.*, Electrical stimulation promotes regeneration of defective peripheral nerves after delayed repair intervals lasting under one month. *PLoS One* **9**, e105045 (2014).

154. X. Hu, J. Hu, L. Dai, B. Trapp, R. Yan, Axonal and Schwann cell BACE1 is equally required for remyelination of peripheral nerves. *J Neurosci* **35**, 3806-3814 (2015).

155. R. G. Perez, H. Zheng, L. H. Van der Ploeg, E. H. Koo, The beta-amyloid precursor protein of Alzheimer's disease enhances neuron viability and modulates neuronal polarity. *J Neurosci* **17**, 9407-9414 (1997).

156. T. L. Young-Pearse, A. C. Chen, R. Chang, C. Marquez, D. J. Selkoe, Secreted APP regulates the function of full-length APP in neurite outgrowth through interaction with integrin beta1. *Neural Dev* **3**, 15 (2008).

157. H. L. Li *et al.*, Defective neurite extension is caused by a mutation in amyloid beta/A4 (A beta) protein precursor found in familial Alzheimer's disease. *J Neurobiol* **32**, 469-480 (1997).

158. C. L. Hinkle, S. Diestel, J. Lieberman, P. F. Maness, Metalloprotease-induced ectodomain shedding of neural cell adhesion molecule (NCAM). *J Neurobiol* **66**, 1378-1395 (2006).

159. S. Barão *et al.*, Antagonistic Effects of BACE1 and APH1B-γ-Secretase Control Axonal Guidance by Regulating Growth Cone Collapse. *Cell Rep* **12**, 1367-1376 (2015).

160. R. Vassar, BACE1 inhibitor drugs in clinical trials for Alzheimer's disease. *Alzheimers Res Ther* **6**, 89 (2014).

161. S. J. Stachel *et al.*, Structure-based design of potent and selective cell-permeable inhibitors of human beta-secretase (BACE-1). *J Med Chem* **47**, 6447-6450 (2004).

162. M. R. Fielden *et al.*, Retinal Toxicity Induced by a Novel β-secretase Inhibitor in the Sprague-Dawley Rat. *Toxicol Pathol* **43**, 581-592 (2015).

163. P. C. May *et al.*, Robust central reduction of amyloid-β in humans with an orally available, non-peptidic β-secretase inhibitor. *J Neurosci* **31**, 16507-16516 (2011).

164. J. D. Scott *et al.*, Discovery of the 3-Imino-1,2,4-thiadiazinane 1,1-Dioxide Derivative Verubecestat (MK-8931)-A β-Site Amyloid Precursor Protein Cleaving Enzyme 1 Inhibitor for the Treatment of Alzheimer's Disease. *J Med Chem* **59**, 10435-10450 (2016).

165. R. Mellick, J. B. Cavanagh, The function of the perineurium and its relation to the flow phenomenon within the endoneurial spaces. *Proc Aust Assoc Neurol* **5**, 521-525 (1968).

166. C. Cheret *et al.*, Bace1 and Neuregulin-1 cooperate to control formation and maintenance of muscle spindles. *EMBO J* **32**, 2015-2028 (2013).

167. M. Weber *et al.*, BACE1 across species: a comparison of the in vivo consequences of BACE1 deletion in mice and rats. *Sci Rep* **7**, 44249 (2017).

168. S. Eketjäll *et al.*, AZD3293: A Novel, Orally Active BACE1 Inhibitor with High Potency and Permeability and Markedly Slow Off-Rate Kinetics. *J Alzheimers Dis* **50**, 1109-1123 (2016).

169. S. Saxena, P. Caroni, Mechanisms of axon degeneration: from development to disease. *Prog Neurobiol* **83**, 174-191 (2007).

170. C. Tallon, K. A. Russell, S. Sakhalkar, N. Andrapallayal, M. H. Farah, Length-dependent axo-terminal degeneration at the neuromuscular synapses of type II muscle in SOD1 mice. *Neuroscience* **312**, 179-189 (2016).

171. M. Schafers, C. Schmidt, C. Vogel, K. V. Toyka, C. Sommer, Tumor necrosis factor-alpha (TNF) regulates the expression of ICAM-1 predominantly through TNF receptor 1 after chronic constriction injury of mouse sciatic nerve. *Acta Neuropathol* **104**, 197-205 (2002).

172. L. Liu *et al.*, Increased TNFR1 expression and signaling in injured peripheral nerves of mice with reduced BACE1 activity. *Neurobiol Dis* **93**, 21-27 (2016).

173. P. Caroni, Overexpression of growth-associated proteins in the neurons of adult transgenic mice. *J Neurosci Methods* **71**, 3-9 (1997).

174. Y. Chen *et al.*, Alzheimer's β-secretase (BACE1) regulates the cAMP/PKA/CREB pathway independently of β-amyloid. *J Neurosci* **32**, 11390-11395 (2012).

175. M. S. Malamas *et al.*, Design and synthesis of 5,5'-disubstituted aminohydantoins as potent and selective human beta-secretase (BACE1) inhibitors. *J Med Chem* **53**, 1146-1158 (2010).

176. G. Cebers *et al.*, AZD3293: Pharmacokinetic and Pharmacodynamic Effects in Healthy Subjects and Patients with Alzheimer's Disease. *J Alzheimers Dis* **55**, 1039-1053 (2017).

177. V. Chaisuksunt *et al.*, The cell recognition molecule CHL1 is strongly upregulated by injured and regenerating thalamic neurons. *J Comp Neurol* **425**, 382-392 (2000).

178. J. L. Bixby, J. Lilien, L. F. Reichardt, Identification of the major proteins that promote neuronal process outgrowth on Schwann cells in vitro. *J Cell Biol* **107**, 353-361 (1988).

179. B. Seilheimer, M. Schachner, Studies of adhesion molecules mediating interactions between cells of peripheral nervous system indicate a major role for L1 in mediating sensory neuron growth on Schwann cells in culture. *J Cell Biol* **107**, 341-351 (1988).

180. F. M. Laird *et al.*, BACE1, a major determinant of selective vulnerability of the brain to amyloid-beta amyloidogenesis, is essential for cognitive, emotional, and synaptic functions. *J Neurosci* **25**, 11693-11709 (2005).

181. R. M. Holsinger, C. A. McLean, K. Beyreuther, C. L. Masters, G. Evin, Increased expression of the amyloid precursor beta-secretase in Alzheimer's disease. *Ann Neurol* **51**, 783-786 (2002).

182. S. J. Tyler, D. Dawbarn, G. K. Wilcock, S. J. Allen, alpha- and beta-secretase: profound changes in Alzheimer's disease. *Biochem Biophys Res Commun* **299**, 373-376 (2002).

183. L. B. Yang *et al.*, Elevated beta-secretase expression and enzymatic activity detected in sporadic Alzheimer disease. *Nat Med* **9**, 3-4 (2003).

184. A. Pestronk, D. B. Drachman, J. W. Griffin, Effects of aging on nerve sprouting and regeneration. *Exp Neurol* **70**, 65-82 (1980).

185. X. Navarro, W. R. Kennedy, Effect of age on collateral reinnervation of sweat glands in the mouse. *Brain Res* **463**, 174-181 (1988).

186. E. Kerezoudi, P. K. Thomas, Influence of age on regeneration in the peripheral nervous system. *Gerontology* **45**, 301-306 (1999).

187. E. Verdú, D. Ceballos, J. J. Vilches, X. Navarro, Influence of aging on peripheral nerve function and regeneration. *J Peripher Nerv Syst* **5**, 191-208 (2000).

188. H. Kang, J. W. Lichtman, Motor axon regeneration and muscle reinnervation in young adult and aged animals. *J Neurosci* **33**, 19480-19491 (2013).

189. H. Fukumoto *et al.*, Beta-secretase activity increases with aging in human, monkey, and mouse brain. *Am J Pathol* **164**, 719-725 (2004).

190. F. R. Fricker *et al.*, Axonally derived neuregulin-1 is required for remyelination and regeneration after nerve injury in adulthood. *J Neurosci* **31**, 3225-3233 (2011).

191. G. Feng *et al.*, Imaging neuronal subsets in transgenic mice expressing multiple spectral variants of GFP. *Neuron* **28**, 41-51 (2000).

Carolyn Tallon

Cell: (410) 591-4632 2515 Boston St. Apt 407
carolynntea@gmail.com or ctallon1@jhmi.edu Baltimore, MD 21224

PhD candidate from Johns Hopkins University expected to graduate in December 2017 studying peripheral nerve regeneration in injury and disease models via molecular, morphological and physiological analysis. Very skilled in nerve surgeries and electrophysiological recordings in mouse models. Expertise using both cell and organotypic slice cultures. Tested drug efficacy both in vitro and in vivo models. Mentored and managed junior lab members in various experimental procedures. Skilled at effectively presenting oral and written scientific information to a variety of audiences. Highly interested in identifying novel drug efficacy in neurodegenerative diseases.

EDUCATION

PhD Candidate in Pathobiology August 2013 – December 2017

Johns Hopkins School of Medicine, Baltimore, MD, USA

PhD Thesis: BACE1 activity levels inversely influence peripheral axon regeneration.

Thesis mentor: Dr. Mohamed H. Farah

- Determined that BACE1 activity levels inversely influence axonal repair in acute peripheral nerve injury mouse models.
- Tested the efficacy of BACE1 inhibitors on enhancing regeneration in acute peripheral nerve injury and neurodegenerative mouse models.

Bachelor of Science in Physiology May 2013

First class honours with distinction, McGill University, Montreal, QC, Canada

Undergraduate Honours Thesis: Attenuated vestibular-only neurons show greater spike train variability during active motion.

Thesis mentor: Dr. Kathleen Cullen

- Explored whether attenuated vestibular-only neurons altered their firing rate variability between self-generated and externally generated head motion.

ADDITIONAL RESEARCH EXPERIENCE

Summer Research Assistant May 2013 – August 2013

Dr. Claire Brown - McGill Imaging Facility, McGill University, Montreal, QC

- Imaged live ErbB2 breast cancer cells to determine whether TGF-β modulates cell motility

Summer Undergraduate Research Assistant May 2011 - August 2011

Dr. Karine Auclair - Chemistry Department, McGill University, Montreal, QC

- Tested novel bisubsrate inhibitors on aminoglycoside resistance enzymes to determine whether the inhibitors were specific to acetyltransferases

WORK EXPERIENCE

Microscope Use Trainer - *Advanced Bioimaging Facility, McGill University* October 2012 - May 2013

- Learned how to operate conventional and confocal microscopy to assist novel users

VOLUNTEER WORK

Sabin Pathology Club - *Johns Hopkins School of Medicine* October 2016 – present

- Prepared and presented biannual hour long lectures on the physiology and pathology of various biological systems of the human body and participated in lively scientific discussions

Pathobiology Social Committee - *Johns Hopkins School of Medicine* July 2014 – June 2015

- Effectively led committee by delegating tasks to efficiently organize events for pathobiology students

Graduate Student Association - *Johns Hopkins School of Medicine* June 2014 – June 2015

- Managed various GSA list serves and created weekly newsletters detailing events for graduate students

TEACHING AND MENTORING

Teaching Assistant Experiences - *Johns Hopkins School of Medicine* Variable months 2014-2017

- Grant Writing – Presented training plan and grant critique sessions, edited student grants
- Neuropathology – Organized lecture notes and exam answers, assisted with scheduling
- Basic Mechanisms of Disease – Presented lecture on bone and muscle physiology and pathology

Chief Pathobiology Graduate Student - *Johns Hopkins School of Medicine* July 2015 – June 2016

- Elected to the position by the chief of pathology, Dr. Ralph Hruban
- Effectively solved student issues and communicated them to the pathobiology executive board
- Helped organize pathobiology events including orientation, retreat, and recruitment
- Successfully mentored first year students through classes and second year students through doctoral board oral exams
- Coordinated and scheduled the pathobiology journal club and Wednesday lunch meetings

PUBLICATIONS

C. Tallon, K. L. Marshall, M. E. Kennedy, and M.H. Farah. (2017) Pharmacological BACE1 inhibition improves nerve regeneration in axonal injury and disease models. *In preparation.*

C. Tallon and M.H. Farah. (2017) Beta secretase activity in peripheral nerve regeneration. *Neural Regener. Res.*12: 1565-74.

C. Tallon, E. Rockenstein, E. Masliah, and M.H. Farah. (2017) Increased BACE1 activity inhibits peripheral nerve regeneration after injury. *Neurobiol. Dis.*106: 147-157.

C. Tallon, K.A. Russell, S. Sakhalkar, N. Andrapallayal, and M.H. Farah. (2016) Length-dependent axo-terminal degeneration at the neuromuscular synapses of type II muscle in SOD1 mice. *Neurosci* 312: 179-189.

PRESENTATIONS AND POSTERS

- "Terminal axonal sprouting is augmented in partially injured motor nerves of BACE1 KO mice" Nanosymposium talk - 2016 Society for Neuroscience Conference. Nov 2016.
- "Reduced BACE1 Activity Enhances Neuromuscular Junction Innervation in SOD1 and Axonal Injury Mouse Models" Flash talk and poster presentation - 2nd Kloster Seeon Meeting on BACE Proteases in Health and Disease. Sept 2016.
- "Inhibition of BACE1 in the SOD1G93A mouse model of ALS enhances neuromuscular junction remodeling" Nanosymposium talk - 2015 Society for Neuroscience Conference. Oct 2015.
- "Reducing BACE1 activity via pharmacological and genetic intervention improves neuromuscular junction remodeling in both ALS and partial motor axon injury models" Research talk and poster presentation - 3rd Ottawa International Conference on Neuromuscular Biology, Disease and Therapy. Sept 2015.
- "Enhancing the plasticity and remodeling of neuromuscular junctions in a motor neuron disease mouse model by inhibiting BACE1" Generated poster – MDA Scientific conference. Mar 2015.

AWARDS & HONOURS

- Golden microscope award for best senior research talk – 2017 Pathobiology Retreat 2017
- Travel award - 2nd Kloster Seeon Meeting on BACE Proteases in Health and Disease 2016
- Best 2nd year poster at the JHU annual pathobiology program retreat 2014
- NSERC Undergraduate Student Research Award 2013
- Science Undergraduate Research Award 2011
- Michael and Lina Chan Scholarship in Science 2010
- Dean's Honour List 2010
- A S Hill Scholarship for academic excellence 2009

CERTIFICATIONS

- CPR (2017), Electronic Information Security and Data Management Training (2017), Research Ethics I (2016), Research Ethics II (2015), Animal Care and Use (2014)

Languages

- English (native), French (basic skills)

SKILLS

- Mouse surgery and electrophysiology
- Muscle dissection, fixation, and sectioning
- Immunofluorescence
- Microscopy (confocal, brightfield, apotome, EM)
- Molecular biology (PCR, ELISA, Western Blot, Protein concentration assays, Enzymatic activity)
- Organotypic spinal cord slice culture
- Primary cell culture and human iPSCs
- Basic MATLAB and java coding
- Scientific writing and presenting
- Lab management and personnel mentoring

MEMBERSHIPS

Golden Key McGill Chapter, Society for Neuroscience